Closed-loop Dynamic Real-time Optimization for Cost-optimal Process Operations

Closed-loop Dynamic Real-time Optimization for Cost-optimal Process Operations

by

Mohammad Zamry Jamaludin, B.Eng., M.Eng.

A Thesis
Submitted to the School of Graduate Studies
in Partial Fulfillment of the Requirements
for the Degree of
Doctor of Philosophy

McMaster University

DOCTOR OF PHILOSOPHY (2016) McMaster University
(Chemical Engineering) Hamilton, Ontario, Canada

TITLE:	Closed-loop Dynamic Real-time Optimization for Cost-optimal Process Operations
AUTHOR:	Mohammad Zamry Jamaludin, B.Eng., M.Eng. Universiti Teknologi Malaysia, Johor, Malaysia
SUPERVISOR:	Dr. Christopher L.E. Swartz
NUMBER OF PAGES:	xi, 130

Abstract

Real-time optimization (RTO) is a supervisory strategy in the hierarchical industrial process automation architecture in which economically optimal set-point targets are computed for the lower level advanced control system, which is typically model predictive control (MPC). Due to highly volatile market conditions, recent developments have considered transforming the conventional steady-state RTO to dynamic RTO (DRTO) to permit economic optimization during transient operation. Published DRTO literature optimizes plant input trajectories without taking into account the presence of the plant control system, constituting an open-loop DRTO (OL-DRTO) approach. The goal of this research is to develop a design framework for a DRTO system that optimizes process economics based on a closed-loop response prediction. We focus, in particular, on DRTO applied to a continuous process operation regulated under constrained MPC. We follow a two-layer DRTO/MPC configuration due to its close tie to the industrial process automation architecture.

We first analyze the effects of optimizing MPC closed-loop response dynamics at the DRTO level. A rigorous DRTO problem structure proposed in this thesis is in the form of a multilevel dynamic optimization problem, as it embeds a sequence of MPC optimization subproblems to be solved in order to generate the closed-loop prediction in the DRTO formulation, denoted here as a closed-loop DRTO (CL-DRTO) strategy. A simultaneous solution approach is applied in which the convex MPC optimization subproblems are replaced by their necessary and sufficient, Karush-Kuhn-Tucker (KKT) optimality conditions, resulting in the reformulation of the original multilevel problem as a single-level mathematical program with complementarity constraints (MPCC) with the complementarities handled using an exact penalty formulation. Performance analysis is carried out, and process conditions under which the CL-DRTO strategy significantly outperforms the traditional open-loop counterpart are identified.

The multilevel DRTO problem with a rigorous inclusion of the future MPC calculations significantly increases the size and solution time of the economic optimization problem. Next, we identify and analyze multiple closed-loop approximation techniques, namely, a hybrid formulation, a bilevel programming formulation, and an input clipping formulation applied to an unconstrained MPC algorithm. Performance analysis based on a linear dynamic system shows that the proposed approximation techniques are able to substantially reduce the size and solution time of the rigorous CL-DRTO problem, while largely retaining its original performance. Application to an industrially-based case study of a polystyrene production described by a nonlinear differential-algebraic equation (DAE) system is also presented.

Often large-scale industrial systems comprise multi-unit subsystems regulated under multiple local controllers that require systematic coordination between them. Utilization of closed-loop prediction in the CL-DRTO formulation is extended for application as a higher-level, centralized supervisory control

strategy for coordination of a distributed MPC system. The advantage of the CL-DRTO coordination formulation is that it naturally considers interaction between the underlying MPC subsystems due to the embedded controller optimization subproblems while optimizing the overall process dynamics. In this case, we take advantage of the bilevel formulation to perform closed-loop prediction in two DRTO coordination schemes, with variations in the coordinator objective function based on dynamic economics and target tracking. Case study simulations demonstrate excellent performance in which the proposed coordination schemes minimize the impact of disturbance propagation originating from the upstream subsystem dynamics, and also reduce the magnitude of constraint violation through appropriate adjustment of the controller set-point trajectories.

Acknowledgments

First and foremost, thank you Almighty God for blessing me with wisdom, patience and strength to complete this PhD research, *alhamdulillah*.

I would like to express my unreserved gratitude to my academic advisor, Dr. Christopher L. E. Swartz, for his support and guidance throughout the course of my graduate study at McMaster University. This work owes its existence to Dr. Swartz's direction and vision. I would also like to recognize my supervisory committee members, Dr. Prashant Mhaskar and Dr. Shahin Sirouspour, for their thought provoking discussions during my committee meetings. Acknowledgement is also due to various institutions that have provided financial support for this work, in particular the Ministry of Higher Education (MOHE) Malaysia, McMaster Advanced Control Consortium (MACC) and McMaster University.

I would like to put on record a heartfelt note of appreciation to my best friends, Nor Farida Harun, Yanan Cao, Erlita Mastan, Zainatul Handani and Han Wang, for their motivation, assistance and companionship. I am also very grateful to my family for their endless prayers, understanding and encouragement. I am forever indebted to my partner, Tim Gray, for his love, care and support in many aspects of my life.

Table of Contents

List of Figures

List of Tables

Chapter 1

Introduction

In this chapter, we present the overall context of our research with a particular emphasis placed on the hierarchical industrial process automation architecture which forms the basis for our research framework. The objectives of our research are stated, and an outline of the thesis is presented.

1.1 Motivation

Current competitive trends in an increasingly global market place, rising costs, and tightening environmental constraints make it increasingly important for process plants to be operated efficiently and in an environmentally responsible manner in order to remain competitive. Besides, an analysis by McKinsey Global Institute [1] reveals that the evolution of process industries is strongly influenced by demand-driven productivity, cost factors, policy and regulation, technology and innovation, and rising risks and uncertainty. Consequently, process automation engineers and scientists are faced with the tasks of designing and revamping process automation strategies to address the aforementioned challenges.

Operation of large-scale processes, such as refineries, manufacturing plants, power generation networks and building automation systems, involve a large number of economic-impacting decisions that must be made online. In chemical process operations, solution approaches to online decision-making problems have been established in a hierarchical fashion, as illustrated in Figure 1.1(a), in which the basic architecture consists of, from the bottom, a regulatory control layer commonly in the form of a proportional-integral-derivative (PID) control, an advanced control layer that is dominated by model predictive control (MPC), and real-time optimization (RTO) at the top.

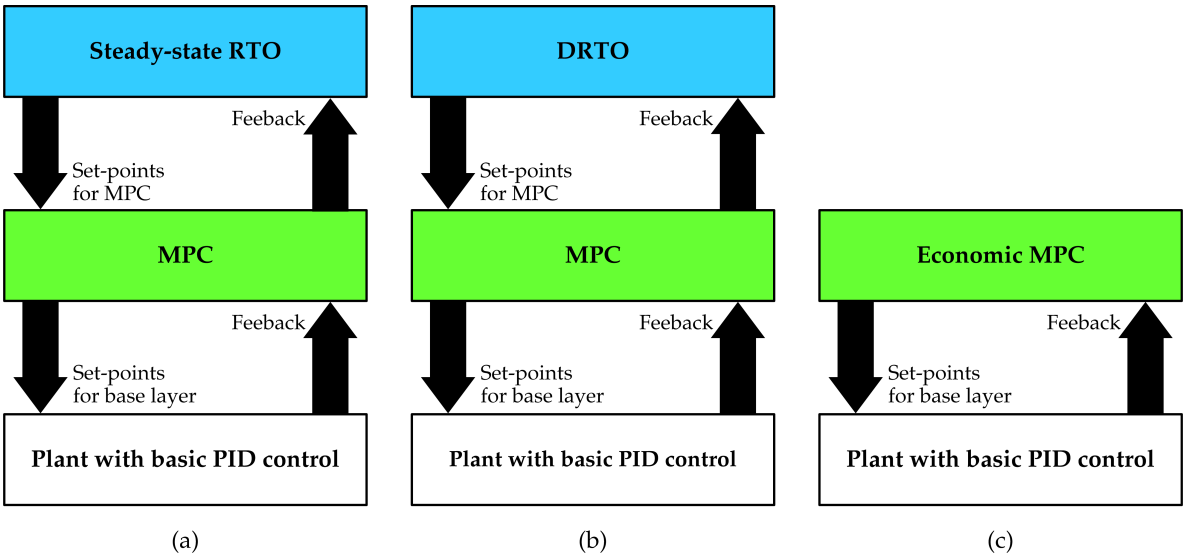

(a) (b) (c)

Figure 1.1: Process automation architectures

After more than seven decades of implementation [2], it is estimated that over 90% of industrial control systems utilize the PID control strategy due to its simple structure, robustness and established stability properties [3]. The variety of implementation approaches include single-loop control, cascade control, ratio control and multiloop control. PID control is installed directly to the process plants together with field instruments such as sensors, transmitters and final control elements. Feedback loops for PID control are typically sampled in the order of seconds. Despite its widespread implementation, the performance of PID control is limited to simple and unconstrained control problems.

MPC is typically installed in a cascade fashion with the local PID controllers to improve process control performance. Key features include its capability to accommodate process interactions and dead time directly, and to handle constraints on manipulated inputs and process outputs explicitly. The MPC algorithm uses a dynamic model to predict future process outputs that optimizes a measure of control performance over a specified prediction horizon. At each controller sampling instance, a sequence of future process inputs are computed to generate the output prediction. The computed control inputs are implemented by following a moving horizon approach in which only the first input changes are

implemented by the final control elements, and the computation is repeated at the next sampling interval. Depending on process and operational requirements, some industrial installations consider a centralized MPC system, and others utilize a distributed MPC environment. Various MPC design approaches and successful industrial applications are reported in a comprehensive review article by Qin and Badgwell [4].

Real-time optimization (RTO) in the two-level process automation architecture is a supervisory strategy that computes the best economics of continuous process operations at a time-scale slower than the lower level process automation activities [5]. RTO interacts with the lower level process control systems in a cascade fashion by providing optimal set-point targets for tracking purposes. The traditional RTO strategy is designed based on a steady-state model. The execution frequency of the steady-state RTO layer is restricted by a requirement for the system to have reached steady-state conditions before the execution of the next optimization calculation. This may result in suboptimal operation for processes that exhibit slow dynamics, experience frequent transitions, or are continuously perturbed by disturbances.

The lack of efficiency in the steady-state RTO system has motivated a recent development that transforms the steady-state RTO system to a dynamic RTO (DRTO) strategy based on a dynamic prediction model, as shown in Figure 1.1(b), thus substantially increasing the frequency at which economic optimization can be performed. DRTO strategies that have been proposed in the literature [6, 7] perform economic optimization in an open-loop fashion without taking into account the presence of the plant control system. In this approach, the set-points prescribed to the underlying control system are constructed from the optimal DRTO open-loop trajectories under an expectation that the closed-loop response dynamics under regulation of controllers at the plant level will follow the trajectories obtained at the DRTO level. An alternative to the two-level DRTO/MPC configuration is a single-level, economic model predictive control (EMPC) strategy that optimizes the plant economics at the controller sampling frequency, as depicted in Figure 1.1(c). Such a strategy aims to address the issues of model inconsistency and time-scale separation between the traditional RTO system and the MPC control layer. In this case, the objective function could be based purely on economics [8], or a hybrid between cost and control performance [9].

In this research, our focus is on the economic optimization of process operations regulated under a constrained MPC system, with an assumption that there exist (D)RTO and MPC systems functioning in the process. We follow the two-level DRTO/MPC configuration in order to be consistent with the typical industrial process automation architecture. In this way, technology advances can be implemented without the requirement for a complete re-design of the original architecture.

1.2 Research Problem Statement

The goal of this research is to develop a dynamic real-time optimization (DRTO) strategy that systematically considers the closed-loop response dynamics of process operations regulated under constrained model predictive controllers (MPC) into its design formulation. The objectives of this research are to:

- Formulate a closed-loop DRTO problem in the form of a multilevel dynamic optimization problem with rigorous inclusion of the future MPC calculations.
- Solve the resulting multilevel problem as a single-level mathematical program with complementarity constraints (MPCC) by replacing the embedded MPC optimization subproblems with their Karush-Kuhn-Tucker (KKT) optimality conditions, and investigate the use of an exact penalty formulation to handle the complementarity constraints.
- Analyze the advantages of optimizing closed-loop response dynamics at the DRTO level in the two-layer process automation architecture, and compare its performance to the open-loop counterpart.
- Formulate and analyze reliable techniques to approximate the rigorous DRTO closed-loop prediction to reduce the size and solution time of the dynamic optimization problem.
- Apply the closed-loop DRTO formulation for process dynamics described by a nonlinear differential-algebraic equation (DAE) system.
- Design coordination schemes for a distributed MPC system via utilization of the closed-loop DRTO formulation with application of a closed-loop approximation technique.

1.3 Thesis Outline

This thesis is organized according to the following chapters.

- In **Chapter 2**, we consider optimization of closed-loop response dynamics at the DRTO level in a two-layer architecture, with constrained MPC applied at the regulatory control level. A simultaneous solution approach is applied to the multilevel DRTO optimization problem, in which the convex MPC optimization subproblems are replaced by their necessary and sufficient Karush-Kuhn-Tucker (KKT) optimality conditions, resulting in a single-level mathematical program with complementarity constraints (MPCC). The performance of the closed-loop DRTO strategy is compared to that of the open-loop prediction counterpart through a multi-part case

study that considers linear dynamic systems with different characteristics. The performance of the proposed strategy is further demonstrated through application to a nonlinear polymerization reactor grade transition problem.

- In **Chapter 3**, we formulate three approximation techniques to the rigorous closed-loop prediction generated from the multilevel closed-loop DRTO problem, which consist of a hybrid formulation, a bilevel formulation, and an input clipping formulation. The hybrid formulation involves application of a rigorous closed-loop prediction applied over a limited DRTO optimization horizon, after which an open-loop optimal control formulation is used. In the bilevel formulation, only a single MPC optimization subproblem is embedded where its prediction and control horizons are extended to match the DRTO optimization horizon, which is significantly longer than that of the MPC. Closed-loop approximation obtained via clipping of inputs computed by an unconstrained MPC algorithm involves utilization of an input saturation mechanism formulated using complementarity constraints. The relative performance of the proposed approximation approaches is analyzed through application of two case studies, the second of which involves economically optimal polymer grade transition.

- In **Chapter 4**, we propose a nonlinear DRTO formulation in the form of a bilevel programming problem. The DRTO performs closed-loop prediction based on a nonlinear DAE system that describes the process dynamic behaviour whereas the embedded MPC optimization subproblem utilizes a linear model prediction. The nonlinear models are discretized using a Backward Euler method with a chosen size of finite element that is consistent with the MPC sampling interval. We investigate the economics and control performance of the proposed strategy based on a polymer grade transition case study in the presence of plant-model mismatch and a high impact disturbance. Also, a comparison is made with the application of a linear DRTO prediction model.

- In **Chapter 5**, we design a DRTO coordination strategy for a distributed MPC system based on a plantwide closed-loop prediction. The DRTO closed-loop formulation that is in the form of a bilevel program embeds the optimization problems of all MPC controllers functioning in the process and computes optimal set-point trajectories for all controllers simultaneously. The process model used within the DRTO module is consistent with the dynamic models used in the MPC controllers, but with the interactions between the process subsystems captured through appropriate linking relationships, such as material flows. The performance of the proposed approach is assessed via case study simulations with variations in the coordinator objective function.

- In **Chapter 6**, we summarize the broad themes covered in this thesis. We present a list of what we consider to be our contributions in this area of study. Future directions are laid out.

References

[1] J. Manyika, J. Sinclair, R. Dobbs, G. Strube, L. Rassey, J. Mischke, J. Remes, C. Roxburgh, K. George, D. O'Halloran, and S. Ramaswamy. *Manufacturing the future: The next era of global growth and innovation*. Tech. rep. McKinsey Global Institute, Nov. 2012, pp. 69 –102.

[2] D. P. Atherton. "Almost Six Decades in Control Engineering [Historical Perspectives]". In: *IEEE Control Systems* 34.6 (2014), pp. 103–110.

[3] C. Knospe. "PID control". In: *IEEE Control Systems* 26.1 (2006), pp. 30–31.

[4] S. J. Qin and T. A. Badgwell. "A survey of industrial model predictive control technology". In: *Control Eng Pract* 11.7 (2003), pp. 733 –764.

[5] M. L. Darby, M. Nikolaou, J. Jones, and D. Nicholson. "RTO: An overview and assessment of current practice". In: *J Process Control* 21.6 (2011), pp. 874 –884.

[6] T. Tosukhowong, J. M. Lee, J. H. Lee, and J. Lu. "An introduction to a dynamic plant-wide optimization strategy for an integrated plant". In: *Comput Chem Eng* 29.1 (2004), pp. 199 –208.

[7] L. Würth, R. Hannemann, and W. Marquardt. "A two-layer architecture for economically optimal process control and operation". In: *J Process Control* 21.3 (2011), pp. 311 –321.

[8] R. Amrit, J. B. Rawlings, and L. T. Biegler. "Optimizing process economics online using model predictive control". In: *Comput Chem Eng* 58.0 (2013), pp. 334 –343.

[9] M. Ellis and P. D. Christofides. "Economic model predictive control with time-varying objective function for nonlinear process systems". In: *AIChE J* 60.2 (2014), pp. 507–519.

Chapter 2

Closed-loop Dynamic Real-time Optimization

The formulations and results in this chapter have been submitted to, and presented in:

[1] M.Z. Jamaludin and C.L.E. Swartz. "Dynamic real-time optimization with closed-loop prediction". *Submitted to AIChE J* (2016), under revision.

[2] M.Z. Jamaludin and C.L.E. Swartz. "Performance analysis of closed-loop dynamic real-time optimization". *CSChE Conference* (2015). Calgary, AB, Canada.

[3] M.Z. Jamaludin and C.L.E. Swartz. "Effects of closed-loop dynamics in dynamic real-time optimization". *AIChE Annual Meeting* (2014). Atlanta, GA, USA.

2.1 Introduction

In order to remain competitive, modern chemical plants have to operate in a cost-optimal fashion, and be responsive to changes that affect their economics and control performance. This has led to a significant research activity towards integrating the control and economic decisions in process operations. Online plant economic optimization has traditionally been addressed via a two-layer architecture with a time-scale separation, as illustrated in Figure 2.1.

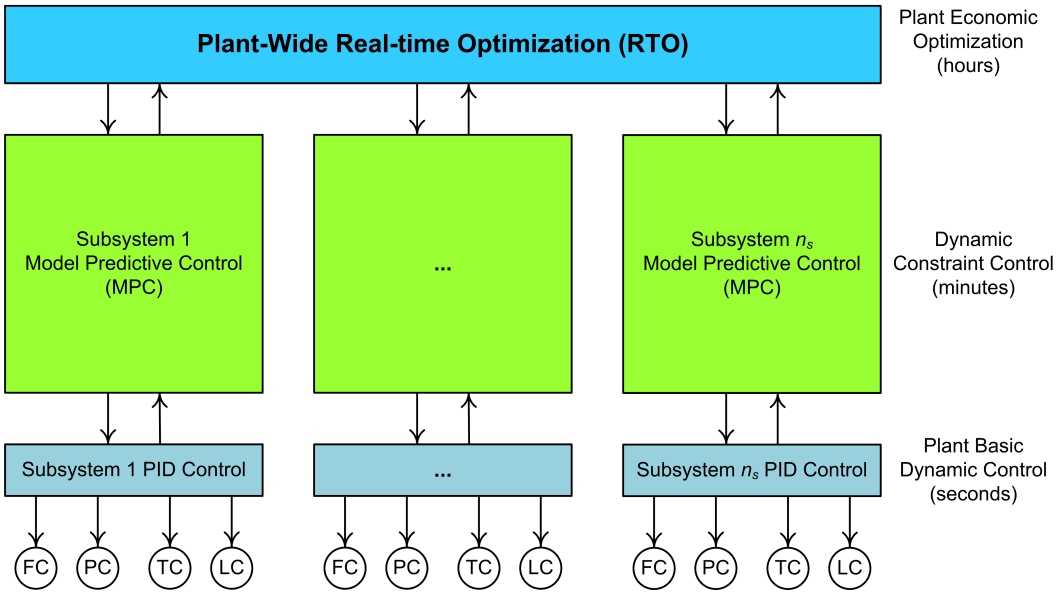

Figure 2.1: Traditional process automation architecture.

A distinct separation between economic optimization and regulatory control enables the upper level to be tuned for economics, and the lower level to be tuned for stability and tracking performance. At the upper-level, plantwide real-time optimization (RTO) optimizes plant economics at a low execution frequency, typically in the order of hours, in response to slow-varying disturbances and economic-driven factors. RTO interacts with the lower-level process automation activities in a cascade fashion by providing economically optimal operating targets (or set-points) to the underlying regulatory control system. Beneath RTO is typically model predictive control (MPC) as an advanced, multivariable control strategy that optimizes control performance by tracking the set-points while rejecting higher frequency disturbances. Most industrial applications use a high fidelity, fundamental nonlinear steady-state process model in the RTO formulation [1, 2]. On the other hand, industrial MPC systems are largely based on linear empirical dynamic models built using plant data [3, 4]. Depending on process and operational requirements, some industrial installations consider a centralized MPC control system, and others utilize a distributed MPC environment. The two-layer approach is considered as robust

for industrial applications due to its multilayer reliability (in the event of convergence or execution failures), accessibility for human supervision, and maintenance flexibility [4, 5, 6].

Key drawbacks cited concerning the traditional RTO approach are model inconsistency between the RTO and control layers, and the requirement for the system to reach steady-state conditions before the execution of the next optimization calculation[6]. The steady-state requirement may result in suboptimal operation for processes that exhibit slow dynamics, experience frequent transitions, or are continuously perturbed by disturbances. An early attempt to narrow the gap between RTO and MPC is to use a steady-state local economic optimizer, formulated as a linear program (LP) or quadratic program (QP) [3] whose function is to track the plant economic optimum and to provide feasible set-points for the MPC. Since process disturbances may cause the plant economic optimum to shift between long RTO intervals, the LP (or QP) optimizer updates the operating targets computed by the RTO system using current feedback information between RTO executions. The LP (or QP) optimizer typically utilizes a steady-state model consistent with the dynamic MPC model and is executed at the same frequency as the MPC. The local optimizer objective function may involve minimization of the (squared) deviation of the MPC set-points from the RTO targets or optimization of an economic criterion directly. The performance and stability of the two-stage LP- and QP-MPC configurations are analyzed in Ying and Joseph [7], and the sensitivity of the LP-MPC system to its model bias update parameters is studied in Nikandrov and Swartz [8].

A more recent approach in the context of the two-layer process automation architecture replaces the steady-state prediction model used at the upper-level economic optimization with a dynamic prediction model, hence transforming the steady-state RTO to dynamic RTO (DRTO). The key incentive for such a transformation is that dynamic models allow for a more frequent reoptimization of plant economics without the need to wait for the plant to stabilize at a steady-state. The output from the DRTO calculation is a set of operating reference trajectories, instead of the steady-state operating targets. This approach mainly benefits processes that experience frequent transitions, for example those in bioprocess [9] and polymerization [10] industries, and also processes that exhibit long transient dynamics such as integrated plants with recycle streams [11]. The DRTO prediction horizon should be sufficiently long to capture the effects of the plant response dynamics on the process economics. Tosukhowong et al. [11] propose a DRTO framework that utilizes a reduced-order linear dynamic model designed to capture the slow plant dynamics, with local MPC controllers implemented for higher frequency trajectory tracking. The DRTO calculation frequency is lower than that of the MPC controllers, and determined through examination of the system eigenvalues. Set-points for the local MPCs are derived from the DRTO trajectories by solving a least-squares coordination problem. Kadam et al. [12] propose a two-level DRTO architecture in which the execution of the DRTO calculation is triggered based on a disturbance sensitivity analysis of the computed reference trajectories. Würth et al. [10] propose a neighboring-extremal MPC strategy for the inner controller, designed to provide

fast updates to the economic-based control trajectories. The algorithm includes time scale separation of the disturbances and consideration of the computational delay.

An alternative to the two-layer architecture is a single-layer economic MPC (EMPC) that merges the RTO and MPC layers into a unified framework, aimed at addressing issues of conflicting objectives and model inconsistencies associated with the traditional two-layer architecture. In this approach, the dynamic optimization problem may be formulated with a purely economic objective function [13], or consider a hybrid objective of plant economics and control tracking weighted with appropriate tuning parameters [13, 14]. Amrit et al. [15] present an EMPC formulation that guarantees stability through application of a terminal constraint region or modification of the regulator cost function. Ellis and Christofides [16] design a Lypunov-based economic MPC (LEMPC) of nonlinear dynamic systems, formulated with a time-varying economic cost function. A union of steady-state stability regions is included as part of the problem constraints, although generation of the union stability region is not trivial for complex dynamic systems. Omell and Chmielewski [17] design an infinite horizon EMPC (IH-EMPC) control strategy for application to integrated gasification combined cycle (IGCC) power plants. A convex optimization problem is solved to determine the gain of an economic linear optimal control (ELOC) policy, which is used to generate weighting matrices for an infinite horizon MPC that takes the form of a QP problem. The IH-EMPC problem is formulated as a constrained QP problem with a terminal cost based on the concept of inverse optimality of an economic-based linear optimal control (ELOC) policy. The algorithm described in Chong and Swartz [18] for optimal control under partial plant shutdown conditions constitutes an EMPC approach. Here, each control calculation involves the solution of a sequence of dynamic optimization problems based on prioritization of multiple objectives.

The proposed single-layer EMPC approaches often do not completely eliminate the economic optimization layer, because the terminal constraint that enforces stability [19], the terminal penalty [19] or the control tracking term in the hybrid economic objective function [14, 16] of the dynamic optimization problem would still require specific operating targets that are usually computed by an economic optimizer. A further challenge associated with the single-level EMPC approach is that computation of the control input may be prohibitive for a sufficiently small sample time for rejection of high frequency disturbances and a sufficiently long prediction horizon to capture longer term economic impacts [6]. However, advances in computational strategies and tools for large-scale dynamic optimization, together with strategies for fast control move updates based on NLP sensitivity information [20, 21] are promising developments toward addressing potential computational bottlenecks. A review of approaches to optimal process operation using feedback is given in Engell[6], while a recent review on EMPC is provided in Ellis et al. [22].

We briefly discuss closed-loop prediction, which is a key feature of the formulation proposed in

this article. The concept of closed-loop prediction has been widely considered in the area of robust MPC [23]. The idea is to account for the effect of feedback action in the propagation of uncertainty in the future response. Lee and Yu [24] describe a dynamic programming approach via Bellman's principle of optimality to account for the feedback mechanism in the closed-loop prediction of a robust min-max MPC formulation that minimizes the worst case cost of uncertain model parameters; but the proposed optimization Kothare et al. [25] and Kouvaritakis et al. [26] develop robust MPC algorithms where the closed-loop predictions are approximated using affine state-feedback control laws without consideration of control input saturation. Sakizlis et al. [27] design robust predictive controllers using a parametric programming formulation. Such an approach performs closed-loop prediction through the inclusion of explicit control laws derived as piecewise affine functions of the state variables constructed offline during the control design stage. Li and Marlin [28] develop a robust MPC approach where the future closed-loop behavior is formulated as a bilevel program. Stochastic uncertainty is considered and chance constraints applied, with control input saturation handled through a clipping technique following the dynamic matrix control (DMC) heuristic. Mastragostino et al. [29] develop a robust MPC approach for supply chain operation where the closed-loop prediction of uncertainty propagation is approximated by following a scenario-based, two-stage stochastic programming approach.

In this chapter, we consider DRTO applied to a continuous process operation regulated under constrained MPC, and follow the two-layer configuration due to its closer tie to the hierarchical industrial process automation architecture. DRTO strategies that have been proposed in the literature typically optimize plant economics utilizing an open-loop prediction of plant response dynamics in which the economic optimization formulations at the upper level do not take into account the presence of the control system functioning in the plant. We denote such formulation approaches as an open-loop DRTO (OL-DRTO) strategy. Here, we propose a closed-loop DRTO (CL-DRTO) strategy that optimizes the economics of the predicted closed-loop response dynamics of the process. The DRTO problem takes the form of a multilevel dynamic optimization problem due to the presence of a MPC optimization subproblem at every sample time over the DRTO prediction horizon in order to generate closed-loop response dynamics. In the CL-DRTO formulation, the MPC set-point trajectories are the primary decision variables as opposed to the process input trajectories computed in the OL-DRTO formulation.

The multilevel programming formulation considered in this study was originally proposed in Baker and Swartz [30] for optimal backoff calculations of steady-state operating targets, while an extension of their work is presented in Lam et al. [31] for reference trajectory optimization of MPC-controlled processes. Here we provide in-depth analysis on the inclusion of MPC closed-loop dynamics in the DRTO calculations, and identify conditions under of which the CL-DRTO strategy most significantly outperforms the conventional open-loop counterpart. The remainder of this chapter is organized as follows. In the next section, we describe the two-layer process automation architecture considered in this study. This is followed by the mathematical formulations that describe the dynamic optimization

problems, a solution strategy to the multilevel programming problem, and a derivation of the economic objective function used for optimization of product grade transitions. Performance analysis of the CL- and OL-DRTO strategies is carried out under various process conditions and linear dynamic plant characteristics, and the application of the proposed CL-DRTO approach to a nonlinear polymer grade transition case study is also demonstrated. Finally, concluding remarks and future research plans are presented.

2.2 Problem Formulation

2.2.1 Two-layer Architecture

A schematic of the two-layer CL-DRTO configuration considered in this study is shown in Figure 2.2. Both the DRTO and MPC levels are implemented based on a moving horizon approach with a time-scale separation between them, which also implies that there are multiple MPC executions within a given DRTO interval.

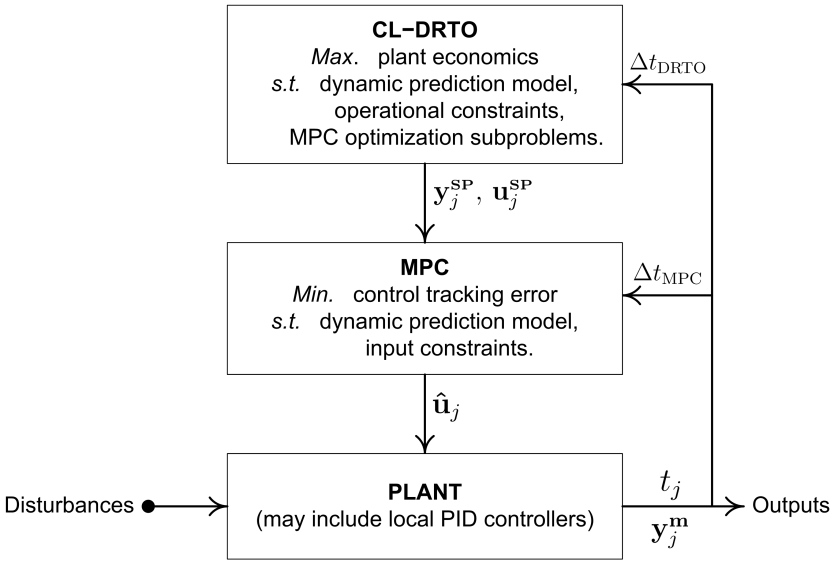

Figure 2.2: CL-DRTO configuration.

At the DRTO level, economic optimization is performed using the predicted closed-loop response dynamics of the process, and is executed at a slower sampling rate than the MPC loop. Closed-loop prediction is obtained from rigorous inclusion of the future MPC control calculations in which the corresponding optimization formulations and tuning parameters are consistent with the actual MPC controller implemented at the lower level. The CL-DRTO formulation computes the controller set-point

trajectories that determine the best economics based on the closed-loop prediction, under an assumption that the process follows the trajectory calculated by the embedded MPC optimization subproblems until the next DRTO execution. The MPC level utilizes an industrial type, input-constrained predictive controller. The plant level generally consists of a continuous process operation, local PID controllers, final control elements and sensors. Output feedback $\mathbf{y}_j^{\mathbf{m}}$ from the plant measurement is used to compute a MPC disturbance estimate which is also used at the DRTO level. The implementation strategy is as follows: at a time instance t_j of every DRTO execution interval Δt_{DRTO}, the DRTO receives feedback information and performs economic optimization to compute the set-point trajectories, $\mathbf{y}_j^{\mathbf{SP}}$ and possibly also $\mathbf{u}_j^{\mathbf{SP}}$, to be prescribed to the MPC level. The MPC tracks the set-point trajectories at a smaller time interval than that of the DRTO. It computes the optimal control inputs, $\hat{\mathbf{u}}_j$, at every controller sampling interval Δt_{MPC} to be issued to the final control elements or as set-points to local PID controllers for plant implementation.

In the absence of modeling error, disturbances and measurement noise, the MPC level computes exactly the same control trajectory as the one obtained from the first MPC control subproblem embedded at the DRTO level because the MPC calculation at the lower level is a subset of the CL-DRTO problem at the upper level. Therefore, the proposed CL-DRTO approach itself may be viewed as a single-layer EMPC approach if it is executed at the controller sampling frequency. However, the CL-DRTO approach has the flexibility to be implemented less frequently at the supervisory level, with controller set-point trajectories as the primary decision variables of the economic optimization problem. This allows the existing process automation architecture to be unaltered, and the higher frequency control calculation remains less complex and computationally inexpensive. We remark here that the two-layer CL-DRTO/MPC configuration can be considered as a cascade MPC scheme, with a primary EMPC controller providing set-points to a secondary, regulatory MPC system. The two-layer architecture with an OL-DRTO strategy also utilizes the configuration in Figure 2, except that there is no MPC optimization subproblem embedded in the upper level DRTO formulation.

2.2.2 MPC

In this study, we consider an input-constrained MPC based on a state-space formulation [32], with the general optimization problem solved at each sample time j taking the form:

$$\begin{aligned}
\min_{\hat{\mathbf{u}}_{j,k}} \phi_j := & \sum_{k=1}^{p} (\hat{\mathbf{y}}_{j,k} - \mathbf{y}^{\mathbf{SP}}_{j,k})^{\mathrm{T}} Q (\hat{\mathbf{y}}_{j,k} - \mathbf{y}^{\mathbf{SP}}_{j,k}) + \sum_{k=0}^{m-1} \Delta\hat{\mathbf{u}}^{\mathrm{T}}_{j,k} R \Delta\hat{\mathbf{u}}_{j,k} \\
& + \sum_{k=0}^{m-1} (\hat{\mathbf{u}}_{j,k} - \mathbf{u}^{\mathbf{SP}}_{j,k})^{\mathrm{T}} S (\hat{\mathbf{u}}_{j,k} - \mathbf{u}^{\mathbf{SP}}_{j,k}) \\
s.t. \quad & \hat{\mathbf{x}}_{j,k+1} = A\hat{\mathbf{x}}_{j,k} + B\hat{\mathbf{u}}_{j,k}, \quad k = 0, \ldots, m-1 \\
& \hat{\mathbf{x}}_{j,k+1} = A\hat{\mathbf{x}}_{j,k} + B\hat{\mathbf{u}}_{j,m-1}, \quad k = m, \ldots, p-1 \\
& \hat{\mathbf{y}}_{j,k} = C\hat{\mathbf{x}}_{j,k} + \hat{\mathbf{d}}_{j,k}, \quad k = 1, \ldots, p \\
& \Delta\hat{\mathbf{u}}_{j,k} = \hat{\mathbf{u}}_{j,k} - \hat{\mathbf{u}}_{j,k-1}, \quad k = 0, \ldots, m-1 \\
& \mathbf{u}_{\min} \leq \hat{\mathbf{u}}_{j,k} \leq \mathbf{u}_{\max}, \quad k = 0, \ldots, m-1
\end{aligned} \tag{2.1}$$

where $\hat{\mathbf{x}} \in \Re^{n_x}$ is a vector of predicted states and $\hat{\mathbf{y}} \in \Re^{n_y}$ is a corresponding vector of the predicted outputs over a prediction horizon p; $\hat{\mathbf{u}} \in \Re^{n_u}$ is a vector of predicted inputs over a control horizon m; $\hat{\mathbf{d}} \in \Re^{n_y}$ is a vector of disturbance estimates for output correction; $\mathbf{y}^{\mathbf{SP}} \in \Re^{n_y}$ and $\mathbf{u}^{\mathbf{SP}} \in \Re^{n_u}$ are vectors of set-point trajectories for the controlled outputs and manipulated inputs; Q, R and S are diagonal positive semidefinite weighting matrices on the output tracking, move suppression penalty, and control tracking in the objective function, respectively. $A \in \Re^{n_x \times n_x}$, $B \in \Re^{n_x \times n_u}$ and $C \in \Re^{n_y \times n_x}$ are linear(ized), discrete-time, state-space matrices; $\mathbf{u}_{\min}$ and $\mathbf{u}_{\max}$ are lower and upper bounds on the manipulated inputs, respectively. $\hat{\mathbf{y}}_{j,k}$ represents the predicted value of the outputs over horizon $k \in [1, \ldots, p]$ based on information available at sample time j.

The disturbance estimate, as proposed in the original DMC and QDMC algorithms [33, 34], is computed as the difference between the current measured outputs and predicted outputs based on the information available at the previous sample time, and is assumed constant over the prediction horizon. The corresponding equations are:

$$\hat{\mathbf{d}}_j = \mathbf{y}^{\mathbf{m}}_j - C\hat{\mathbf{x}}_{j-1,1} \tag{2.2a}$$

$$\hat{\mathbf{d}}_{j,k} = \hat{\mathbf{d}}_j, \quad k = 1, \ldots, p \tag{2.2b}$$

where $\mathbf{y}^{\mathbf{m}}_j$ is the set of measured outputs at current time step j. To compute $\Delta\hat{\mathbf{u}}_{j,0}$, the previously

implemented manipulated input vector $\hat{\mathbf{u}}_{j-1}$ is written in the above formulation as $\hat{\mathbf{u}}_{j,-1}$ and given by:

$$\hat{\mathbf{u}}_{j,-1} = \hat{\mathbf{u}}_{j-1,0} \tag{2.3}$$

The predicted states at sampling instance j may be obtained from:

$$\hat{\mathbf{x}}_{j,0} = \hat{\mathbf{x}}_{j-1,1} \tag{2.4a}$$

$$= A\hat{\mathbf{x}}_{j-1,0} + B\hat{\mathbf{u}}_{j-1,0} \tag{2.4b}$$

This DMC output disturbance estimation scheme is also equivalent to a state observer under the assumptions of a constant disturbance applied on the predicted outputs, and no measurement noise, as discussed in Maciejowski [32] and Lee et al. [35]. The observer model is a composite of the plant model and output disturbance model, with the augmented state vector composed of the plant and disturbance predictions. The observer gain is a combination of zeros and the identity matrix with respect to the plant and disturbance predictions.

Remarks

1. The MPC formulation Eq. (2.1) could be transformed to a standard quadratic programming (QP) formulation with $\boldsymbol{\Delta}\hat{\mathbf{u}}_{j,k}$ being the decision variables, as shown in Maciejowski [32]. Although this results in a compact QP problem of smaller dimension, it also involves the computation of matrix powers, A^i, which for large prediction horizons could lead to numerical problems [32]. Therefore, we use the direct form of the model equations as stated in Eq. (2.1).

2. The DRTO approach presented in this article is not restricted to a particular MPC formulation. Other MPC formulations, such as those that include terminal constraints [36] are readily accomodated by making corresponding modifications to the first-order optimality conditions of the MPC optimization subproblems presented later.

3. The control tracking term in the MPC cost function could be useful for nonsquare systems where the number of manipulated inputs exceeds the number controlled outputs, that is, ideal resting values (IRVs) [3] may be required for some of the manipulated inputs to generate a unique solution to the control problem. Control input set-points, $\mathbf{u}_{j,k}^{\mathbf{SP}}$, for the IRVs are usually computed by a plant economic optimizer.

4. While input constraints for physical limitations, such as control valve opening, can be simply included in the MPC formulation, the inclusion of output constraints, such as those arising from economic, safety and environmental considerations, could lead to closed-loop instability [37]

or infeasible QP problems [3], and are often avoided in practice. We impose them instead at the upper level DRTO formulation; they are indirectly applied at the regulatory level through appropriate set-point calculation.

2.2.3 OL–DRTO

We formulate the OL-DRTO problem similar to the formulations reported in the literature [9, 10, 11]. The objective is to minimize an economic cost, and the control input trajectory is optimized based on the predicted open-loop response dynamics of the process. For a discrete-time dynamic system, the OL-DRTO formulation may be written as:

$$\begin{aligned} &\min_{\hat{\mathbf{u}}^{\mathbf{DRTO}}} \Phi^{\mathrm{Econ}}(\hat{\mathbf{x}}^{\mathbf{DRTO}},\ \hat{\mathbf{y}}^{\mathbf{DRTO}},\ \hat{\mathbf{u}}^{\mathbf{DRTO}}) \\ s.t.\quad &\hat{\mathbf{x}}^{\mathbf{DRTO}}_{j+1} = \mathbf{f}^{\mathbf{DRTO}}(\hat{\mathbf{x}}^{\mathbf{DRTO}}_{j}, \hat{\mathbf{u}}^{\mathbf{DRTO}}_{j}), \qquad j = 0,\ldots,N-1 \\ &\hat{\mathbf{y}}^{\mathbf{DRTO}}_{j} = \mathbf{h}^{\mathbf{DRTO}}(\hat{\mathbf{x}}^{\mathbf{DRTO}}_{j}), \qquad j = 1,\ldots,N \\ &\mathbf{0} \leq \mathbf{g}^{\mathbf{DRTO}}(\hat{\mathbf{x}}^{\mathbf{DRTO}}_{j},\ \hat{\mathbf{y}}^{\mathbf{DRTO}}_{j},\ \hat{\mathbf{u}}^{\mathbf{DRTO}}_{j}), \qquad j = 0,\ldots,N \\ &\mathbf{0} = \mathbf{h}^{\mathbf{Fix}}(\hat{\mathbf{u}}^{\mathbf{DRTO}}) \end{aligned} \tag{2.5}$$

where $\hat{\mathbf{x}}^{\mathbf{DRTO}}_{j} \in \Re^{n_x}$ is a vector of DRTO model states, $\hat{\mathbf{y}}^{\mathbf{DRTO}}_{j} \in \Re^{n_y}$ is a corresponding vector of DRTO model outputs, and $\hat{\mathbf{u}}^{\mathbf{DRTO}}_{j} \in \Re^{n_u}$ is a vector of DRTO inputs. $\hat{\mathbf{u}}^{\mathbf{DRTO}}$, $\hat{\mathbf{x}}^{\mathbf{DRTO}}$ and $\hat{\mathbf{y}}^{\mathbf{DRTO}}$ are composite vectors comprising all the DRTO inputs, states and outputs over the optimization horizon $j \in [0,\ldots,N-1]$:

$$\begin{aligned} \hat{\mathbf{u}}^{\mathbf{DRTO}} &= \left[(\hat{\mathbf{u}}^{\mathbf{DRTO}}_{0})^{\mathrm{T}},\ (\hat{\mathbf{u}}^{\mathbf{DRTO}}_{1})^{\mathrm{T}},\ldots,(\hat{\mathbf{u}}^{\mathbf{DRTO}}_{N-1})^{\mathrm{T}}\right]^{\mathrm{T}} \\ \hat{\mathbf{x}}^{\mathbf{DRTO}} &= \left[(\hat{\mathbf{x}}^{\mathbf{DRTO}}_{1})^{\mathrm{T}},\ (\hat{\mathbf{x}}^{\mathbf{DRTO}}_{2})^{\mathrm{T}},\ldots,(\hat{\mathbf{x}}^{\mathbf{DRTO}}_{N})^{\mathrm{T}}\right]^{\mathrm{T}} \\ \hat{\mathbf{y}}^{\mathbf{DRTO}} &= \left[(\hat{\mathbf{y}}^{\mathbf{DRTO}}_{1})^{\mathrm{T}},\ (\hat{\mathbf{y}}^{\mathbf{DRTO}}_{2})^{\mathrm{T}},\ldots,(\hat{\mathbf{y}}^{\mathbf{DRTO}}_{N})^{\mathrm{T}}\right]^{\mathrm{T}} \end{aligned}$$

Φ^{Econ} is an economic objective function, $\mathbf{f}^{\mathbf{DRTO}}$ represents the dynamic model utilized for DRTO prediction, $\mathbf{h}^{\mathbf{DRTO}}$ are constraints that relate the states to the outputs, and $\mathbf{g}^{\mathbf{DRTO}}$ comprises inequality constraints on the inputs, outputs and possibly some of the states. Equality $\mathbf{h}^{\mathbf{Fix}}$ may be used to fix the input trajectory as piecewise constants over each DRTO interval, for instance, in cases where input set-points are required for the underlying controller.

In the OL-DRTO strategy, the reference trajectories are constructed based on the resulting optimal open-loop trajectories, with the outputs at the end of each DRTO interval used as the reference points

for all MPC sample intervals contained within it. At the MPC layer, the selection of these reference trajectories for controller set-point tracking is shifted in time following the MPC moving horizon window, and new reference trajectories will be issued at the subsequent DRTO calculation.

2.2.4 CL–DRTO

We propose a CL-DRTO approach with rigorous inclusion of the future MPC control calculations, which for constrained MPC cannot be expressed as an explicit function to be included in the algebraic constraints, such as P-control or unconstrained MPC. The overall CL-DRTO problem structure is in the form of a multilevel dynamic optimization problem with embedded MPC optimization subproblems in order to generate the closed-loop response dynamics, as illustrated in Figure 2.3.

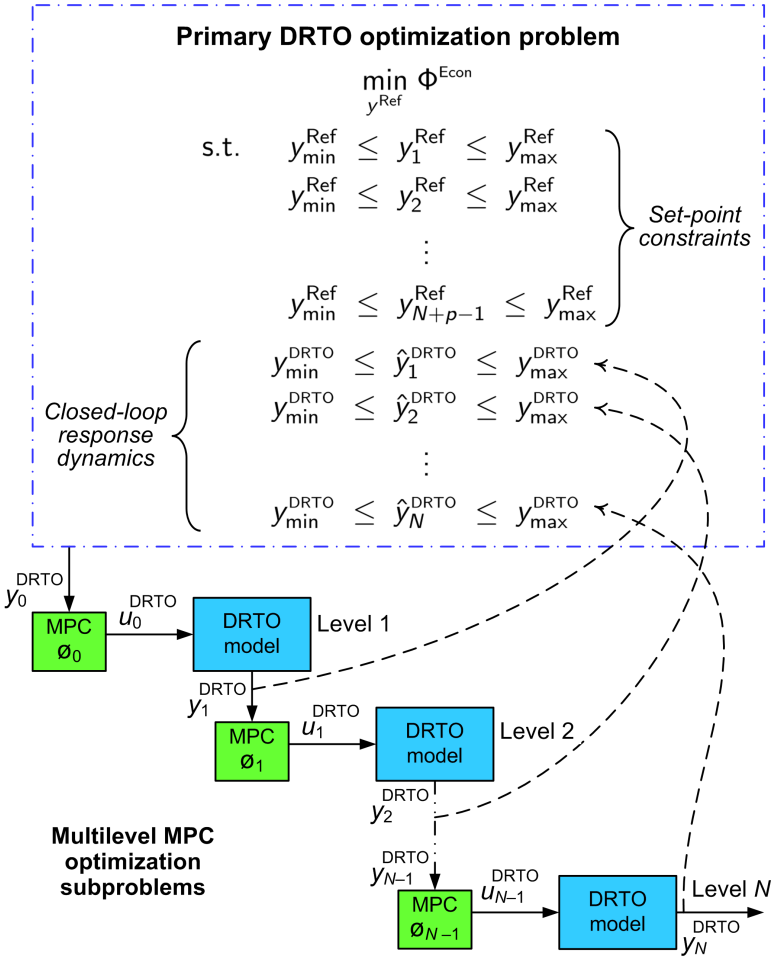

Figure 2.3: Illustration of the multilevel dynamic optimization problem.

Interaction between the primary DRTO optimization problem and the inner MPC optimization sub-

problems occurs in a bidirectional way. The DRTO provides an internal dynamic model of the process to generate plant outputs required by the MPC subproblems at each DRTO prediction step, and the MPC subproblems provide an optimal control input vector to the DRTO model.

Mathematically, we have a primary DRTO optimization problem Eq. (2.6a) that computes controller reference trajectories that determine the best economics over a finite DRTO optimization horizon, N. The primary DRTO optimization problem requires a sequence of MPC controller optimization subproblems Eq. (2.6b), corresponding to the MPC formulation given in Eq. (2.1) to compute the optimal control input trajectories. The subproblem indices $j = 1, \ldots, N-1$ in Eq. (2.6b) correspond to the sequence of MPC optimization blocks shown in Figure 2.3. The first control move from each MPC subproblem solution is applied in the primary DRTO optimization problem to predict the closed-loop response dynamics for economic optimization. Constraints on the outputs and reference trajectories are imposed at the primary DRTO problem, whereas input constraints are addressed by the inner MPC subproblems. The DRTO problem is stated as follows.

$$
\begin{aligned}
&\min_{\mathbf{y}^{\mathbf{Ref}},\, \mathbf{u}^{\mathbf{Ref}}} \Phi^{\text{Econ}}(\hat{\mathbf{x}}^{\mathbf{DRTO}},\ \hat{\mathbf{y}}^{\mathbf{DRTO}},\ \hat{\mathbf{u}}^{\mathbf{DRTO}}) \\
s.t.\quad & \hat{\mathbf{x}}^{\mathbf{DRTO}}_{j+1} = \mathbf{f}^{\mathbf{DRTO}}(\hat{\mathbf{x}}^{\mathbf{DRTO}}_{j},\ \hat{\mathbf{u}}^{\mathbf{DRTO}}_{j}), \quad j = 0, \ldots, N-1 \\
& \hat{\mathbf{y}}^{\mathbf{DRTO}}_{j} = \mathbf{h}^{\mathbf{DRTO}}(\hat{\mathbf{x}}^{\mathbf{DRTO}}_{j}), \quad j = 1, \ldots, N \\
& \mathbf{0} \le \mathbf{g}^{\mathbf{DRTO}}(\hat{\mathbf{x}}^{\mathbf{DRTO}}_{j},\ \hat{\mathbf{y}}^{\mathbf{DRTO}}_{j}), \quad j = 1, \ldots, N \\
& \mathbf{0} = \mathbf{h}^{\mathbf{Ref}}(\mathbf{y}^{\mathbf{Ref}},\ \mathbf{u}^{\mathbf{Ref}},\ \mathbf{y}^{\mathbf{SP}},\ \mathbf{u}^{\mathbf{SP}}) \\
& \mathbf{0} \le \mathbf{g}^{\mathbf{Ref}}(\mathbf{y}^{\mathbf{Ref}}_{j+1},\ \mathbf{u}^{\mathbf{Ref}}_{j}), \quad j = 0, \ldots, N-1 \\
& \hat{\mathbf{u}}^{\mathbf{DRTO}}_{j} = \hat{\mathbf{u}}_{j,0}, \quad j = 0, \ldots, N-1 \\
& \hat{\mathbf{d}}_{0,k} = \mathbf{y}^{\mathbf{m}}_{j^*} - C\hat{\mathbf{x}}_{j^*-1,1} \\
& \hat{\mathbf{d}}_{j,k} = \hat{\mathbf{y}}^{\mathbf{DRTO}}_{j} - C\hat{\mathbf{x}}_{j-1,1}, \quad j = 1, \ldots, N-1, \quad k = 1, \ldots, p \\
& \hat{\mathbf{u}}_{j,0} \in \arg\min_{\hat{\mathbf{u}}_{j,k}} \phi_j := \textstyle\sum_{k=1}^{p} (\hat{\mathbf{y}}_{j,k} - \mathbf{y}^{\mathbf{SP}}_{j,k})^{\mathrm{T}} Q (\hat{\mathbf{y}}_{j,k} - \mathbf{y}^{\mathbf{SP}}_{j,k}) + \sum_{k=0}^{m-1} \boldsymbol{\Delta}\hat{\mathbf{u}}_{j,k}^{\mathrm{T}} R \boldsymbol{\Delta}\hat{\mathbf{u}}_{j,k} \\
& \qquad\qquad + \textstyle\sum_{k=0}^{m-1} (\hat{\mathbf{u}}_{j,k} - \mathbf{u}^{\mathbf{SP}}_{j,k})^{\mathrm{T}} S (\hat{\mathbf{u}}_{j,k} - \mathbf{u}^{\mathbf{SP}}_{j,k}) \\
& \qquad s.t. \quad \hat{\mathbf{x}}_{j,k+1} = A\hat{\mathbf{x}}_{j,k} + B\hat{\mathbf{u}}_{j,k}, \quad k = 0, \ldots, m-1 \\
& \qquad\qquad \hat{\mathbf{x}}_{j,k+1} = A\hat{\mathbf{x}}_{j,k} + B\hat{\mathbf{u}}_{j,m-1}, \quad k = m, \ldots, p-1 \\
& \qquad\qquad \hat{\mathbf{y}}_{j,k} = C\hat{\mathbf{x}}_{j,k} + \hat{\mathbf{d}}_{j,k}, \quad k = 1, \ldots, p \\
& \qquad\qquad \boldsymbol{\Delta}\hat{\mathbf{u}}_{j,k} = \hat{\mathbf{u}}_{j,k} - \hat{\mathbf{u}}_{j,k-1}, \quad k = 0, \ldots, m-1 \\
& \qquad\qquad \mathbf{u}_{\min} \le \hat{\mathbf{u}}_{j,k} \le \mathbf{u}_{\max}, \quad k = 0, \ldots, m-1
\end{aligned}
\qquad \left.\begin{array}{l} \\ \\ \\ \\ \\ \\ \\ \\ \\ \\ \\ \end{array}\right\} \begin{array}{l}\text{MPC}\\ \text{subproblems,}\\ j = 0, \ldots, N-1\end{array}
\tag{2.6a, 2.6b}
$$

where $\hat{\mathbf{x}}_j^{\mathbf{DRTO}}$, $\hat{\mathbf{y}}_j^{\mathbf{DRTO}}$, $\hat{\mathbf{u}}_j^{\mathbf{DRTO}}$, $\hat{\mathbf{x}}^{\mathbf{DRTO}}$, $\hat{\mathbf{y}}^{\mathbf{DRTO}}$, $\hat{\mathbf{u}}^{\mathbf{DRTO}}$, Φ^{Econ}, $\mathbf{f}^{\mathbf{DRTO}}$ and $\mathbf{h}^{\mathbf{DRTO}}$ are similarly defined as in the previous section. Inequality $\mathbf{g}^{\mathbf{DRTO}}$ consists of constraints on the outputs and possibly some of the states. Note that input constraints are not imposed at the primary DRTO optimization problem, but they addressed by the input-constrained MPC optimization subproblems. The time index j corresponds to the MPC sample interval.

Variables $\mathbf{y}_{j,k}^{\mathbf{SP}}$ and $\mathbf{u}_{j,k}^{\mathbf{SP}}$ represent set-point trajectories of MPC subproblem j, and are extracted from the DRTO reference trajectories, $\mathbf{y}^{\mathbf{Ref}}$ and $\mathbf{u}^{\mathbf{Ref}}$. Equality $\mathbf{h}^{\mathbf{Ref}}$ enforces the reference trajectories to be constant for every DRTO interval within the optimization horizon, and also defines the relationship between the overall reference trajectories and the set-point trajectories for the MPC optimization subproblems (described in more detail later). Inequality $\mathbf{g}^{\mathbf{Ref}}$ defines the upper and lower bounds of the reference trajectories.

$\hat{\mathbf{d}}_{0,k}$ defines the disturbance estimate of the MPC subproblem at DRTO prediction step $j = 0$, which is computed based on the output measurement $(\mathbf{y}_{j^*}^{\mathbf{m}})$ at the current time instance t_{j^*}, and the output prediction at the previous controller sampling instance. Index j^* is used to denote the current time step, as opposed to j which represents the time indices corresponding to the MPC subproblems internal to the DRTO optimization framework. $\hat{\mathbf{x}}_{j^*-1,1}$ is a state prediction obtained from the lower level MPC calculation at the previous sampling instance (t_{j^*-1}), and is utilized to compute disturbance estimate of the first MPC subproblem at the DRTO prediction step $j = 0$. On the other hand, $\hat{\mathbf{x}}_{j-1,1}$ are state predictions of the embedded MPC subproblems within the DRTO prediction horizon, and are utilized to compute disturbance estimate of the remaining MPC subproblems.

In this study, the DRTO and MPC prediction models are consistent, and output feedback to the primary DRTO optimization problem Eq. (2.6a) occurs through the model bias update mechanism, described in Eqs. (2.2a) and (2.2b), for the first MPC subproblem. Initialization of the states in the primary DRTO problem and MPC optimization subproblems is performed in the same fashion as the standard MPC algorithm described in Eqs. (2.4a) and (2.4b). The DRTO closed-loop prediction is performed through implementation of the first vector of the MPC input trajectory from each MPC optimization subproblem.

At each DRTO prediction step, the MPC optimization subproblem will select a subset of the overall reference trajectories, $\mathbf{y}^{\mathbf{Ref}}$ and $\mathbf{u}^{\mathbf{Ref}}$, computed by the primary DRTO optimization problem for the purpose of set-point tracking. $\mathbf{y}^{\mathbf{Ref}}$ and $\mathbf{u}^{\mathbf{Ref}}$ are composite vectors comprising the output and input reference trajectories for the MPC subproblems embedded over the optimization horizon, extended to provide set-point trajectories for MPC subproblems in the latter part of the DRTO horizon:

$$\mathbf{y}^{\mathbf{Ref}} = \left[(\mathbf{y}_1^{\mathbf{Ref}})^{\mathrm{T}},\ (\mathbf{y}_2^{\mathbf{Ref}})^{\mathrm{T}}, \ldots, (\mathbf{y}_{N+p-1}^{\mathbf{Ref}})^{\mathrm{T}} \right]^{\mathrm{T}}$$
$$\mathbf{u}^{\mathbf{Ref}} = \left[(\mathbf{u}_0^{\mathbf{Ref}})^{\mathrm{T}},\ (\mathbf{u}_1^{\mathbf{Ref}})^{\mathrm{T}}, \ldots, (\mathbf{u}_{N+m-2}^{\mathbf{Ref}})^{\mathrm{T}} \right]^{\mathrm{T}}$$

The reference trajectories beyond the DRTO prediction horizon, $j \in [0, \ldots, N-1]$, are kept constant at the last values ($\mathbf{y}_N^{\mathbf{Ref}}$ and $\mathbf{u}_{N-1}^{\mathbf{Ref}}$ respectively for the output and input reference trajectories). Over the optimization horizon, the selection of the reference trajectories to become the inner MPC set-point trajectories is shifted in time to account for the moving horizon window of the MPC controller, as illustrated in Figure 2.4. This mechanism can be mathematically written as follows:

$$\mathbf{y}_{j,k}^{\mathbf{SP}} = \mathbf{y}_{j+k}^{\mathbf{Ref}} \qquad j = 0, \ldots, N-1\ ,\ \ k = 1, \ldots, p$$
$$\mathbf{u}_{j,k}^{\mathbf{SP}} = \mathbf{u}_{j+k}^{\mathbf{Ref}} \qquad j = 0, \ldots, N-1\ ,\ \ k = 0, \ldots, m-1$$

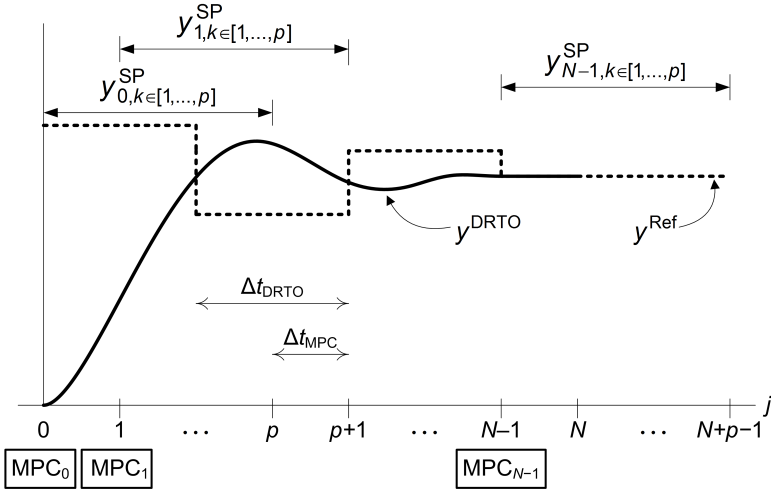

Figure 2.4: Illustration of set-point selection by the inner MPC subproblems.

where $\mathbf{y}_{j,k}^{\mathbf{SP}}$ and $\mathbf{u}_{j,k}^{\mathbf{SP}}$ are the tracking set-points for the output and input at MPC prediction step k, which corresponds to an MPC optimization subproblem embedded at DRTO prediction step j. $\mathbf{y}_{j,k}^{\mathbf{SP}}$ and $\mathbf{u}_{j,k}^{\mathbf{SP}}$ are concatenated into composite vectors $\mathbf{y}^{\mathbf{SP}}$ and $\mathbf{u}^{\mathbf{SP}}$, respectively, used in constraint $\mathbf{h}^{\mathbf{Ref}}$. The reference trajectories are held constant based on the DRTO sampling interval, which is an integer multiple of the MPC sampling interval, using equality constraints to provide consistency with the OL-DRTO formulation in constructing the reference trajectories. Implementation of the reference trajectories on the actual plant follows the same procedures as illustrated in Figure 2.4 until new updates are available at the subsequent DRTO calculation.

2.2.5 Solution Strategy

Closed-loop Problem Reformulation

One possible method to solve a multilevel programming problem is to use a sequential solution approach in which the primary DRTO optimization problem and a closed-loop simulation involving the MPC optimization subproblems are solved iteratively until convergence to an optimum. A potential drawback of such an approach is the presence of derivative discontinuities at the primary DRTO optimization problem induced by input constraints of the MPC optimization subproblems whenever control saturation occurs, which may hinder convergence of the NLP iterations. We consequently follow instead a simultaneous solution approach that involves replacement of the MPC optimization subproblems with algebraic equations corresponding to their equivalent first-order, Karush-Kuhn-Tucker (KKT) optimality conditions [30]. For a constrained MPC problem formulated as a convex QP problem considered in this study, such a transformation is both necessary and sufficient for optimality of the MPC optimization subproblems. This reformulates the original multilevel dynamic optimization problem as a single-level mathematical program with complementarity constraints (MPCC), hence permitting simultaneous convergence of the primary DRTO optimization problem and the MPC optimization subproblems. Such a reformulation approach is valid for a vast majority of MPC approaches that utilize a quadratic cost function and a linear prediction model.

The Lagrangian of the MPC optimization subproblems at each DRTO prediction step j may be written as:

$$\begin{aligned}
\mathcal{L}_j = &\sum_{k=1}^{p} (\hat{\mathbf{y}}_{j,k} - \mathbf{y}_{j,k}^{\mathbf{SP}})^{\mathrm{T}} Q (\hat{\mathbf{y}}_{j,k} - \mathbf{y}_{j,k}^{\mathbf{SP}}) + \sum_{k=0}^{m-1} \boldsymbol{\Delta}\hat{\mathbf{u}}_{j,k}^{\mathrm{T}} R \boldsymbol{\Delta}\hat{\mathbf{u}}_{j,k} + \sum_{k=0}^{m-1} (\hat{\mathbf{u}}_{j,k} - \mathbf{u}_{j,k}^{\mathbf{SP}})^{\mathrm{T}} S (\hat{\mathbf{u}}_{j,k} - \mathbf{u}_{j,k}^{\mathbf{SP}}) \\
&- \sum_{k=0}^{m-1} \left(\boldsymbol{\lambda}_{j,k+1}^{1}\right)^{\mathrm{T}} (\hat{\mathbf{x}}_{j,k+1} - A\hat{\mathbf{x}}_{j,k} - B\hat{\mathbf{u}}_{j,k}) - \sum_{k=m}^{p-1} \left(\boldsymbol{\lambda}_{j,k+1}^{1}\right)^{\mathrm{T}} (\hat{\mathbf{x}}_{j,k+1} - A\hat{\mathbf{x}}_{j,k} - B\hat{\mathbf{u}}_{j,m-1}) \\
&- \sum_{k=1}^{p} \left(\boldsymbol{\lambda}_{j,k}^{2}\right)^{\mathrm{T}} (\hat{\mathbf{y}}_{j,k} - C\hat{\mathbf{x}}_{j,k} - \hat{\mathbf{d}}_{j,k}) - \sum_{k=0}^{m-1} \left(\boldsymbol{\lambda}_{j,k}^{3}\right)^{\mathrm{T}} (\hat{\mathbf{u}}_{j,k} - \hat{\mathbf{u}}_{j,k-1} - \boldsymbol{\Delta}\hat{\mathbf{u}}_{j,k}) \\
&- \sum_{k=0}^{m-1} \left(\boldsymbol{\eta}_{j,k}^{1}\right)^{\mathrm{T}} (\hat{\mathbf{u}}_{j,k} - \mathbf{u}_{\min}) - \sum_{k=0}^{m-1} \left(\boldsymbol{\eta}_{j,k}^{2}\right)^{\mathrm{T}} (\mathbf{u}_{\max} - \hat{\mathbf{u}}_{j,k})
\end{aligned}$$

where $\boldsymbol{\lambda}^{i}, i = 1, \ldots, 3$ and $\boldsymbol{\eta}^{i}, i = 1, 2$ are Lagrange multipliers for equality and inequality constraints, respectively. Suppose the set V contains all the decision variables in an original MPC optimization subproblem, then the KKT conditions require:

- Lagrange gradients

$$\nabla_v \mathcal{L}_j = \mathbf{0}, \qquad v \in V \tag{2.7}$$

  where the corresponding algebraic expressions are given in Table 2.1.

- Primal feasibility of equality constraints, with inequalities posed by input constraints transformed to equalities using slack variables $\boldsymbol{\mu}^i$, $\forall i \in I = \{1, 2\}$

$$\hat{\mathbf{u}}_{j,k} - \mathbf{u}_{\min} - \boldsymbol{\mu}^1_{j,k} = \mathbf{0}, \quad k = 0, \ldots, m-1 \tag{2.8a}$$

$$\mathbf{u}_{\max} - \hat{\mathbf{u}}_{j,k} - \boldsymbol{\mu}^2_{j,k} = \mathbf{0}, \quad k = 0, \ldots, m-1 \tag{2.8b}$$

$$\boldsymbol{\mu}^i_{j,k} \geq \mathbf{0}, \quad k = 0, \ldots, m-1, \quad i \in I \tag{2.8c}$$

- Dual feasibility of inequality constraints Eq. (2.8c)

$$\boldsymbol{\eta}^i_{j,k} \geq \mathbf{0}, \quad k = 0, \ldots, m-1, \quad i \in I \tag{2.9}$$

- Complementarity constraints

$$\boldsymbol{\eta}^i_{j,k} \boldsymbol{\mu}^i_{j,k} = \mathbf{0}, \quad k = 0, \ldots, m-1, \quad i \in I \tag{2.10}$$

In our solution approach, Eqs. (2.7)-(2.10) replace the MPC subproblems Eq. (2.6b), yielding a single-level MPCC problem. We describe in the next section how the MPCC is solved.

Table 2.1: Lagrange derivatives.

Derivative	Time step, k	Algebraic equation
$\nabla_{\hat{\mathbf{y}}_{j,k}} \mathcal{L}_j$	$1 \dots p$	$2\hat{\mathbf{y}}_{j,k} Q - 2\mathbf{y}^{\mathbf{SP}}_{j,k} Q - \boldsymbol{\lambda}^2_{j,k} = \mathbf{0}$
$\nabla_{\boldsymbol{\Delta}\hat{\mathbf{u}}_{j,k}} \mathcal{L}_j$	$0 \dots m-1$	$2R\boldsymbol{\Delta}\hat{\mathbf{u}}_{j,k} + \boldsymbol{\lambda}^3_{j,k} = \mathbf{0}$
$\nabla_{\hat{\mathbf{x}}_{j,k}} \mathcal{L}_j$ [†]	$1 \dots p-1$	$-\boldsymbol{\lambda}^1_{j,k} + A^{\mathrm{T}}\boldsymbol{\lambda}^1_{j,k+1} + C^{\mathrm{T}}\boldsymbol{\lambda}^2_{j,k} = \mathbf{0}$
	p	$-\boldsymbol{\lambda}^1_{j,k} + C^{\mathrm{T}}\boldsymbol{\lambda}^2_{j,k} = \mathbf{0}$
$\nabla_{\hat{\mathbf{u}}_{j,k}} \mathcal{L}_j$ [†]	$0 \dots m-2$	$2S\hat{\mathbf{u}}_{j,k} - 2S\mathbf{u}^{\mathbf{SP}}_{j,k} + B^{\mathrm{T}}\boldsymbol{\lambda}^1_{j,k+1} - \boldsymbol{\lambda}^3_{j,k} + \boldsymbol{\lambda}^3_{j,k+1}$ $-\boldsymbol{\eta}^1_{j,k} + \boldsymbol{\eta}^2_{j,k} = \mathbf{0}$
	$m-1$	$2S\hat{\mathbf{u}}_{j,k} - 2S\mathbf{u}^{\mathbf{SP}}_{j,k} + B^{\mathrm{T}}\boldsymbol{\lambda}^1_{j,m} + B^{\mathrm{T}}\boldsymbol{\lambda}^1_{j,m+1} + \ldots + B^{\mathrm{T}}\boldsymbol{\lambda}^1_{j,p}$ $-\boldsymbol{\lambda}^3_{j,k} - \boldsymbol{\eta}^1_{j,k} + \boldsymbol{\eta}^2_{j,k} = \mathbf{0}$

[†] $\hat{\mathbf{x}}_{j,0}$ and $\hat{\mathbf{u}}_{j,-1}$ are assumed known at each DRTO prediction step j, hence they are not considered as KKT variables.

Handling Complementarity Constraints

MPCC problems are generally hard to solve using standard nonlinear programming (NLP) solvers because they fail to satisfy the NLP constraint qualifications typically required in the design of the algorithms, as discussed in Fletcher et al. [38]. In particular, the complementarity constraints, which take the form of $\eta^i \mu^i = 0$ cause the MPCC problems to violate the linear independence constraint qualification (LICQ) that requires the gradient of active constraints to be linearly independent. This leads to a weaker regularity condition in which the multiplier set of the KKT conditions of the MPCC problems becomes nonunique and unbounded at any feasible solution, hence violating the Mangasarian-Fromovitz constraint qualification (MFCQ). Solving MPCC problems require reformulation of the complementarity constraints or alternative algorithm strategies that internally treat the constraints. Common approaches to handle complementarity constraints related to this work include: 1) regularization or constraint relaxation approach as implemented in Baker and Swartz [30] and Lam et al. [31], 2) mixed-integer approach as implemented in Baker and Swartz [30] and Soliman et al. [39], and 3) exact penalty approach. An extensive review on MPCC problems is beyond the scope of this thesis, and readers are referred to more detailed and in-depth discussions on MPCCs, inter alia, Raghunathan and Biegler [40], Ralph and Wright [41], Baumrucker et al. [42] and the references therein.

In this study, the complementarity constraints are handled using an exact penalty formulation by including them in a weighted penalty term appended to the economic objective function. Convergence

properties of the exact penalty formulation are presented in Ralph and Wright [41]. The penalty term is formulated as:

$$w_c = \rho \sum_{i=1}^{I} \boldsymbol{\eta}^i \boldsymbol{\mu}^i \tag{2.11}$$

where $\boldsymbol{\eta}^i$ and $\boldsymbol{\mu}^i$ represent composite vectors of the $\boldsymbol{\eta}^i_{j,k}$ and $\boldsymbol{\mu}^i_{j,k}$ respectively. ρ is a complementarity penalty parameter, whose value is not known a priori and is therefore treated as a tuning parameter for the MPCC problem. Also, the complementarity penalty term Eq. (2.11) is always positive due to the non-negativity constraints imposed on the slack variables $\boldsymbol{\mu}^i$ and their corresponding Lagrange multipliers $\boldsymbol{\eta}^i$. Tuning of the complementarity penalty parameter ρ starts from a small value, roughly of the same order of magnitude as the decision variables, and increased until it exceeds a critical value of $\rho > \rho_c$, at which point the original complementarity constraints will be approximately satisfied. However, choosing too large a penalty parameter may lead to scaling issues and longer solution times. At the optimum, the value of the complementarity penalty term will be close to zero, and the optimal solution recovers the original economic objective function of the MPCC problem due to the negligible contribution of the penalty term. The penalty transformed MPCC is solved in this study using the NLP solver, `IPOPT 3.12.0`[43].

2.2.5 Economic Objective Function

In general, any appropriate economic objective function for process optimization at the DRTO level may be used, but our cases are particularly motivated by product grade transition problems, such as those arising in polymerization and bioprocess industries. The DRTO objective function is formulated to minimize the input cost while at the same time taking into account the revenue when the product quality is within the desired target tolerance. In this section, we formulate an economic objective function that tracks the revenue of a target-specific output based on a hyperbolic tangent function construct originally proposed by Tousain [44]. The function is used as a continuous approximation of a switching function constructed to indicate when the variable enters a specification tolerance band. These may be used in combination to capture specification bands with upper and lower limits around a desired target, and included in the objective function in order for revenue to apply only when the product quality falls within specification limits. A general expression of a hyperbolic tangent function is given by

$$R(x) = \frac{1}{2}\tanh(\gamma x) + \frac{1}{2} \approx \begin{cases} 0, & x < 0 \\ 1, & x > 0 \end{cases}$$

where γ is a weighting parameter used to define the steepness of the switching function that produces a function value either smoothly or sharply approaching 0 or 1.

Consider a transition of an output from an initial specification (y^{init}) to a new target (y^{target}), as illustrated in Figure 2.5, where the output is allowed to vary within a strict tolerance, for example $\pm\delta\%$. The economic objective function is formulated to take into account the revenue when the output is within the desired specification limits. Thus, the tolerances of the desired output target may be defined mathematically as follows,

- Region 1 (lower tolerance band):

$$R^1(y) = \frac{1}{2}\tanh\left[\gamma(y - y^{\text{target}} + \delta y^{\text{target}})\right] + \frac{1}{2} \approx \begin{cases} 0, & y < y^{\text{target}} - \delta y^{\text{target}} \\ 1, & y > y^{\text{target}} - \delta y^{\text{target}} \end{cases}$$

- Region 2 (upper tolerance band):

$$R^2(y) = \frac{1}{2}\tanh\left[\gamma(y^{\text{target}} + \delta y^{\text{target}} - y)\right] + \frac{1}{2} \approx \begin{cases} 0, & y > y^{\text{target}} + \delta y^{\text{target}} \\ 1, & y < y^{\text{target}} + \delta y^{\text{target}} \end{cases}$$

Therefore $R^1R^2 \approx 1$ if y lies in the intersection of regions 1 and 2 of the target tolerance, and is approximately zero otherwise. This construct of tracking the dynamic economics of the output will be applied in following case studies.

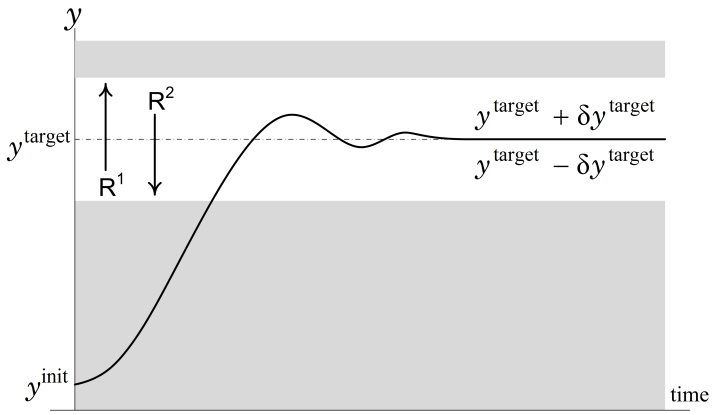

Figure 2.5: Illustration of specification tolerance bands.

2.3 Case Studies

In the following subsection, the performance of the CL- and OL-DRTO approaches is demonstrated through case studies involving linear dynamic systems. Next, we implement the CL-DRTO strategy

for optimal grade transition applied to a nonlinear dynamic model of a polystyrene production reactor system with consideration of plant-model mismatch. In all case studies, steady-state transitions are considered, with the objective of maximizing profit. Dynamic models describing the system behavior are discretized to state-space models in MATLAB based on the controller sampling time for implementation in the MPC and DRTO calculations.

The implementation procedure follows the DRTO framework described earlier in Figure 2.2. In this work, MATLAB R2012b is chosen as a supervisory computational platform to solve the MPC problem using the `quadprog` solver, and also to perform process simulation. The DRTO problem, the size of which is significantly larger than that of the MPC problem, is modeled in AMPL and solved using `IPOPT 3.12.0` [43] utilizing the linear solver `ma27`. Also, a warm-start is provided for the primal variables of the DRTO problems. An in-house interface written in PHYTON allows data transmission between AMPL and MATLAB. All case studies are solved using a 3.4GHz INTEL CORE-i7 with 8GB RAM running Windows 7.

2.3.1 Case Study 1: Linear Dynamic Systems

In this section, we first analyze the impact of controller tuning on the economics and control performance of both the OL- and CL-DRTO strategies using a single-input single-output (SISO) system. Thereafter, we consider its impact on the DRTO performance of process dynamics with control performance-limiting characteristics, which include the presence of plant-model mismatch, right-half plane transmission (RHPT) zeros and time delay, where controller detuning is required to maintain stability and robustness.

Our hypothesis is that under aggressive controller tuning, it is expected that the performance of the OL-DRTO strategy will be similar to that of the CL-DRTO approach proposed in this chapter. This is because the underlying predictive controller then approaches perfect control behavior in tracking the set-point trajectories issued by DRTO at the upper level. Conversely, factors that limit aggressive controller tuning are likely result in poor prediction capability at the DRTO level using the open-loop approach, hence a rigorous inclusion of controller tracking properties is potentially advantageous when optimizing the process economics. Achievable control performance is limited by right-half plane transmission (RHPT) zeros, time delays, input constraints and plant-model mismatch [45, 46]. We consider these factors in the context of OL- versus CL-DRTO in this multi-part case study.

The SISO transfer function models, DRTO parameters, MPC parameters, economic objective, and constraints are given in Table 2.2. Both the actual MPC controller at the lower level and the embedded MPC optimization subproblems at the upper level utilize the same tuning parameters. The systems are initialized at zero, and the desired target value is 1.0 with $\pm 10\%$ of acceptable target tolerance.

The economic objective function computes the economic return over a finite DRTO optimization horizon of $j \in [1, \ldots, N]$, with revenue accruing when the output is within the specification tolerance limits. R^1 and R^2 are outputs of hyperbolic tangent switching function approximations that indicate satisfaction of the lower and upper output specification tolerances respectively, as described earlier. A complementarity penalty parameter of 100, and a hyperbolic switching parameter of 10 are chosen for all cases. For the purpose of simplicity and clarity of comparison, we only show the reference trajectories computed at the initial simulation time ($t = 0$), but these trajectories are continuously updated at every DRTO optimization interval.

Table 2.2: Case Study 1. Linear dynamic systems.

Case study	Parameters	Economic objective and constraints
SISO system (Cases 1a and 1b): $y(s) = \frac{1}{125s^3 + 75s^2 + 15s + 1} u(s)$	$\Delta t_{\text{DRTO}} = 5$, $\Delta t_{\text{MPC}} = 1$ $Q = 1$, $R = 1$ (base case) $N = 50$, $p = 30$, $m = 3$	min $\Delta t_{\text{MPC}} \sum_{j=1}^{N} u_j - 10 R_j^1 R_j^2$ $0 \leq u \leq 1.2$ $0 \leq y \leq 1.2$ $0 \leq y^{\text{Ref}} \leq 1.5$
SISO system w/ RHPT zeros (Case 1c): $y(s) = \frac{-1.2s + 0.16}{s^2 + 1.4s + 0.16} u(s)$	$\Delta t_{\text{DRTO}} = 3$, $\Delta t_{\text{MPC}} = 1$ $Q = 1$, $R = 10$ $N = 45$, $p = 30$, $m = 3$	min $\Delta t_{\text{MPC}} \sum_{j=1}^{N} u_j - 10 R_j^1 R_j^2$ $0 \leq u \leq 1.2$ $-0.2 \leq y \leq 1.2$ $-0.2 \leq y^{\text{Ref}} \leq 1.5$
SISO system w/ time delay (Case 1d): $y(s) = \frac{e^{-4s}}{343s^3 + 147s^2 + 21s + 1} u(s)$	$\Delta t_{\text{DRTO}} = 10$, $\Delta t_{\text{MPC}} = 1$ $Q = 1$, $R = 10$ $N = 100$, $p = 40$, $m = 5$	min $\Delta t_{\text{MPC}} \sum_{j=1}^{N} u_j - 10 R_j^1 R_j^2$ $0 \leq u \leq 1.2$ $-0.2 \leq y \leq 1.2$ $-0.2 \leq y^{\text{Ref}} \leq 1.5$

Case 1a: Effect of Tuning

Figure 2.6(a) and Figure 2.6(b) show the closed-loop response dynamics of the SISO system corresponding to Case 1a in Table 2.2, based on the CL and OL-DRTO implementations, respectively. The upper figures depicts the output dynamics and the reference trajectories under aggressive MPC tuning of $R = 1$ while the lower figures represent the profiles under conservative MPC tuning of $R = 20$. The output tracking weight Q is fixed at 1 in all simulations. Also indicated are the resulting profits of the SISO system by evaluating the economic based objective function indicated in Table 2.2 over the simulation horizon.

Aggressive controller tuning with $R = 1$ results in an economic return of the CL-DRTO to be 8% higher than that of the OL-DRTO. Exploiting the reference trajectory as a degree of freedom at the primary

DRTO optimization problem contributes to the economic benefit of the closed-loop formulation. The economic gap is increased to 23% when the MPC controller is detuned with $R = 20$. Also, the CL-DRTO assists a fast transition to the desired target even under detuned control settings. The overall reference trajectory is therefore adjusted based on the controller tracking capability defined by its tuning parameters. Constraints on the reference trajectory can also be imposed independently. In this case, the upper bound for the output response and the reference trajectory are 1.2 and 1.5, respectively. As shown in Figure 2.6, the MPC reference trajectory from the DRTO calculation at the initial simulation time $(t = 0)$ is at the upper bound over five DRTO intervals (i.e. 25 min); it is continuously updated at every DRTO optimization interval over the simulation horizon. When the controller is detuned, the CL-DRTO takes the advantage of placing the reference trajectory at its upper bound for a longer period in order to improve process agility, before moving it to the desired target. By contrast, the OL-DRTO approach does not have this advantage because the underlying MPC controller tracks set-points taken directly from the optimal open-loop output trajectory computed at the DRTO level.

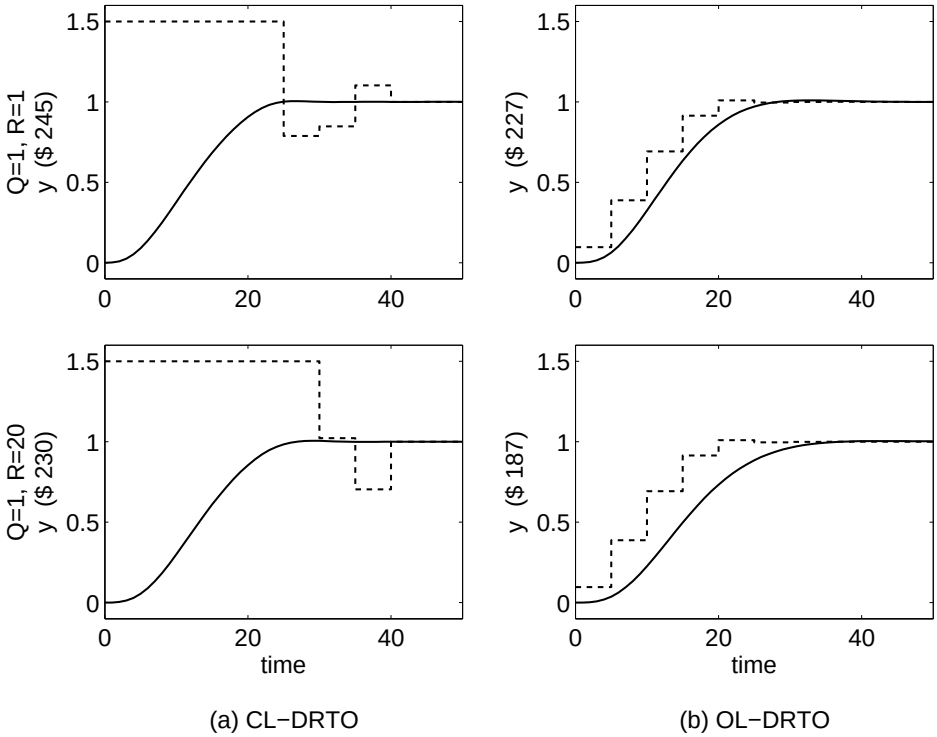

Figure 2.6: Effect of controller tuning (Case 1a).
Legend: *solid lines* = output trajectories, *dashed lines* = reference trajectories generated at $t = 0$.

In addition to the MPC move suppression weight, detuning the controller by limiting the length of control horizon also demonstrates significant advantages of the CL-DRTO strategy [47]. Although the economic gap is smaller when the MPC is tuned to be aggressive, this may be risky for system with model uncertainty, RHPT zeros and time delay as these process characteristics may lead to

internal instability as shown in the next case studies. Therefore, the multilevel closed-loop formulation provides a strategy for enhancing economic performance whenever detuning is required under such control performance limiting conditions.

Case 1b: Effect of Plant-model Mismatch

In this section, we use the model from the previous SISO case study. To introduce plant-model mismatch, the actual process gain is set to be 33% higher than that of the prediction model. The DRTO optimization horizon is $N = 100$ and the MPC controller is detuned with $Q = 0.1$ and $R = 30$. The reference trajectory is allowed to vary with in a range of $0 \leq y^{\text{Ref}} \leq 1.2$. Simulation results in Figure 2.7(a) and Figure 2.7(b) show that the CL-DRTO strategy assists a faster process transition as compared to its open-loop counterpart with economic returns of \$641 and \$565, respectively.

In the closed-loop prediction, the effect of plant-model mismatch during set-point tracking is taken into account via output feedback to the DRTO layer. Although the controller is tuned to be conservative, the CL-DRTO strategy exploits process agility through appropriate adjustment of reference trajectory in an economically-optimal fashion, hence permitting a rapid process transition, as demonstrated in Figure 2.7(a). However, further simulation studies with larger magnitudes of mismatch or aggressive MPC tunings show that output constraint violation at the plant level can only be reduced to some degree. Therefore, complete constraint satisfaction is not guaranteed by the actual plant due to behavior such as process overshoot.

By contrast, MPC tracking of the reference trajectory constructed from the optimal open-loop prediction at the OL-DRTO level requires a longer process settling time to the desired target, even though the reference trajectory exhibits fast dynamics, as depicted in Figure 2.7(b). The closed-loop process time constant is found to be 22% larger than that of the open-loop prediction at the OL-DRTO layer due to conservative controller tuning in the presence of plant-model mismatch. Performance of the CL-DRTO strategy is further enhanced relative to the OL-DRTO when mismatch in process time constant is also considered in addition to the process gain.

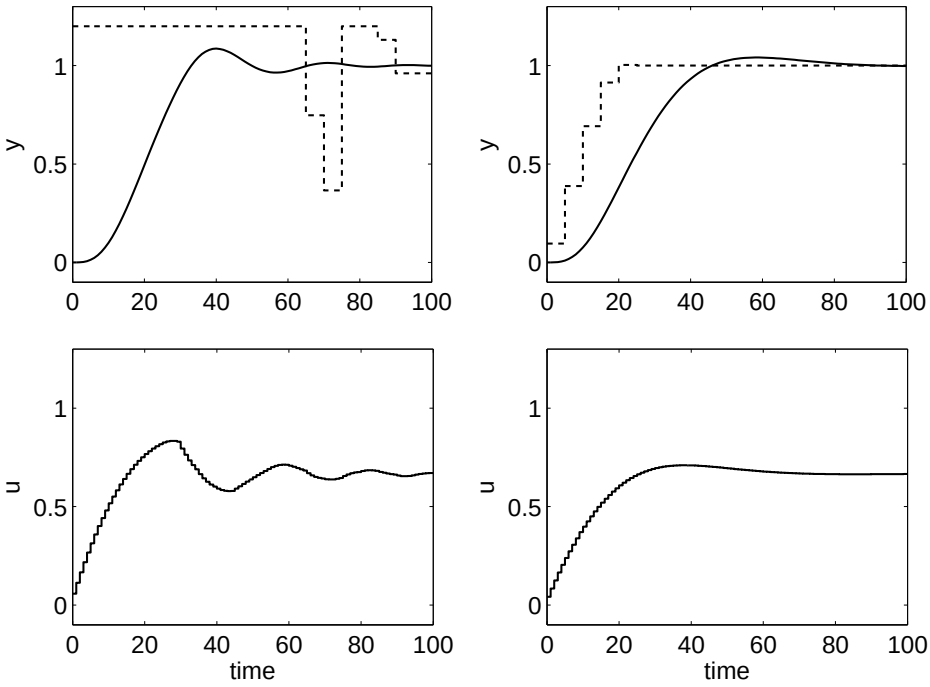

(a) CL−DRTO ($ 641) (b) OL−DRTO ($ 565)

Figure 2.7: SISO system with plant-model mismatch (Case 1b).
Legend: *solid lines* = input and output trajectories, *dashed lines* = reference trajectories generated at $t = 0$.

Case 1c: Effect of RHPT Zeros

We focus in this section on a SISO system with a right-half plane transmission (RHPT) zeros, resulting in inverse response behavior. Systems with RHPT zeros pose challenging control problems due to stability limits they place on traditional feedback controllers, and inversion of unstable process zeros to unstable poles in model-based control systems. For the case of unconstrained MPC where the length of prediction and control horizons are equal, the RHPT zeros induce internal instability if the move suppression penalty is not included in the MPC cost function [48].

Simulation results in Figure 2.8(a) show that the CL-DRTO approach outperforms the OL-DRTO in handling RHPT zeros in terms of process agility and feasibility. The CL-DRTO formulation regulates the reference trajectory based on the controller tracking properties while it simultaneously assists a fast process transition of the output to the specified target. The closed-loop prediction also identifies the possibility of output constraint violation under closed-loop regulation, hence allowing the CL-DRTO to perform preventative action in a cost-optimal fashion by adjusting the reference trajectory within the constraint limits.

By contrast, the OL-DRTO approach does not have this mechanism because the open-loop prediction

does not recognize the impact of closed-loop regulation on the process dynamics. Set-point tracking based on the optimal open-loop trajectory causes operational infeasibility due to severe output constraint violation during the initial transition period, as shown in Figure 2.8(b). Although the process closed-loop behavior is stable, the input trajectory from the OL-DRTO calculations mimics internally unstable behavior before it saturates at the lower bound of zero. This could be problematic for non-square systems where set-points are needed for some of the manipulated inputs, because control tracking of such an undesirable input trajectory may drive the process to infeasibility, potentially leading to an expensive process shutdown.

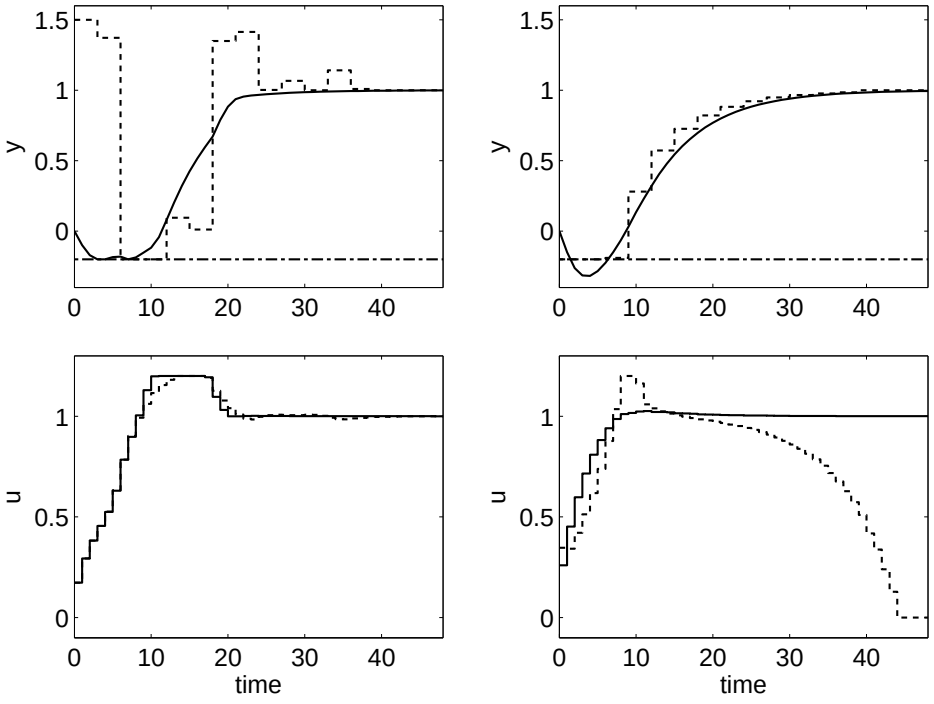

Figure 2.8: SISO system with RHPT zeros (Case 1c).
Legend: *solid lines* = input and output trajectories, *dashed lines* = reference and DRTO input trajectories, *dashed-dotted lines* = output constraints.

Application of the CL-DRTO approach generates an economic return that is 40% higher than the OL-RTO. This economic gap may be significantly larger if a penalty cost is charged on the output constraint violation, hence making the economics of the OL-DRTO strategy deteriorate substantially.

Case 1d: Effect of Time Delay

In this section, we consider a steady-state transition of a SISO system with a time delay of four minutes, as shown in Table 2.2. As shown Figure 2.9(a), the proposed CL-DRTO strategy exhibits good performance, smoothly driving the process to the desired target. The reference trajectory for the output is temporarily driven to the upper limit during the first 40 hr of the DRTO optimization horizon to assist a rapid process transition before settling at the specified target. This mechanism causes input saturation between time 4 and 22 hr, which also illustrates that the constraint-handling functionality formulated using complementary constraints is utilized at the DRTO level.

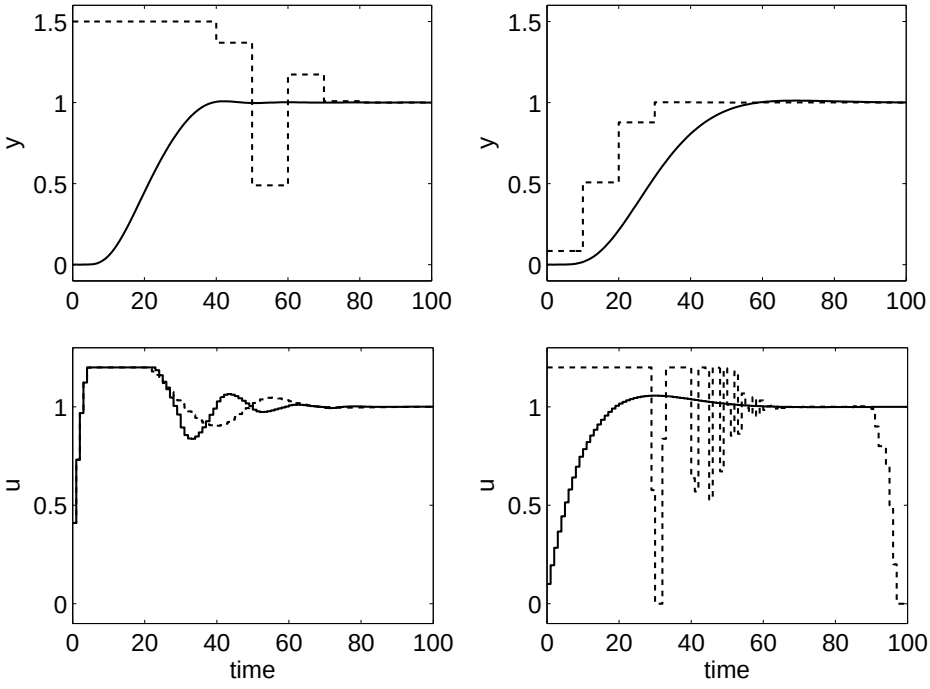

Figure 2.9: SISO system with time delay (Case 1d).
Legend: *solid lines* = input and output trajectories, *dashed lines* = reference and DRTO input trajectories.

Despite a smooth output transition to the desired target, the input trajectory from the OL-DRTO calculation exhibits high frequency and large amplitude of oscillations when the process undergoes transition within the first 60 hr of the optimization horizon before it eventually saturates at the lower bound, as illustrated in Figure 2.9(b). Control saturation does not occur under OL-DRTO implementation due to gradual changes of the reference trajectory, constructed from the optimal open-loop prediction, to the specified target. Overall, implementation of the CL-DRTO strategy gives a 35% higher economic return than the OL-DRTO strategy.

2.3.2 Case Study 2: Application to Polymer Grade Transition

In this section, we apply the CL-DRTO strategy for optimal grade transitions in polystyrene production in a jacketed CSTR with consideration of plant-model mismatch. The process exhibits slow dynamic economics because the overall process settling time can take up to 20 hr, thus making it suitable as a benchmark problem for implementation of the proposed CL-DRTO strategy. As depicted in Figure 2.10, the reactor has three feed streams comprising styrene monomer, isopropyl benzene solvent, and azobisisobutyronitrile (AIBN) initiator dissolved in isopropyl benzene. The solvent is used to keep the monomer conversion and viscosity of the polymerization mixture low. The reaction is exothermic and cooling water is used to absorb the heat of polymerization. The reactor discharge contains polymer, unreacted monomer, residual initiator and solvent.

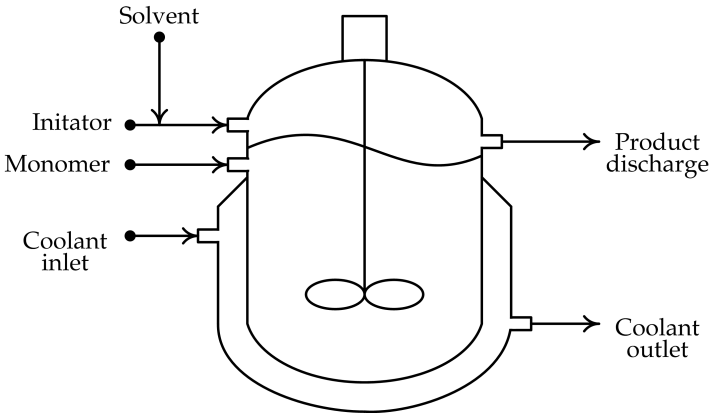

Figure 2.10: Polystyrene reactor.

The polystyrene reactor model is taken from Maner et al. [49], and based on the original work by Hidalgo and Brosilow [50]. Since the process variables vary from 10^{-5} to 10^{5}, the polystyrene reactor model is scaled to a dimensionless form following Russo and Bequette [51] in order to avoid numerical problems during optimization and simulation. The manipulated inputs, controlled outputs, and problem parameters are given in Table 2.3. Monomer feed is mainly used to maximize production rate, initiator is mainly used to control the polymer grade, and the cooling supply is used to absorb the heat of polymerization. We assume a sufficient solvent feed ratio to the monomer feed flowrate to keep the viscosity of the reaction mixture low, and therefore the solvent feed flowrate is kept constant at its nominal value. In addition to the controlled outputs, we also provide a set-point to the monomer feed flowrate as a degree of freedom to help maximize the polymer productivity. The scaled polystyrene model is linearized at the nominal steady-state operating point for implementation at the MPC and DRTO levels, whereas the nonlinear dynamic model is utilized to perform plant simulations. Linearization is carried out in MATLAB by computing the Jacobian of the reactor model at the nominal

operating data using complex-step differentiation to generate the continuous state-space model, which is subsequently discretized based on the MPC sample time of 1 hr.

Table 2.3: Case study 2 data.

Variables	Parameters	
	MPC	DRTO
Manipulated inputs:	$p = 15$	$N = 50$
Initiator feed, Q_i (L/hr)	$m = 3$	$\rho = 5$
Monomer feed, Q_m (L/hr)	$Q = I$	$\gamma = 5$
Coolant supply, Q_c (L/hr)	$R = \text{diag}(50,15,2)$	$\Delta t_{\text{DRTO}} = 5$ hr
Controlled outputs:	$S = \text{diag}(0,1,0)$	
Polymer grade, $NAMW$ (kg/mol)	$\Delta t_{\text{MPC}} = 1$ hr	
Reactor temperature, T (K)		

The economics of the polymer grade transition problem are formulated to maximize the profit of producing the specified polymer grades, characterized by the number average molecular weight (NAMW). The reactor discharge flowrate, Q_t is used as an inferred estimate of the polymer production rate. The economic objective function is formulated as:

$$\min \Phi = \Delta t_{\text{MPC}} \sum_{j=1}^{N} \left(c_i Q_{i,j} + c_m Q_{m,j} + c_c Q_{c,j} - p_p Q_{t,j} R_j^1 R_j^2 \right) \tag{2.12}$$

where c_i is the cost of the initiator (\$0.1/L), c_m is the cost of the monomer (\$0.50/L), c_c is the cost of the cooling supply (\$0.01/L), p_p is the price of the desired polymer product (\$20/L), and R^1 and R^2 are outputs of hyperbolic tangent switching function approximations that indicate satisfaction of the lower and upper bounds of the polymer grade specification tolerances. The solvent and unreacted monomer are assumed to be recovered and recycled, and their effects on the transition cost are not taken into account. Constraints on the inputs, outputs and set-points are applied as follows:

$$0 \leq Q_i \leq 300$$
$$0 \leq Q_m,\ Q_m^{\text{Ref}} \leq 400$$
$$0 \leq Q_c \leq 700$$
$$46 \leq NAMW,\ NAMW^{\text{Ref}} \leq 71$$
$$315 \leq T,\ T^{\text{Ref}} \leq 325$$

with variable units as indicated in Table 2.3.

An end-point constraint is also enforced to ensure that the DRTO reference trajectory of the polymer NAMW meets the desired specification at the end of the optimization horizon. The desired polymer grades are allowed to vary within a tolerance of $\pm 3\%$.

The polymer reactor runs two production campaigns over a 100 hr simulation time frame. The polystyrene grade change from the nominal conditions to Grade A (58 kg/mol) is imposed at the initial simulation time, and then to Grade B (69 kg/mol) at time 50 hr. We assume that the polymer grade transition schedule is obtained from a higher level of production planning and scheduling. It is desirable that the DRTO reoptimization interval be smaller than the process settling time to allow appropriate adjustments to be made during the course of grade transition by periodically updating the reference trajectories. Since the settling time of the system can take up to 20 hr, we choose an optimization interval of 5 hr for the DRTO calculations. The set-point hold mechanism described earlier is applied to the DRTO reference trajectories using equality constraints to hold them constant over each DRTO interval. We found this helpful to reduce aggressive changes in the reference trajectories. An average solution time for the CL-DRTO calculations in the following simulations is 4.8 CPU(s).

Simulation results for the nominal case are depicted in Figure 2.11. The production profit over the simulation horizon is computed using the economic formulation given in Eq. (2.12), which returns a profit of $\$15,770$. The overall set-point trajectories plotted are composed of the first period of the reference trajectories computed at every DRTO interval. The reference trajectory for the monomer feed is continuously forced to the upper bound to achieve a high reactor throughput. In addition, the polymerization temperature is mostly kept at the upper bound, which signifies a low cost for the cooling supply. Reference trajectories for the polymer NAMW and reactor temperature are appropriately adjusted to assist a rapid polymer grade transition, maintain the polymer grade specification, and prevent output constraint violation based on the closed-loop prediction at the DRTO level. The backoff mechanism that arises naturally from the closed-loop prediction helps to minimize overshoot during the polymer grade transition, which can be observed between time 60 and 65 hr. The monomer feed is slightly reduced during the course of transitions to minimize the production of off-specification polymer, but remains at the upper limit as the desired polymer grades are settling within the acceptable tolerance bands. Figure 2.11 also illustrates that production of polymer Grade A with a lower NAMW consumes more monomer units than polymer grade B that has a higher NAMW, and this results in a lower monomer concentration (C_m) in the polymerization mixture in the initial 50 hr of the simulation horizon. Although output constraints are fully satisfied at the DRTO level after the polymer NAMW reached the specified tolerance for Grade B, these constraints are temporarily violated in negligible magnitudes at the plant level from time 61 to 63 hr due to plant-model mismatch between the successive DRTO intervals.

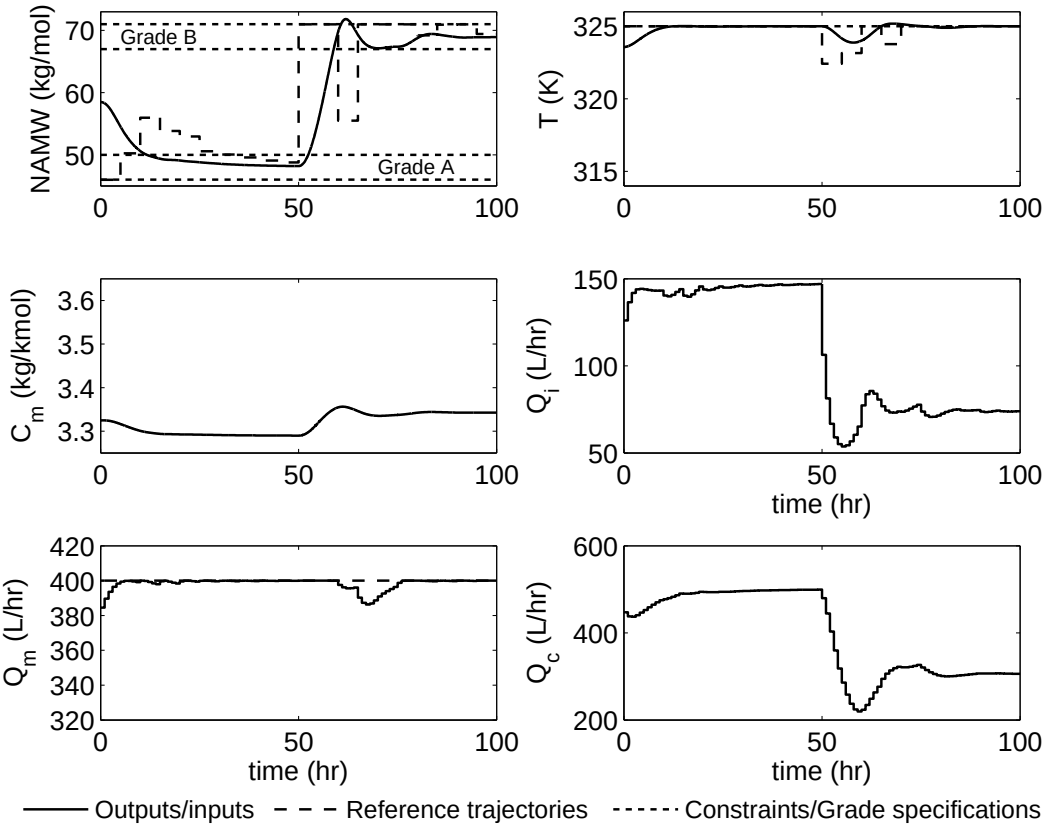

Figure 2.11: Optimal polymer grade transition for nominal case.

We now consider a disturbance scenario involving a positive pulse change in the monomer feed concentration of magnitude 0.7 kg/kmol introduced to the system between time 40 and 75 hr; the resulting dynamic responses are shown in Figure 2.12. Such a disturbance accelerates the rate of polymerization as soon as it enters the system, and consequently causes perturbations in the polymer NAMW as well as reactor temperature. The disturbance also increases the monomer concentration in the reactor mixture. Consequently, the controller decreases the monomer feed flowrate between time 40 and 55 hr to allow polymer productivity to remain economically feasible within the specified target tolerance of polymer Grade A, and also to avoid overshoot during the transition from Grade A to Grade B. The reference trajectory of the polymer NAMW is decreased to its lower bound for 5 hr starting at time 45 hr, while both the monomer and initiator feeds are simultaneously manipulated to maintain the polymer NAMW within the specified tolerance. Similar to the nominal case, a slight overshoot occurs between time 65 and 70 hr. On the other hand, the reference trajectory of the reactor temperature is drastically plunged to its lower bound over a single DRTO interval starting at time 45 hr to prevent constraint violation at the DRTO level, although it is slightly violated at the plant level between time 45 and 48 hr.

Although the dynamics of the polymer NAMW are similar for both the nominal and disturbance cases, productivity is reduced to a large extent when the disturbance enters the system. This can be seen by a substantial reduction of the monomer feed between time 40 and 55 hr to help keep polymer Grade A within the specified tolerance. Also, more cooling water is utilized to prevent temperature overshoot caused by an increase in the monomer feed concentration. This results in a profit of \$14,840, which is 6% less than the nominal case.

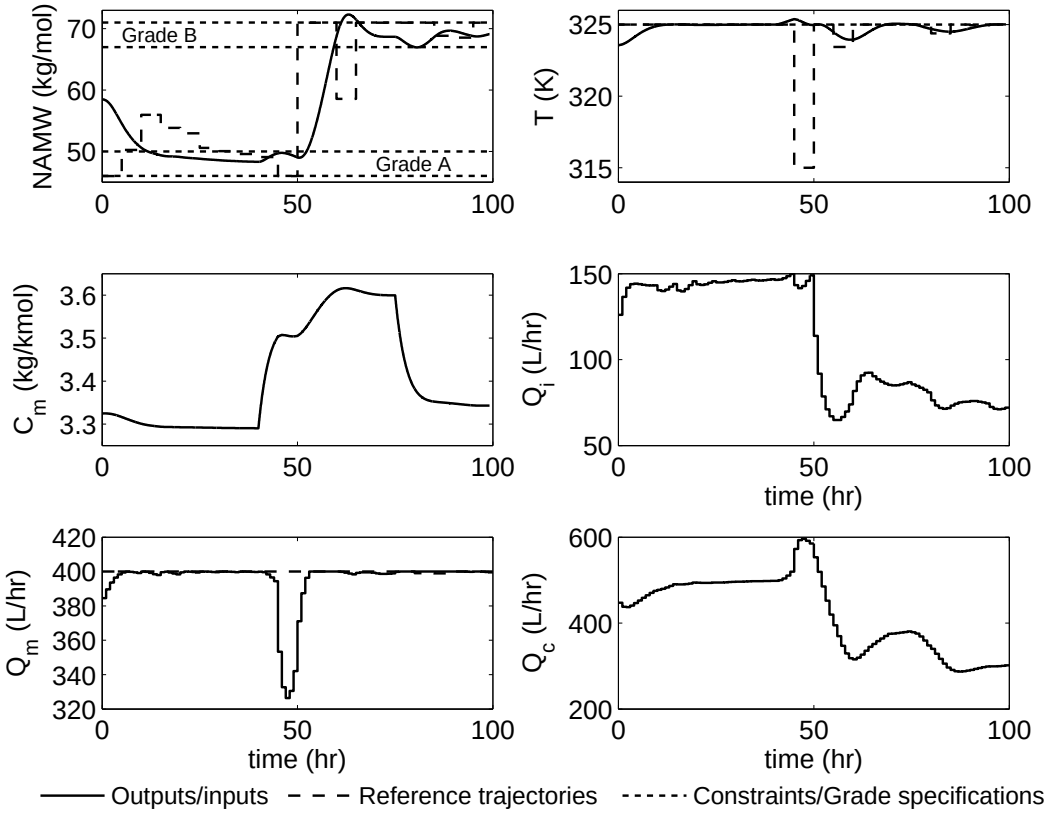

Figure 2.12: Optimal polymer grade transition with a pulse disturbance.

2.4 Conclusion

This chapter proposes and analyzes the performance of a CL-DRTO strategy in the two-layer process automation architecture. It computes the economics based on the closed-loop response dynamics of the process, formulated as a multilevel dynamic optimization problem with rigorous inclusion of the underlying MPC optimization subproblems. The multilevel problem is subsequently reformulated as a single-level MPCC problem by transforming the convex MPC QP-subproblems to algebraic equations using their first-order KKT optimality conditions.

Excellent performance is achieved in which the proposed CL-DRTO strategy outperforms the traditional open-loop counterpart, particularly under detuned control settings due to control performance limitations posed by plant-model mismatch, RHPT zeros and dead time. It generates higher economic performance, inherits the embedded MPC tracking capability, improves process agility, and helps aid operational feasibility through appropriate adjustment of the controller set-point trajectories. Application to a polystyrene production case study also shows that the CL-DRTO strategy is able to drive the polymer grade transition in a cost-optimal fashion and maintain the polymer grades within the desired specifications in the presence of plant-model mismatch and disturbances.

The multilevel CL-DRTO formulation however significantly increases the problem size and solution time of the economic optimization problem due to the embedded MPC optimization subproblems. In the next chapter, we will investigate multiple approaches to approximate the rigorous closed-loop prediction for application to complex dynamic systems.

References

[1] T. E. Marlin and A. N. Hrymak. "Real-time operations optimization of continuous processes". In: *AIChE Symposium Series: Proceedings of the 5th International Conference on Chemical Process Control*. Ed. by J. C. Kantor, C. E. Garcia, and B. Carnahan. Vol. 93. 316. AIChE and CACHE, 1997, pp. 156 –164.

[2] M. L. Darby, M. Nikolaou, J. Jones, and D. Nicholson. "RTO: An overview and assessment of current practice". In: *J Process Control* 21.6 (2011), pp. 874 –884.

[3] S. J. Qin and T. A. Badgwell. "A survey of industrial model predictive control technology". In: *Control Eng Pract* 11.7 (2003), pp. 733 –764.

[4] M. L. Darby and M. Nikolaou. "MPC: Current practice and challenges". In: *Control Eng Pract* 20.4 (2012), pp. 328 –342.

[5] J. Kadam and W. Marquardt. "Integration of economical optimization and control for intentionally transient process operation". In: *Assessment and Future Directions of Nonlinear Model Predictive Control*. Ed. by R. Findeisen, F. Allgöwer, and L. T. Biegler. Vol. 358. Lecture Notes in Control and Information Sciences. Springer Berlin Heidelberg, 2007, pp. 419–434.

[6] S. Engell. "Feedback control for optimal process operation". In: *J Process Control* 17.3 (2007), pp. 203 –219.

[7] C.-M. Ying and B. Joseph. "Performance and stability analysis of LP-MPC and QP-MPC cascade control systems". In: *AIChE J* 45.7 (1999), pp. 1521–1534.

[8] A. Nikandrov and C. L. E. Swartz. "Sensitivity analysis of LP-MPC cascade control systems". In: *J Process Control* 19.1 (2009), pp. 16 –24.

[9] S. Ochoa, J.-U. Repke, and G. Wozny. "Integrating real-time optimization and control for optimal operation: Application to the bio-ethanol process". In: *Biochem Eng J* 53.1 (2010), pp. 18 –25.

[10] L. Würth, R. Hannemann, and W. Marquardt. "A two-layer architecture for economically optimal process control and operation". In: *J Process Control* 21.3 (2011), pp. 311 –321.

[11] T. Tosukhowong, J. M. Lee, J. H. Lee, and J. Lu. "An introduction to a dynamic plant-wide optimization strategy for an integrated plant". In: *Comput Chem Eng* 29.1 (2004), pp. 199 –208.

[12] J. Kadam, M. Schlegel, W. Marquardt, R. Tousain, D. van Hessem, J. van den Berg, and O. Bosgra. "A two-level strategy of integrated dynamic optimization and control of industrial processes – a case study". In: *European Symposium on Computer Aided Process Engineering-12*. Ed. by J. Grievink and J. van Schijndel. Vol. 10. Computer Aided Chemical Engineering. Elsevier, 2002, pp. 511 –516.

[13] R. Amrit, J. B. Rawlings, and L. T. Biegler. "Optimizing process economics online using model predictive control". In: *Comput Chem Eng* 58.0 (2013), pp. 334 –343.

[14] A. Zanin, M. T. de GouvÃła, and D. Odloak. "Integrating real-time optimization into the model predictive controller of the FCC system". In: *Control Eng Pract* 10.8 (2002), pp. 819 –831.

[15] R. Amrit, J. B. Rawlings, and D. Angeli. "Economic optimization using model predictive control with a terminal cost". In: *Annual Reviews in Control* 35.2 (2011), pp. 178 –186.

[16] M. Ellis and P. D. Christofides. "Economic model predictive control with time-varying objective function for nonlinear process systems". In: *AIChE J* 60.2 (2014), pp. 507–519.

[17] B. P. Omell and D. J. Chmielewski. "IGCC power plant dispatch using infinite-horizon economic model predictive control". In: *Ind Eng Chem Res* 52.9 (2013), pp. 3151–3164.

[18] Z. Chong and C. L. E. Swartz. "Optimal operation of process plants under partial shutdown conditions". In: *AIChE J* 59.11 (2013), pp. 4151–4168.

[19] J. B. Rawlings and R. Amrit. "Optimizing process economic performance using model predictive control". In: *Nonlinear Model Predictive Control*. Ed. by L. Magni, D. Raimondo, and F. Allgöwer. Vol. 384. Lecture Notes in Control and Information Sciences. Springer Berlin Heidelberg, 2009, pp. 119–138.

[20] V. M. Zavala and L. T. Biegler. "The advanced-step NMPC controller: Optimality, stability and robustness". In: *Automatica* 45.1 (2009), pp. 86 –93.

[21] R. Huang, V. M. Zavala, and L. T. Biegler. "Advanced step nonlinear model predictive control for air separation units". In: *J Process Control* 19 (2009), pp. 678 –685.

[22] M. Ellis, H. Durand, and P. D. Christofides. "A tutorial review of economic model predictive control methods". In: *J Process Control* 24.8 (2014), pp. 1156 –1178.

[23] A. Bemporad and M. Morari. "Robust model predictive control: A survey". In: *Robustness in identification and control*. Ed. by A. Garulli and A. Tesi. Vol. 245. Lecture Notes in Control and Information Sciences. Springer London, 1999, pp. 207–226.

[24] J. Lee and Z. Yu. "Worst-case formulations of model predictive control for systems with bounded parameters". In: *Automatica* 33.5 (1997), pp. 763 –781.

[25] M. V. Kothare, V. Balakrishnan, and M. Morari. "Robust constrained model predictive control using linear matrix inequalities". In: *Automatica* 32.10 (1996), pp. 1361–1379.

[26] B. Kouvaritakis, J. A. Rossiter, and J. Schuurmans. "Efficient robust predictive control". In: *IEEE Trans Automat Contr* 45.8 (2000), pp. 1545–1549.

[27] V. Sakizlis, N. M. Kakalis, V. Dua, J. D. Perkins, and E. N. Pistikopoulos. "Design of robust model-based controllers via parametric programming". In: *Automatica* 40.2 (2004), pp. 189 –201.

[28] X. Li and T. E. Marlin. "Model predictive control with robust feasibility". In: *J Process Control* 21.3 (2011), pp. 415 –435.

[29] R. Mastragostino, S. Patel, and C. L. E. Swartz. "Robust decision making for hybrid process supply chain systems via model predictive control". In: *Comput Chem Eng* 62 (2014), pp. 37–55.

[30] R. Baker and C. L. E. Swartz. "Interior point solution of multilevel quadratic programming problems in constrained model predictive control applications". In: *Ind Eng Chem Res* 47.1 (2008), pp. 81–91.

[31] D. K. Lam, R. Baker, and C. L. E. Swartz. "Reference trajectory optimization under constrained predictive control". In: *Can J Chem Eng* 85.4 (2007), pp. 454–464.

[32] J. M. Maciejowski. *Predictive Control with Constraints*. Essex, England: Prentice Hall, 2002.

[33] C. R. Cutler and B. L. Ramaker. "Dynamic Matrix Control - a computer control algorithm". In: *AIChE 86th National Meeting*. Houston, TX, USA, 1979.

[34] C. E. Garcia and A. M. Morshedi. "Quadratic programming solution of dynamic matrix control (QDMC)". In: *Chem Eng Commun* 46.1-3 (1986), pp. 73–87.

[35] J. H. Lee, M. Morari, and C. E. Garcia. "State-space Interpretation of Model Predictive Control". In: *Automatica* 30.4 (Apr. 1994), pp. 707–717.

[36] D. Mayne, J. Rawlings, C. Rao, and P. Scokaert. "Constrained model predictive control: Stability and optimality". In: *Automatica* 36.6 (2000), pp. 789 –814.

[37] E. Zafiriou and A. L. Marchal. "Stability of SISO quadratic dynamic matrix control with hard output constraints". In: *AIChE J* 37.10 (1991), pp. 1550–1560.

[38] R. Fletcher, S. Leyffer, D. Ralph, and S. Scholtes. "Local convergence of SQP methods for mathematical programs with equilibrium constraints". In: *SIAM J. on Optimization* 17.1 (Jan. 2006), pp. 259–286.

[39] M. Soliman, C. L. E. Swartz, and R. Baker. "A mixed-integer formulation for back-off under constrained predictive control". In: *Comput Chem Eng* 32.10 (2008), pp. 2409 –2419.

[40] A. U. Raghunathan and L. T. Biegler. "Mathematical programs with equilibrium constraints (MPECs) in process engineering". In: *Comput Chem Eng* 27.10 (2003), pp. 1381 –1392.

[41] D. Ralph and S. J. Wright. "Some properties of regularization and penalization schemes for MPECs". In: *Optimization Methods and Software* 19.5 (2004), pp. 527–556.

[42] B. Baumrucker, J. Renfro, and L. Biegler. "MPEC problem formulations and solution strategies with chemical engineering applications". In: *Comput Chem Eng* 32.12 (2008), pp. 2903 –2913.

[43] A. Wächter and L. T. Biegler. "On the implementation of an interior-point filter line-search algorithm for large-scale nonlinear programming". In: *Math Prog* 106.1 (2006), pp. 25–57.

[44] R. L. Tousain. "Dynamic Optimization in Business-Wide Process Control". Ph.D. Thesis. Delft University of Technology, Delft, The Netherlands, 2002.

[45] M. Morari. "Design of resilient processing plants – III. A general framework for the assessment of dynamic resilience". In: *Chem Eng Sci* 38 (1983), pp. 1881 –1891.

[46] C. L. E. Swartz. "A computational framework for dynamic operability assessment". In: *Comput Chem Eng* 20.4 (1996), pp. 365 –371.

[47] M. Z. Jamaludin and C. L. Swartz. "IFAC Symposium on Advanced Control of Chemical Processes (ADCHEM): A Bilevel Programming Formulation for Dynamic Real-time Optimization". In: *IFAC-PapersOnLine* 48.8 (2015), pp. 906 –911.

[48] C. E. García, D. M. Prett, and M. Morari. "Model predictive control: Theory and practice – A survey". In: *Automatica* 25.3 (1989), pp. 335 –348.

[49] B. R. Maner, F. J. Doyle III, B. A. Ogunnaike, and R. K. Pearson. "Nonlinear model predictive control of a simulated multivariable polymerization reactor using second-order Volterra models". In: *Automatica* 32.9 (1996), pp. 1285 –1301.

[50] P. Hidalgo and C. Brosilow. "Nonlinear model predictive control of styrene polymerization at unstable operating points". In: *Comput Chem Eng* 14.4/5 (1990), pp. 481 –494.

[51] L. P. Russo and B. Bequette. "Operability of chemical reactors: multiplicity behavior of a jacketed styrene polymerization reactor". In: *Chem Eng Sci* 53.1 (1998), pp. 27 –45.

Chapter 3

Approximation of Closed-loop Prediction

The formulations and results in this chapter have been submitted to, and presented in:

[1] M.Z. Jamaludin and C.L.E. Swartz. "Approximation of closed-loop prediction for dynamic real-time optimization calculations". *Submitted to Comput Chem Eng* (2016), under review.

[2] M.Z. Jamaludin and C.L.E. Swartz. "IFAC International Symposium on Advanced Control of Chemical Processes (ADCHEM): A bilevel programming formulation for dynamic real-time optimization". *IFAC-PapersOnLine* 48-8 (2015), pp 906-911.

[3] M.Z. Jamaludin and C.L.E. Swartz. "Approximation of closed-loop dynamics for dynamic real-time optimization calculations". *AIChE Annual Meeting* (2015). Salt Lake City, UT, USA.

3.1 Introduction

Competitive global market conditions and demand-driven production are characteristics of the present day environment in which industries operate. Consequently, engineers confront a challenging task in operating production plants in a cost-optimal fashion while satisfying the prevailing constraints. Industrial plant economic optimization has conventionally been addressed via a multilevel process automation architecture with time-scale separation, as illustrated in Figure 3.1(a). At the upper level, a real-time optimization (RTO) system exploits the economics of process operation in response to changes in pricing factors and slow-varying disturbances that affect production profit [1, 2]. RTO interacts with the lower level process automation activities in a cascade fashion by providing economically optimal operating targets (or set-points) for the underlying regulatory control system. Beneath RTO is typically model predictive control (MPC) as an advanced, multivariable control strategy that optimizes process control performance by tracking the set-points while rejecting higher frequency disturbances.

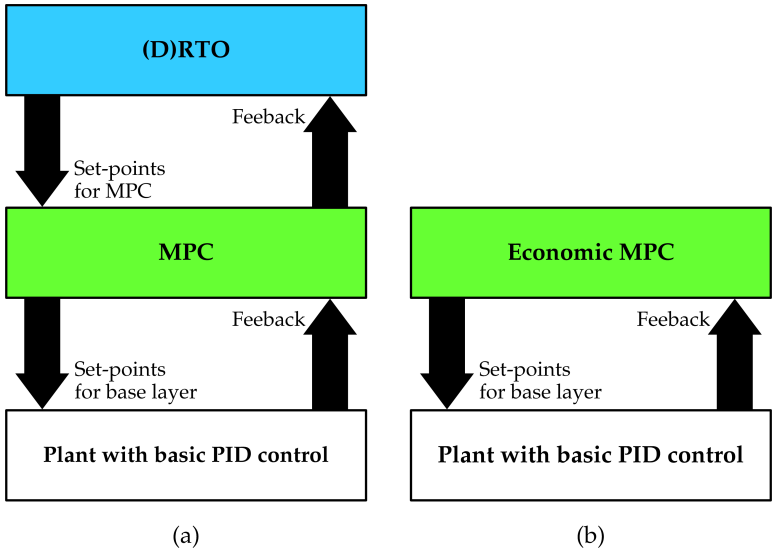

Figure 3.1: Process automation architecture: (a) a hierarchical approach, (b) a single-layer approach.

The static RTO strategy utilizes a steady-state model for economic optimization in its framework. This prohibits frequent economic assessment of process operation since RTO calculations can only be executed once the process is deemed to have reached steady state. Such an approach generally does not account for the economic performance of the plant during transition from one steady-state to another, resulting in suboptimal operation for processes that exhibit slow dynamics, experience frequent transitions, or are continuously perturbed by disturbances. In an attempt to address this shortcoming, commercial MPC applications typically include a linear programming (LP) or quadratic programming (QP) steady-state optimizer, whose key function is to track the economic optimum given

by the less frequently executed RTO system [3, 4]. This cascade LP(QP)-MPC configuration provides feasible set-point updates for the MPC layer based on minimization of the (squared) deviation of the MPC set-points from the RTO targets or optimization of an economic criterion directly. The optimizer uses a steady-state model consistent with the dynamic MPC model in its formulation, and is executed at the same frequency as the MPC. Ying and Joseph [5] analyze the performance and stability of LP-MPC and QP-MPC, while Nikandrov and Swartz [6] investigate the sensitivity of the LP-MPC system to its model bias update parameters.

Recent advances have transformed the steady-state RTO to dynamic RTO (DRTO) based on a dynamic prediction model, thus substantially increasing the frequency at which economic optimization can be performed by eliminating the steady-state requirement in the traditional RTO implementation. This transformation mainly benefits processes that experience frequent transitions, or that exhibit long transient dynamics such as integrated process networks with recycle streams. Proposed DRTO strategies typically perform economic optimization in an open-loop fashion without taking into account the presence of the plant control system. In this approach, reference trajectories for the lower level controller are constructed from the optimal open-loop response dynamics under an expectation that the closed-loop response dynamics at the plant level will follow the trajectories obtained at the DRTO level. Tosukhowong et al. [7] propose a DRTO strategy that optimizes operation of networked processes regulated using multiple MPC subsystems, and suggest that the frequency of execution for the DRTO should be lower than that of the MPC to capture the slow plantwide dynamics without being affected by local disturbances. An additional coordination layer is placed between the DRTO and MPC layers whose function is to provide locally feasible set-point trajectories for the MPC controllers. Kadam et al. [8] propose a hierarchical decomposition approach based on a two-level architecture, in which the upper level optimizes the economics and provides reference control trajectories to the lower level controller for tracking purposes. Instead of performing rigorous optimization at a fixed frequency, the DRTO calculation at the upper level is only executed when disturbances entering the system exceed a certain predetermined threshold. In a subsequent study, Würth et al. [9] propose utilization of a neighboring-extremal (NE) control strategy for plant regulation, designed to provide a linear update to the economic-based control trajectory using sensitivity information computed at the DRTO level. The algorithm also considers decomposing disturbances to slow and fast time-scales, handled by the DRTO and the NE controller, respectively. Wolf et al. [10] propose a two-layer DRTO architecture for hybrid discrete-continuous dynamic systems that integrates a predefined production schedule into online control calculations with application to a polymerization reactor system. Two similar versions of the architecture are presented with distinction in the assignment of layer(s) that compute the optimal polymer grade switching times.

An alternative paradigm for optimizing the process economics is to use a single-layer economic MPC (EMPC) strategy, as depicted in Figure 3.1(b). In the single-layer approach, EMPC computes the

manipulated input moves directly at every controller sample instance. It solves a dynamic optimization problem with a purely economic objective function or a hybrid objective of plant economics and control tracking, weighted by appropriate tuning parameters. Zanin et al. [11] proposed a single-layer approach that includes an economic function as a penalty term in the objective function of the MPC controller for application to a fluid catalytic cracking (FCC) system. Although successful implementation is demonstrated, their study revealed a difficulty in apportioning of weights in the optimization problem for achieving regulation and economic objectives. Amrit et al. [12] present an EMPC formulation that optimizes process economics with stability properties achieved by imposing a terminal region constraint and the terminal state, under an assumption that the system satisfies a certain dissipativity condition. Heidarinejad et al. [13] present Lyapunov-based economic MPC (LEMPC) strategies for nonlinear systems. They consider two operating modes, the first in which the economics are optimized with the process maintained within a stability region, and the second in which the system is driven to a predefined steady-state. Asynchronous and delayed measurements, and uncertain variables are also considered. Gopalakrishnan and Biegler [14] consider application of an EMPC strategy to a gas pipeline network, in which convergence to a periodic steady-state, as dictated by the demand pattern, is achieved through imposition of an appropriate terminal constraint. The EMPC approach is shown to yield superior economic performance over a set-point tracking approach. Chong and Swartz [15] design a multi-tiered economic-based MPC strategy for optimal control of plant under partial shutdown operation, in which each control execution involves the solution of a sequence of dynamic optimization problems based on prioritization of multiple competing objectives.

Proposed EMPC strategies often require an additional steady-state economic optimizer functioning in conjunction with the controller to provide tracking set-points, terminal penalty, or terminal state variable constraints to enforce stability in its formulation, computed either offline or online [11, 16, 14]. The single-level approach is also faced with a computational challenge of solving a complex dynamic optimization problem for a long prediction horizon that may be required to capture long term economic impacts, while being implemented at a sufficiently small controller sampling interval for disturbance rejection. However, significant progress has been made in recent years to speed up the solution time of large-scale dynamic optimization problems arising in real-time applications. For instance, Biegler and co-workers [17, 18, 19] fully discretize a dynamic optimization problem to form a nonlinear program (NLP) and take advantage of the NLP sensitivity information to compute a fast approximate online solution applicable to nonlinear MPC (NMPC), EMPC, and moving horizon estimation (MHE). Reviews on the hierarchical optimal control configuration are discussed in Tatjewski [20] and Scattolini [21], while a recent review on the EMPC approach can be found in Ellis et al. [22].

In previous work [23], we considered a two-level DRTO/MPC configuration applied to a continuous process operation that fits within the hierarchical industrial process automation architecture. We proposed a closed-loop DRTO (CL-DRTO) approach in the form of a multilevel dynamic optimization

problem involving a sequence of constrained MPC optimization subproblems embedded over the DRTO optimization horizon. The multilevel problem is subsequently reformulated as a single-level mathematical program with complementarity constraints (MPCC) by transforming the MPC subproblems to algebraic constraint equations using their first-order, Karush-Kuhn-Tucker (KKT) optimality conditions. The performance of the CL-DRTO approach is examined through multiple case studies with different problem characteristics, with the objective of maximizing profit. Case study results demonstrated that the proposed CL-DRTO approach outperforms the traditional open-loop counterpart, particularly under detuned controller settings due to control performance limitations posed by plant-model mismatch, right half-plane transmission (RHPT) zeros and dead time. Also, application to a polystyrene reactor system demonstrates the ability the CL-DRTO strategy to drive polymer grade transitions in a cost-optimal fashion. Despite its advantages, rigorous closed-loop prediction generated from the formulation of a multilevel dynamic optimization problem significantly increases the size and solution time of the DRTO problem, and approximation approaches are therefore desirable.

This chapter analyzes multiple approaches to approximate the closed-loop prediction for utilization in the CL-DRTO formulation to allow the economic optimization problem to remain manageable and computationally tractable. Three formulations for approximate closed-loop prediction are studied: (i) a hybrid formulation, (ii) a bilevel formulation, and (iii) an input clipping formulation. The remainder of this chapter is organized as follows. Section 2 presents mathematical formulations that describe the dynamic optimization problems for the rigorous and approximate CL-DRTO formulations, a solution strategy to handle the embedded MPC optimization subproblem(s), and the economic objective function used for optimization of product grade transitions. In Section 3, we analyze the performance of the proposed approaches using a multi-input single-output (MISO) case study involving steady-state transitions, with the objective of maximizing profit. This is followed by a case study application to a polystyrene grade transition problem with consideration of plant-model mismatch and a disturbance. Finally, Section 4 concludes with some remarks and outlines future research avenues.

3.2 Problem Formulation

3.2.1 MPC Formulation

In this work, we consider an input-constrained MPC algorithm based on a state-space formulation [3, 24], with the general optimization problem solved at each sample time j taking the form:

$$\begin{aligned}
\min_{\hat{\mathbf{u}}_{j,k}} \phi_j := & \sum_{k=1}^{p} (\hat{\mathbf{y}}_{j,k} - \mathbf{y}^{\mathbf{SP}}_{j,k})^{\mathrm{T}} Q (\hat{\mathbf{y}}_{j,k} - \mathbf{y}^{\mathbf{SP}}_{j,k}) + \sum_{k=0}^{m-1} \Delta\hat{\mathbf{u}}^{\mathrm{T}}_{j,k} R \Delta\hat{\mathbf{u}}_{j,k} \\
& + \sum_{k=0}^{m-1} (\hat{\mathbf{u}}_{j,k} - \mathbf{u}^{\mathbf{SP}}_{j,k})^{\mathrm{T}} S (\hat{\mathbf{u}}_{j,k} - \mathbf{u}^{\mathbf{SP}}_{j,k}) \\
s.t. \quad & \hat{\mathbf{x}}_{j,k+1} = A\hat{\mathbf{x}}_{j,k} + B\hat{\mathbf{u}}_{j,k}, \quad k = 0, \ldots, m-1 \\
& \hat{\mathbf{x}}_{j,k+1} = A\hat{\mathbf{x}}_{j,k} + B\hat{\mathbf{u}}_{j,m-1}, \quad k = m, \ldots, p-1 \\
& \hat{\mathbf{y}}_{j,k} = C\hat{\mathbf{x}}_{j,k} + \hat{\mathbf{d}}_{j,k}, \quad k = 1, \ldots, p \\
& \Delta\hat{\mathbf{u}}_{j,k} = \hat{\mathbf{u}}_{j,k} - \hat{\mathbf{u}}_{j,k-1}, \quad k = 0, \ldots, m-1 \\
& \mathbf{u}_{\min} \leq \hat{\mathbf{u}}_{j,k} \leq \mathbf{u}_{\max}, \quad k = 0, \ldots, m-1
\end{aligned} \tag{3.1}$$

where $\hat{\mathbf{x}} \in \Re^{n_x}$ is a vector of predicted states and $\hat{\mathbf{y}} \in \Re^{n_y}$ is a corresponding vector of the predicted outputs over a prediction horizon p; $\hat{\mathbf{u}} \in \Re^{n_u}$ is a vector of predicted inputs over a control horizon m; $\hat{\mathbf{d}} \in \Re^{n_y}$ is a vector of disturbance estimates for output correction; $\mathbf{y}^{\mathbf{SP}} \in \Re^{n_y}$ and $\mathbf{u}^{\mathbf{SP}} \in \Re^{n_u}$ are vectors of set-point trajectories for the controlled outputs and manipulated inputs; and Q, R and S are diagonal positive semidefinite weighting matrices on the output tracking, move suppression, and control tracking terms in the objective function, respectively. $A \in \Re^{n_x \times n_x}$, $B \in \Re^{n_x \times n_u}$ and $C \in \Re^{n_y \times n_x}$ are linear(ized), discrete-time, state-space matrices; and $\mathbf{u}_{\min}$ and $\mathbf{u}_{\max}$ are lower and upper bounds on the manipulated inputs, respectively. $\hat{\mathbf{y}}_{j,k}$ represents the predicted value of the outputs over horizon $k \in [1, \ldots, p]$ based on information available at sample time j.

The disturbance estimate, as proposed in the original DMC and QDMC algorithms [25, 26], is computed as the difference between the current measured outputs and predicted outputs based on the information available at the previous sample time, and is assumed constant over the prediction horizon. The corresponding equations are

$$\begin{aligned}
\hat{\mathbf{d}}_j &= \mathbf{y}^{\mathbf{m}}_j - C\hat{\mathbf{x}}_{j-1,1} \\
\hat{\mathbf{d}}_{j,k} &= \hat{\mathbf{d}}_j, \quad k = 1, \ldots, p
\end{aligned}$$

where $\mathbf{y}_j^{\mathbf{m}}$ is the set of measured outputs at current time step j. To compute $\boldsymbol{\Delta}\hat{\mathbf{u}}_{j,0}$, the previously implemented manipulated input vector $\hat{\mathbf{u}}_{j-1}$ is written in the above formulation as $\hat{\mathbf{u}}_{j,-1}$ and given by

$$\hat{\mathbf{u}}_{j,-1} = \hat{\mathbf{u}}_{j-1,0} \tag{3.2}$$

The predicted states at sampling instance j may be obtained from

$$\begin{aligned} \hat{\mathbf{x}}_{j,0} &= \hat{\mathbf{x}}_{j-1,1} \\ &= A\hat{\mathbf{x}}_{j-1,0} + B\hat{\mathbf{u}}_{j-1,0} \end{aligned} \tag{3.3}$$

We remark that the DRTO approach presented in this article is not restricted to a particular MPC formulation, with other MPC formulations, such as those that include terminal constraints [27], readily accommodated by making corresponding modifications to the first-order optimality conditions of the MPC optimization subproblems presented later. Also, the input tracking set-point term in the objective function is particularly useful for non-square systems, with the input set-points corresponding to so-called ideal resting values [24]. However, specification of more set-points than available degrees of freedom could result in offset [6]. We note finally that output constraints are not included in the MPC formulation, as they could lead to infeasibility and/or instability [3, 28]; they are imposed instead at the DRTO level where the set-point trajectories constitute the optimization degrees of freedom.

3.2.2 Rigorous CL-DRTO Formulation

For clarity of exposition, we first describe the rigorous CL-DRTO formulation as it forms a basis for the derivation of the closed-loop approximation approaches to be presented in the subsequent sections. The closed-loop response required for evaluation of the economics and application of constraints on the dynamic response can be generated by a sequence of calculations involving the determination of MPC control inputs followed by the response of the plant to the applied control inputs, repeated over the DRTO horizon. Thus, a CL-DRTO approach with rigorous inclusion of the future MPC closed-loop response dynamics forms a multilevel dynamic optimization problem with embedded MPC optimization subproblems, as illustrated in Figure 3.2. Interaction between the primary DRTO optimization problem and the inner MPC optimization subproblems occurs in a bidirectional way. The DRTO provides an internal dynamic model of the process to generate plant outputs required by the MPC subproblems at each DRTO prediction step, and the MPC subproblems provide an optimal control input vector to the DRTO model.

Mathematically, we have a primary DRTO optimization problem Eq. (3.4a) that computes controller

reference trajectories that determine the best economics over a finite DRTO optimization horizon, N. The DRTO optimization horizon is chosen to be sufficiently long to capture the effects of the overall plant response dynamics on the process economics, and may be significantly longer than the MPC prediction horizon. The primary DRTO optimization problem requires a sequence of MPC controller optimization subproblems Eq. (3.4b), corresponding to the MPC formulation given in Eq. (3.1) to compute the optimal control input trajectories. The first control move from each MPC subproblem solution is applied in the primary DRTO optimization problem to predict the closed-loop response dynamics for economic optimization. Constraints on the outputs and reference trajectories are imposed at the primary DRTO problem, whereas input constraints are addressed by the inner MPC subproblems. The DRTO problem is stated as follows.

$$
\begin{aligned}
&\min_{\mathbf{y}^{\mathbf{Ref}},\ \mathbf{u}^{\mathbf{Ref}}} \Phi^{\text{Econ}}(\hat{\mathbf{x}}^{\mathbf{DRTO}},\ \hat{\mathbf{y}}^{\mathbf{DRTO}},\ \hat{\mathbf{u}}^{\mathbf{DRTO}}) \\
s.t.\quad & \hat{\mathbf{x}}_{j+1}^{\mathbf{DRTO}} = \mathbf{f}^{\mathbf{DRTO}}(\hat{\mathbf{x}}_j^{\mathbf{DRTO}},\ \hat{\mathbf{u}}_j^{\mathbf{DRTO}}), \quad j = 0, \ldots, N-1 \\
& \hat{\mathbf{y}}_j^{\mathbf{DRTO}} = \mathbf{h}^{\mathbf{DRTO}}(\hat{\mathbf{x}}_j^{\mathbf{DRTO}}), \quad j = 1, \ldots, N \\
& \mathbf{0} \leq \mathbf{g}^{\mathbf{DRTO}}(\hat{\mathbf{x}}_j^{\mathbf{DRTO}},\ \hat{\mathbf{y}}_j^{\mathbf{DRTO}}), \quad j = 1, \ldots, N \\
& \mathbf{0} = \mathbf{h}^{\mathbf{Ref}}(\mathbf{y}^{\mathbf{Ref}},\ \mathbf{u}^{\mathbf{Ref}},\ \mathbf{y}^{\mathbf{SP}},\ \mathbf{u}^{\mathbf{SP}}) \\
& \mathbf{0} \leq \mathbf{g}^{\mathbf{Ref}}(\mathbf{y}_{j+1}^{\mathbf{Ref}},\ \mathbf{u}_j^{\mathbf{Ref}}), \quad j = 0, \ldots, N-1 \\
& \hat{\mathbf{u}}_j^{\mathbf{DRTO}} = \hat{\mathbf{u}}_{j,0}, \quad j = 0, \ldots, N-1 \\
& \hat{\mathbf{d}}_{0,k} = \mathbf{y}_{j^*}^{\mathbf{m}} - C\hat{\mathbf{x}}_{j^*-1,1}, \quad k = 1, \ldots, p \\
& \hat{\mathbf{d}}_{j,k} = \hat{\mathbf{y}}_j^{\mathbf{DRTO}} - C\hat{\mathbf{x}}_{j-1,1}, \quad j = 1, \ldots, N-1, \quad k = 1, \ldots, p
\end{aligned} \tag{3.4a}
$$

$$
\left.
\begin{aligned}
\hat{\mathbf{u}}_{j,0} \in \arg \min_{\hat{\mathbf{u}}_{j,k}} \ & \phi_j := \textstyle\sum_{k=1}^{p} (\hat{\mathbf{y}}_{j,k} - \mathbf{y}_{j,k}^{\mathbf{SP}})^{\mathrm{T}} Q (\hat{\mathbf{y}}_{j,k} - \mathbf{y}_{j,k}^{\mathbf{SP}}) + \sum_{k=0}^{m-1} \boldsymbol{\Delta}\hat{\mathbf{u}}_{j,k}^{\mathrm{T}} R \boldsymbol{\Delta}\hat{\mathbf{u}}_{j,k} \\
& \quad + \textstyle\sum_{k=0}^{m-1} (\hat{\mathbf{u}}_{j,k} - \mathbf{u}_{j,k}^{\mathbf{SP}})^{\mathrm{T}} S (\hat{\mathbf{u}}_{j,k} - \mathbf{u}_{j,k}^{\mathbf{SP}}) \\
s.t.\quad & \hat{\mathbf{x}}_{j,k+1} = A\hat{\mathbf{x}}_{j,k} + B\hat{\mathbf{u}}_{j,k}, \quad k = 0, \ldots, m-1 \\
& \hat{\mathbf{x}}_{j,k+1} = A\hat{\mathbf{x}}_{j,k} + B\hat{\mathbf{u}}_{j,m-1}, \quad k = m, \ldots, p-1 \\
& \hat{\mathbf{y}}_{j,k} = C\hat{\mathbf{x}}_{j,k} + \hat{\mathbf{d}}_{j,k}, \quad k = 1, \ldots, p \\
& \boldsymbol{\Delta}\hat{\mathbf{u}}_{j,k} = \hat{\mathbf{u}}_{j,k} - \hat{\mathbf{u}}_{j,k-1}, \quad k = 0, \ldots, m-1 \\
& \mathbf{u}_{\min} \ \leq \ \hat{\mathbf{u}}_{j,k} \ \leq \ \mathbf{u}_{\max}, \quad k = 0, \ldots, m-1
\end{aligned}
\right\}
\begin{array}{c}\text{MPC}\\ \text{subproblems,}\\ j = 0, \ldots, N-1\end{array} \tag{3.4b}
$$

where $\hat{\mathbf{x}}_j^{\mathbf{DRTO}} \in \Re^{n_x}$ is a vector of DRTO model states, $\hat{\mathbf{y}}_j^{\mathbf{DRTO}} \in \Re^{n_y}$ is a corresponding vector of DRTO model outputs, and $\hat{\mathbf{u}}_j^{\mathbf{DRTO}} \in \Re^{n_u}$ is a vector of DRTO inputs. $\hat{\mathbf{u}}^{\mathbf{DRTO}}$, $\hat{\mathbf{x}}^{\mathbf{DRTO}}$ and $\hat{\mathbf{y}}^{\mathbf{DRTO}}$ are composite vectors comprising all the DRTO inputs, states and outputs over the optimization horizon

$j \in [0, \ldots, N-1]$:

$$\hat{\mathbf{u}}^{\mathbf{DRTO}} = \left[(\hat{\mathbf{u}}_0^{\mathbf{DRTO}})^{\mathrm{T}},\ (\hat{\mathbf{u}}_1^{\mathbf{DRTO}})^{\mathrm{T}}, \ldots, (\hat{\mathbf{u}}_{N-1}^{\mathbf{DRTO}})^{\mathrm{T}} \right]^{\mathrm{T}}$$
$$\hat{\mathbf{x}}^{\mathbf{DRTO}} = \left[(\hat{\mathbf{x}}_1^{\mathbf{DRTO}})^{\mathrm{T}},\ (\hat{\mathbf{x}}_2^{\mathbf{DRTO}})^{\mathrm{T}}, \ldots, (\hat{\mathbf{x}}_N^{\mathbf{DRTO}})^{\mathrm{T}} \right]^{\mathrm{T}}$$
$$\hat{\mathbf{y}}^{\mathbf{DRTO}} = \left[(\hat{\mathbf{y}}_1^{\mathbf{DRTO}})^{\mathrm{T}},\ (\hat{\mathbf{y}}_2^{\mathbf{DRTO}})^{\mathrm{T}}, \ldots, (\hat{\mathbf{y}}_N^{\mathbf{DRTO}})^{\mathrm{T}} \right]^{\mathrm{T}}$$

Φ^{Econ} is an economic objective function, $\mathbf{f}^{\mathbf{DRTO}}$ represents the dynamic model utilized for DRTO prediction, $\mathbf{h}^{\mathbf{DRTO}}$ are equality constraints that relate the states to the outputs, and $\mathbf{g}^{\mathbf{DRTO}}$ comprises inequality constraints on the outputs and possibly some of the states. Note that input constraints are not imposed at the primary DRTO optimization problem, but they addressed by the input-constrained MPC optimization subproblems. The time index j corresponds to the MPC sample interval. Equality $\mathbf{h}^{\mathbf{Ref}}$ enforces the reference trajectories to be piecewise constant for every DRTO interval within the optimization horizon (found to be useful to reduce aggressive changes in the optimal trajectory of the tracking set-points) and also relates the overall reference trajectories to the set-point trajectories for the MPC optimization subproblems (described in more detail later). Inequality $\mathbf{g}^{\mathbf{Ref}}$ defines the upper and lower bounds of the reference trajectories. $\hat{\mathbf{d}}_{0,k}$ defines the disturbance estimate of MPC subproblem at DRTO prediction step $j = 0$, which is computed based on the current output measurement ($\mathbf{y}^{\mathbf{m}}_{j^*}$) and the output prediction at the previous controller sampling instance.

The DRTO closed-loop prediction is performed through implementation of the first vector of the MPC input trajectory from each MPC optimization subproblem. Input initialization and the initial state estimate in the MPC optimization subproblems are determined as in Eqs. (3.2) and (3.3), and applied as well in the closed-loop approximation formulations presented in the next sections.

Tracking set-points $\mathbf{y}^{\mathbf{SP}}$ and $\mathbf{u}^{\mathbf{SP}}$ for each MPC optimization subproblem are constructed from the DRTO composite reference trajectories, $\mathbf{y}^{\mathbf{Ref}}$ and $\mathbf{u}^{\mathbf{Ref}}$, as

$$\mathbf{y}^{\mathbf{SP}}_{j,k} = \mathbf{y}^{\mathbf{Ref}}_{j+k} \qquad j = 0, \ldots, N-1\ ,\ \ k = 1, \ldots, p$$
$$\mathbf{u}^{\mathbf{SP}}_{j,k} = \mathbf{u}^{\mathbf{Ref}}_{j+k} \qquad j = 0, \ldots, N-1\ ,\ \ k = 0, \ldots, m-1$$

with $\mathbf{y}^{\mathbf{Ref}}$ and $\mathbf{u}^{\mathbf{Ref}}$ defined as

$$\mathbf{y}^{\mathbf{Ref}} = \left[(\mathbf{y}_1^{\mathbf{Ref}})^{\mathrm{T}},\ (\mathbf{y}_2^{\mathbf{Ref}})^{\mathrm{T}}, \ldots, (\mathbf{y}_{N+p-1}^{\mathbf{Ref}})^{\mathrm{T}} \right]^{\mathrm{T}}$$
$$\mathbf{u}^{\mathbf{Ref}} = \left[(\mathbf{u}_0^{\mathbf{Ref}})^{\mathrm{T}},\ (\mathbf{u}_1^{\mathbf{Ref}})^{\mathrm{T}}, \ldots, (\mathbf{u}_{N+m-2}^{\mathbf{Ref}})^{\mathrm{T}} \right]^{\mathrm{T}}$$

The reference points beyond the DRTO prediction horizon are kept constant at the values corresponding

to time step $N-1$. The relationship between the DRTO reference trajectory and the MPC subproblem set-point trajectories is illustrated in Figure 3.3.

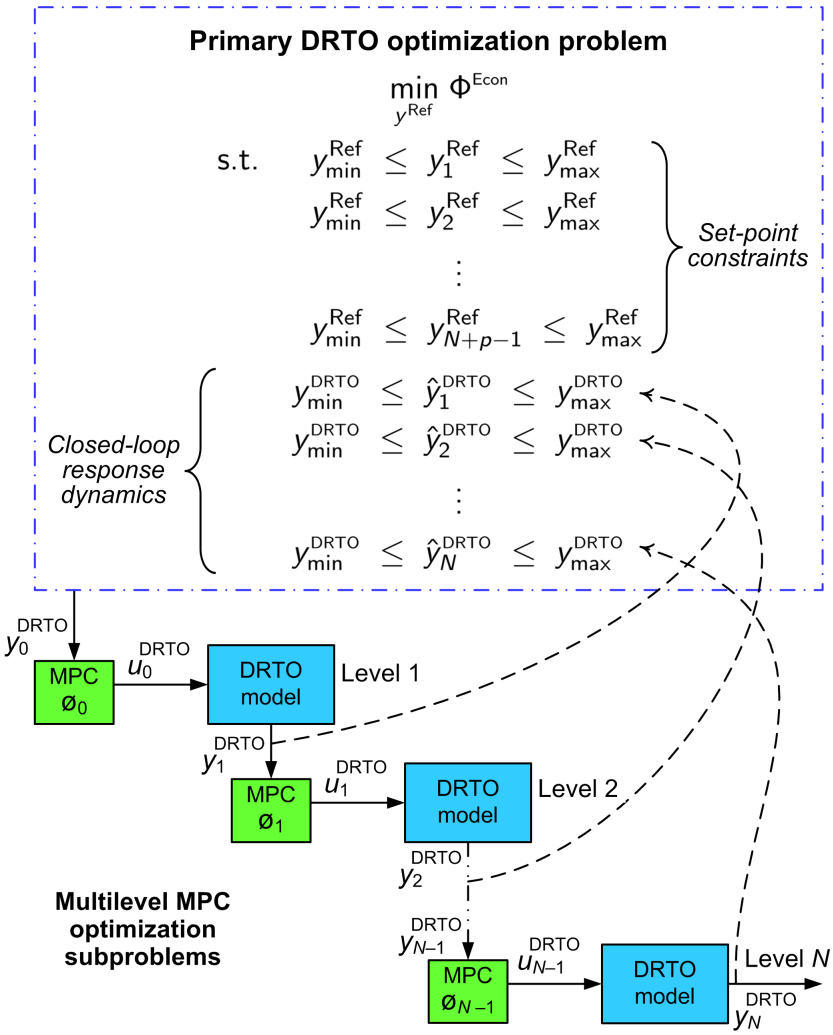

Figure 3.2: Illustration of the rigorous closed-loop prediction for DRTO calculations.

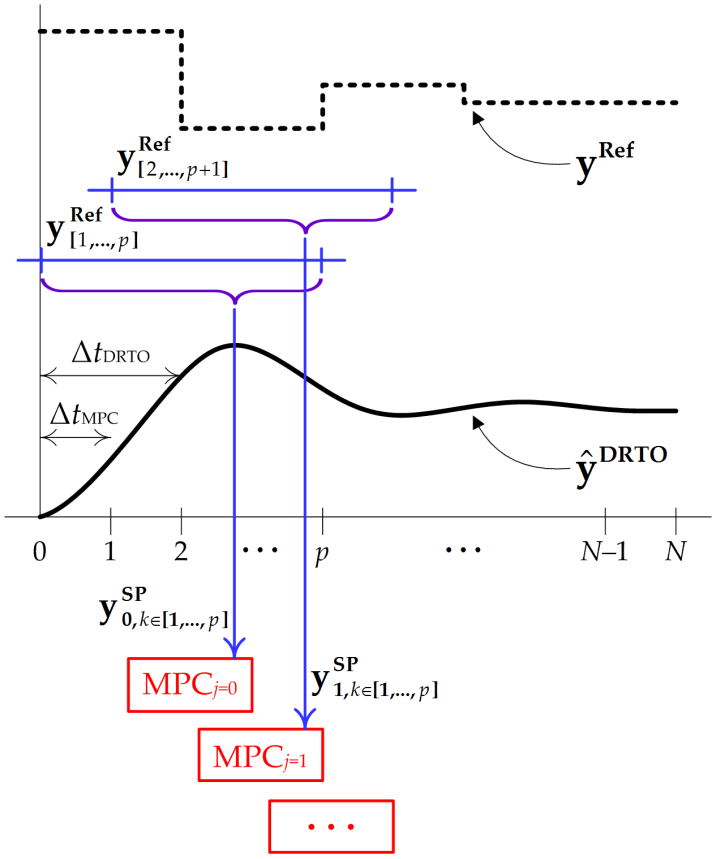

Figure 3.3: Illustration of set-point selection by the inner MPC subproblems.

In the following, we will present approximation approaches to predict the closed-loop response dynamics at the DRTO level. Although the construction of set-point trajectories for each approximation approach varies slightly from the rigorous formulation, implementation of the overall set-point (or reference) trajectories at the lower level controller is the same for all approaches.

3.2.3 Hybrid CL-DRTO Formulation

The hybrid prediction formulation involves the application of a rigorous closed-loop prediction from multilevel MPC optimization subproblems applied over a limited DRTO optimization horizon, after which an approximate closed-loop prediction from a single MPC calculation is used, as illustrated in Figure 3.4. The number of MPC optimization subproblems required for the rigorous closed-loop prediction portion of the DRTO horizon is determined by the number of MPC sampling intervals contained within the first DRTO optimization interval, given by $n = \Delta t_{\mathrm{DRTO}}/\Delta t_{\mathrm{MPC}}$; another MPC subproblem is needed to provide control inputs for the subsequent DRTO intervals. Here we have a primary DRTO economic optimization problem Eq. (3.5a), rigorous multilevel MPC optimization

subproblems Eq. (3.5b) that provide a control trajectory for the first DRTO interval, and another MPC subproblem Eq. (3.5c) that provides the control trajectory for the remainder of the optimization horizon. Rigorous closed-loop prediction entails application the control vector corresponding to the first control interval of each MPC subproblem at time steps $j \in [0, \ldots, n-1]$, whereas the approximate closed-loop prediction is generated from the full control trajectory of the last MPC subproblem at time step $j = n$.

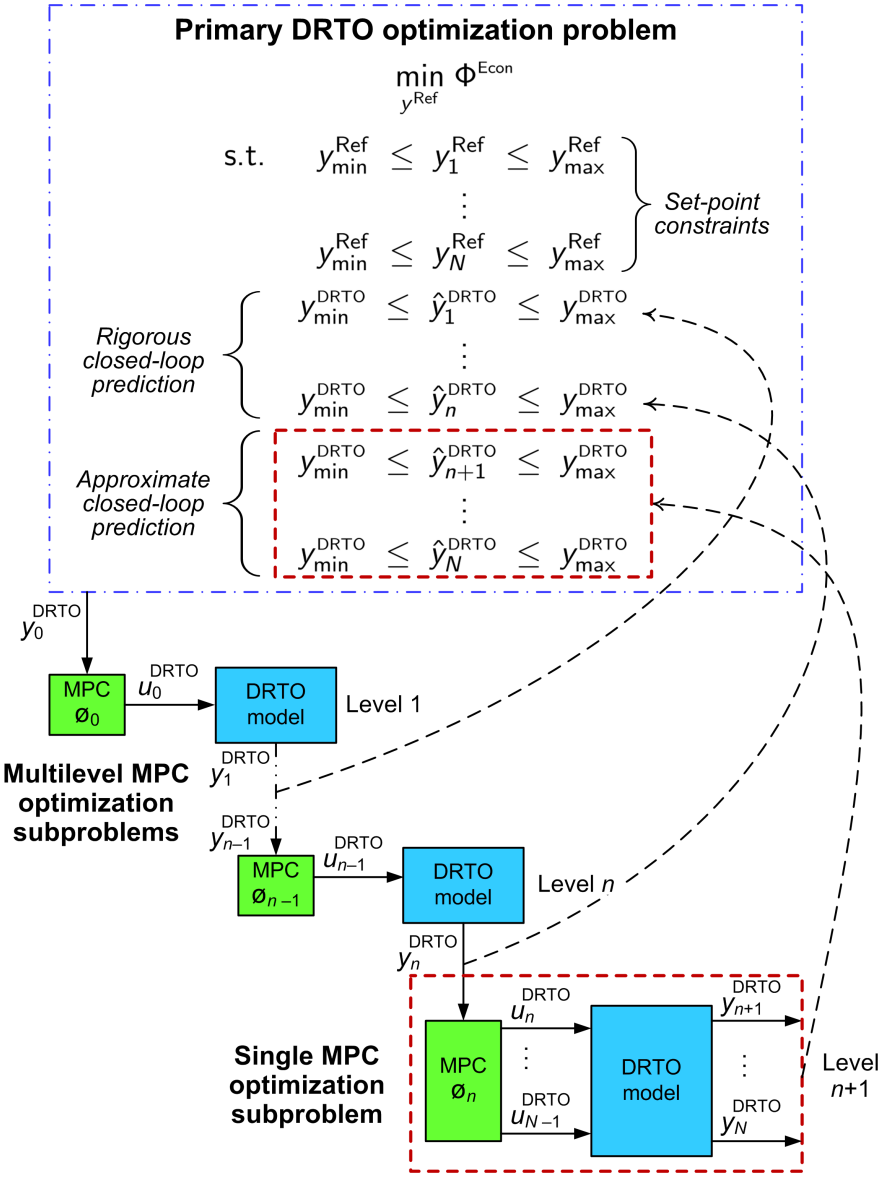

Figure 3.4: Illustration of the hybrid closed-loop prediction.

$$
\begin{aligned}
&\min_{\mathbf{y}^{\mathbf{Ref}},\,\mathbf{u}^{\mathbf{Ref}}} \Phi^{\text{Econ}}(\hat{\mathbf{x}}_j^{\mathbf{DRTO}},\,\hat{\mathbf{y}}_j^{\mathbf{DRTO}},\,\hat{\mathbf{u}}_j^{\mathbf{DRTO}}) \\
s.t.\quad & \hat{x}_{j+1}^{\mathbf{DRTO}} = \mathbf{f}^{\mathbf{DRTO}}(\hat{\mathbf{x}}_j^{\mathbf{DRTO}},\,\hat{\mathbf{u}}_j^{\mathbf{DRTO}}), \quad j = 0,\ldots,N-1 \\
& \hat{\mathbf{y}}_j^{\mathbf{DRTO}} = \mathbf{h}^{\mathbf{DRTO}}(\hat{\mathbf{x}}_j^{\mathbf{DRTO}}), \quad j = 1,\ldots,N \\
& \mathbf{0} \le \mathbf{g}^{\mathbf{DRTO}}(\hat{\mathbf{x}}_j^{\mathbf{DRTO}},\,\hat{\mathbf{y}}_j^{\mathbf{DRTO}}), \quad j = 1,\ldots,N \\
& \mathbf{0} = \mathbf{h}^{\mathbf{Ref}}(\mathbf{y}^{\mathbf{Ref}},\,\mathbf{u}^{\mathbf{Ref}},\,\hat{\mathbf{y}}^{\mathbf{SP}},\,\hat{\mathbf{u}}^{\mathbf{SP}},\,\tilde{\mathbf{y}}^{\mathbf{SP}},\,\tilde{\mathbf{u}}^{\mathbf{SP}}) \\
& \mathbf{0} \le \mathbf{g}^{\mathbf{Ref}}(\mathbf{y}_{j+1}^{\mathbf{Ref}},\,\mathbf{u}_j^{\mathbf{Ref}}), \quad j = 0,\ldots,N-1 \\
& \hat{\mathbf{u}}_j^{\mathbf{DRTO}} = \hat{\mathbf{u}}_{j,0}, \qquad j = 0,\ldots,n-1 \\
& \mathbf{u}_{j+k}^{\mathbf{DRTO}} = \tilde{\mathbf{u}}_k, \qquad j = n, \quad k = 0,\ldots,N-n-1 \\
& \hat{\mathbf{d}}_{0,k} = \mathbf{y}_{j^*}^{\mathbf{m}} - C\hat{\mathbf{x}}_{j^*-1,1}, \qquad k = 1,\ldots,p \\
& \hat{\mathbf{d}}_{j,k} = \hat{\mathbf{y}}_j^{\mathbf{DRTO}} - C\hat{\mathbf{x}}_{j-1,1}, \qquad j = 1,\ldots,n-1, \quad k = 1,\ldots,p \\
& \tilde{\mathbf{d}}_k = \hat{\mathbf{y}}_j^{\mathbf{DRTO}} - C\hat{\mathbf{x}}_{j-1,1}, \qquad j = n, \quad k = 1,\ldots,N-n
\end{aligned}
\tag{3.5a}
$$

$$
\left.
\begin{aligned}
\hat{\mathbf{u}}_{j,0} \in \arg\min_{\hat{\mathbf{u}}_{j,k}} \phi_j &:= \textstyle\sum_{k=1}^{p}(\hat{\mathbf{y}}_{j,k} - \hat{\mathbf{y}}_{j,k}^{\mathbf{SP}})^{\mathrm{T}} Q (\hat{\mathbf{y}}_{j,k} - \hat{\mathbf{y}}_{j,k}^{\mathbf{SP}}) + \textstyle\sum_{k=0}^{m-1} \boldsymbol{\Delta}\hat{\mathbf{u}}_{j,k}^{\mathrm{T}} R \boldsymbol{\Delta}\hat{\mathbf{u}}_{j,k} \\
&\quad + \textstyle\sum_{k=0}^{m-1}(\hat{\mathbf{u}}_{j,k} - \hat{\mathbf{u}}_{j,k}^{\mathbf{SP}})^{\mathrm{T}} S (\hat{\mathbf{u}}_{j,k} - \hat{\mathbf{u}}_{j,k}^{\mathbf{SP}}) \\
s.t.\quad \hat{\mathbf{x}}_{j,k+1} &= A\hat{\mathbf{x}}_{j,k} + B\hat{\mathbf{u}}_{j,k}, \quad k = 0,\ldots,m-1 \\
\hat{\mathbf{x}}_{j,k+1} &= A\hat{\mathbf{x}}_{j,k} + B\hat{\mathbf{u}}_{j,m-1}, \quad k = m,\ldots,p-1 \\
\hat{\mathbf{y}}_{j,k} &= C\hat{\mathbf{x}}_{j,k} + \hat{\mathbf{d}}_{j,k}, \quad k = 1,\ldots,p \\
\boldsymbol{\Delta}\hat{\mathbf{u}}_{j,k} &= \hat{\mathbf{u}}_{j,k} - \hat{\mathbf{u}}_{j,k-1}, \quad k = 0,\ldots,m-1 \\
\mathbf{u}_{\min} \;\le\; \hat{\mathbf{u}}_{j,k} \;&\le\; \mathbf{u}_{\max}, \quad k = 0,\ldots,m-1
\end{aligned}
\right\}
\begin{array}{c}\text{MPC} \\ \text{subproblems} \\ j = 0,\ldots,n-1\end{array}
\tag{3.5b}
$$

$$
\left.
\begin{aligned}
\tilde{\mathbf{u}} = \arg\min_{\tilde{\mathbf{u}}} \phi &:= \textstyle\sum_{k=1}^{N-n}(\tilde{\mathbf{y}}_k - \tilde{\mathbf{y}}_k^{\mathbf{SP}})^{\mathrm{T}} Q (\tilde{\mathbf{y}}_k - \tilde{\mathbf{y}}_k^{\mathbf{SP}}) + \textstyle\sum_{k=0}^{N-n-1} \boldsymbol{\Delta}\tilde{\mathbf{u}}_k^{\mathrm{T}} R \boldsymbol{\Delta}\tilde{\mathbf{u}}_k \\
&\quad + \textstyle\sum_{k=0}^{N-n-1}(\tilde{\mathbf{u}}_k - \tilde{\mathbf{u}}_k^{\mathbf{SP}})^{\mathrm{T}} S (\tilde{\mathbf{u}}_k - \tilde{\mathbf{u}}_k^{\mathbf{SP}}) \\
s.t.\quad \tilde{\mathbf{x}}_{k+1} &= A\tilde{\mathbf{x}}_k + B\tilde{\mathbf{u}}_k, \quad k = 0,\ldots,N-n-1 \\
\tilde{\mathbf{y}}_k &= C\tilde{\mathbf{x}}_k + \tilde{\mathbf{d}}_k, \quad k = 1,\ldots,N-n \\
\boldsymbol{\Delta}\tilde{\mathbf{u}}_k &= \tilde{\mathbf{u}}_k - \tilde{\mathbf{u}}_{k-1}, \quad k = 0,\ldots,N-n-1 \\
\mathbf{u}_{\min} \le \tilde{\mathbf{u}}_k &\le \mathbf{u}_{\max}, \quad k = 0,\ldots,N-n-1
\end{aligned}
\right\}
\begin{array}{c}\text{MPC} \\ \text{subproblem} \\ j = n\end{array}
\tag{3.5c}
$$

The controller design parameters of the embedded MPC optimization subproblems are identical to those of the controller implemented on the plant, except that the last MPC optimization subproblem has extended prediction and control horizons of $\tilde{p} = \tilde{m} = N - n$ so that there will be sufficient control vectors to generate the closed-loop response dynamics at the primary DRTO optimization problem, the prediction horizon of which is usually longer than that of the MPC.

The definition of variables involved in the hybrid formulation Eqs. (3.5a)-(3.5c) is analogous to the rigorous CL-DRTO formulation Eqs. (3.4a)-(3.4b) presented earlier. However, we differentiate the variables belonging to the rigorous and approximate MPC subproblems with a hat (ˆ) and a tilde (˜), respectively. MPC variables in subproblems Eq. (3.5b) are defined analogously to those in Eq. (3.1). $\tilde{\mathbf{u}}$ is a composite vector of control inputs of the final MPC optimization subproblem:

$$\tilde{\mathbf{u}} = \left[(\tilde{\mathbf{u}}_0)^{\mathrm{T}},\ (\tilde{\mathbf{u}}_1)^{\mathrm{T}}, \ldots, (\tilde{\mathbf{u}}_{N-n-1})^{\mathrm{T}}\right]^{\mathrm{T}}$$

The composite DRTO reference trajectories are defined as before, except that the hybrid formulation does not require the reference trajectories to be extended beyond the DRTO horizon (in contrast to the rigorous formulation):

$$\mathbf{y}^{\mathbf{Ref}} = \left[(\mathbf{y}_1^{\mathbf{Ref}})^{\mathrm{T}},\ (\mathbf{y}_2^{\mathbf{Ref}})^{\mathrm{T}}, \ldots, (\mathbf{y}_N^{\mathbf{Ref}})^{\mathrm{T}}\right]^{\mathrm{T}}$$
$$\mathbf{u}^{\mathbf{Ref}} = \left[(\mathbf{u}_0^{\mathbf{Ref}})^{\mathrm{T}},\ (\mathbf{u}_1^{\mathbf{Ref}})^{\mathrm{T}}, \ldots, (\mathbf{u}_{N-1}^{\mathbf{Ref}})^{\mathrm{T}}\right]^{\mathrm{T}}$$

The selection of the MPC set-point trajectories from the DRTO reference trajectories is the same as that given in Section 3.2.2 for the first DRO interval, but the set-points thereafter require only one index due to the single MPC formulation for the remainder of the optimization horizon:

$$\begin{aligned}
\hat{\mathbf{y}}_{j,k}^{\mathbf{SP}} &= \mathbf{y}_{j+k}^{\mathbf{Ref}}, \qquad j = 0, \ldots, n-1, \quad k = 1, \ldots, p \\
\hat{\mathbf{u}}_{j,k}^{\mathbf{SP}} &= \mathbf{u}_{j+k}^{\mathbf{Ref}}, \qquad j = 0, \ldots, n-1, \quad k = 0, \ldots, m-1 \\
\tilde{\mathbf{y}}_{k}^{\mathbf{SP}} &= \mathbf{y}_{k+n}^{\mathbf{Ref}}, \qquad k = 1, \ldots, N-n \\
\tilde{\mathbf{u}}_{k}^{\mathbf{SP}} &= \mathbf{u}_{k+n}^{\mathbf{Ref}}, \qquad k = 0, \ldots, N-n-1
\end{aligned}$$

where $\hat{\mathbf{y}}_{j,k}^{\mathbf{SP}}$ and $\hat{\mathbf{u}}_{j,k}^{\mathbf{SP}}$ are tracking set-points for the outputs and inputs at MPC prediction step k, for the MPC optimization subproblem embedded at DRTO prediction step $j \in [0, \ldots, n-1]$; $\tilde{\mathbf{y}}_{k}^{\mathbf{SP}}$ and $\tilde{\mathbf{u}}_{k}^{\mathbf{SP}}$ are the set-points at prediction step k for the final MPC optimization subproblem at time step $j = n$.

3.2.4 Bilevel CL-DRTO Formulation

In the bilevel formulation, as illustrated in Figure 3.5, only a single MPC optimization subproblem is utilized in which the prediction and control horizons are extended to match the DRTO optimization horizon such that $\tilde{p} = \tilde{m} = N$, while other controller tuning parameters are exactly the same as the MPC implemented at the lower level. Mathematically, we have a primary DRTO optimization problem Eq. (3.6a) and an inner MPC optimization subproblem Eq. (3.6b). The control trajectory from the MPC

optimization subproblem is assumed to be fully implemented to generate the closed-loop prediction at the primary optimization problem.

$$
\begin{aligned}
&\min_{\tilde{\mathbf{y}}^{\mathbf{SP}},\, \tilde{\mathbf{u}}^{\mathbf{SP}}} \Phi^{\text{Econ}}(\hat{\mathbf{x}}_j^{\mathbf{DRTO}},\ \hat{\mathbf{y}}_j^{\mathbf{DRTO}},\ \hat{\mathbf{u}}_j^{\mathbf{DRTO}}) \\
s.t.\quad & \hat{\mathbf{x}}_{j+1}^{\mathbf{DRTO}} = \mathbf{f}^{\mathbf{DRTO}}(\hat{\mathbf{x}}_j^{\mathbf{DRTO}},\ \hat{\mathbf{u}}_j^{\mathbf{DRTO}}), \quad j = 0,\ldots,N-1 \\
& \hat{\mathbf{y}}_j^{\mathbf{DRTO}} = \mathbf{h}^{\mathbf{DRTO}}(\hat{\mathbf{x}}_j^{\mathbf{DRTO}}), \quad j = 1,\ldots,N \\
& \mathbf{0} \le \mathbf{g}^{\mathbf{DRTO}}(\hat{\mathbf{x}}_j^{\mathbf{DRTO}},\ \hat{\mathbf{y}}_j^{\mathbf{DRTO}}), \quad j = 1,\ldots,N \\
& \mathbf{0} = \mathbf{h}^{\mathbf{Ref}}(\tilde{\mathbf{y}}^{\mathbf{SP}},\ \tilde{\mathbf{u}}^{\mathbf{SP}}) \\
& \mathbf{0} \le \mathbf{g}^{\mathbf{Ref}}(\tilde{\mathbf{y}}_{k+1}^{\mathbf{SP}},\ \tilde{\mathbf{u}}_k^{\mathbf{SP}}), \quad k = 0,\ldots,N-1 \\
& \tilde{\mathbf{d}}_k = \mathbf{y}_{j^*}^{\mathbf{m}} - C\hat{\mathbf{x}}_{j^*-1,1}, \quad k = 1,\ldots,N
\end{aligned}
\tag{3.6a}
$$

$$
\left.
\begin{aligned}
\hat{\mathbf{u}}^{\mathbf{DRTO}} = \arg\ \min_{\tilde{\mathbf{u}}}\ & \phi := \textstyle\sum_{k=1}^{N}(\tilde{\mathbf{y}}_k - \tilde{\mathbf{y}}_k^{\mathbf{SP}})^{\mathrm{T}} Q(\tilde{\mathbf{y}}_k - \tilde{\mathbf{y}}_k^{\mathbf{SP}}) + \textstyle\sum_{k=0}^{N-1} \boldsymbol{\Delta}\tilde{\mathbf{u}}_k^{\mathrm{T}} R \boldsymbol{\Delta}\tilde{\mathbf{u}}_k \\
& \qquad + \textstyle\sum_{k=0}^{N-1}(\tilde{\mathbf{u}}_k - \tilde{\mathbf{u}}_k^{\mathbf{SP}})^{\mathrm{T}} S(\tilde{\mathbf{u}}_k - \tilde{\mathbf{u}}_k^{\mathbf{SP}}) \\
s.t.\quad & \tilde{\mathbf{x}}_{k+1} = A\tilde{\mathbf{x}}_k + B\tilde{\mathbf{u}}_k, \quad k = 0,\ldots,N-1 \\
& \tilde{\mathbf{y}}_k = C\tilde{\mathbf{x}}_k + \tilde{\mathbf{d}}_k, \quad k = 1,\ldots,N \\
& \boldsymbol{\Delta}\tilde{\mathbf{u}}_k = \tilde{\mathbf{u}}_k - \tilde{\mathbf{u}}_{k-1}, \quad k = 0,\ldots,N-1 \\
& \mathbf{u}_{\min} \le \tilde{\mathbf{u}}_k \le \mathbf{u}_{\max}, \quad k = 0,\ldots,N-1
\end{aligned}
\right\} \text{MPC subproblem}
\tag{3.6b}
$$

The definitions in problems Eq. (3.6a) and Eq. (3.6b) are analogous to those in the hybrid formulation described earlier. Vectors $\tilde{\mathbf{y}}^{\mathbf{SP}}$ and $\tilde{\mathbf{u}}^{\mathbf{SP}}$ are the output and input set-point trajectories over the horizon of the embedded MPC optimization subproblem, written as

$$
\begin{aligned}
\tilde{\mathbf{y}}^{\mathbf{SP}} &= \left[(\tilde{\mathbf{y}}_1^{\mathbf{SP}})^{\mathrm{T}}, (\tilde{\mathbf{y}}_2^{\mathbf{SP}})^{\mathrm{T}}, \ldots, (\tilde{\mathbf{y}}_N^{\mathbf{SP}})^{\mathrm{T}}\right]^{\mathrm{T}} \\
\tilde{\mathbf{u}}^{\mathbf{SP}} &= \left[(\tilde{\mathbf{u}}_0^{\mathbf{SP}})^{\mathrm{T}}, (\tilde{\mathbf{u}}_1^{\mathbf{SP}})^{\mathrm{T}}, \ldots, (\tilde{\mathbf{u}}_{N-1}^{\mathbf{SP}})^{\mathrm{T}}\right]^{\mathrm{T}}
\end{aligned}
$$

In this formulation, there is a direct correspondence between the DRTO variables $\hat{\mathbf{x}}_j^{\mathbf{DRTO}}$, $\hat{\mathbf{y}}_j^{\mathbf{DRTO}}$, and $\hat{\mathbf{u}}_j^{\mathbf{DRTO}}$ with the MPC variables $\tilde{\mathbf{x}}_j$, $\tilde{\mathbf{y}}_j$, and $\tilde{\mathbf{u}}_j$, respectively. However, we utilize notation that differentiates between the DRTO variables in the primary problem and the MPC variables in the optimization subproblem for consistency with multilevel formulation, where the direct correspondence does not carry over.

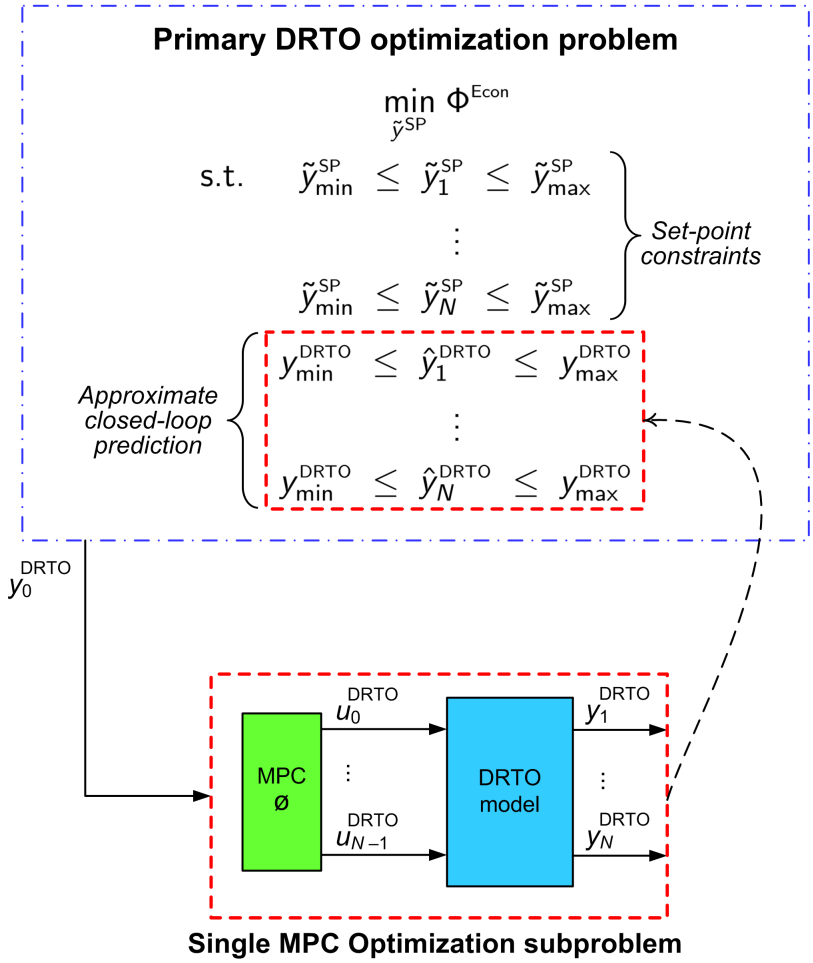

Figure 3.5: Illustration of the bilevel closed-loop prediction.

3.2.5 Input Clipping Formulation

Closed-loop approximation via input clipping involves use of an unconstrained MPC algorithm where an input saturation mechanism is applied over the DRTO optimization horizon using complementarity constraints. The input saturation mechanism is derived from logical conditions that determine the relationship between the controller output $\hat{\mathbf{u}}_j^{\mathbf{MPC}}$ computed by the unconstrained MPC optimization subproblems at each DRTO prediction step $j \in [0, \ldots, N-1]$ and the implemented DRTO input $\hat{\mathbf{u}}_j^{\mathbf{DRTO}}$ at the primary optimization problem, given as follows:

$$\hat{\mathbf{u}}_j^{\mathbf{DRTO}} = \begin{cases} \mathbf{u}_{\min}, & \hat{\mathbf{u}}_j^{\mathbf{MPC}} < \mathbf{u}_{\min} \\ \hat{\mathbf{u}}_j^{\mathbf{MPC}}, & \mathbf{u}_{\min} \leq \hat{\mathbf{u}}_j^{\mathbf{MPC}} \leq \mathbf{u}_{\max} \\ \mathbf{u}_{\max}, & \hat{\mathbf{u}}_j^{\mathbf{MPC}} > \mathbf{u}_{\max} \end{cases} \tag{3.7}$$

The logical conditions Eq. (3.7) are transformed to a continuous form amendable to standard optimization solvers as proposed in Baker and Swartz [29]. This involves introduction of slack variables $\boldsymbol{\eta}^1$ and $\boldsymbol{\eta}^2$ associated with the DRTO inputs, written as follows:

$$\hat{\mathbf{u}}_j^{\mathbf{DRTO}} = \hat{\boldsymbol{u}}_j^{\mathbf{MPC}} + \boldsymbol{\eta}_j^1 - \boldsymbol{\eta}_j^2 \tag{3.8}$$

The definition of these slack variables is such that if the control signal is in range with respect to the saturation limits of $\mathbf{u}_{\min}$ and $\mathbf{u}_{\max}$, then $\hat{\mathbf{u}}_j^{\mathbf{DRTO}} = \hat{\boldsymbol{u}}_j^{\mathbf{MPC}}$. In the event that one of the saturation limits becomes active, only then does the respective slack variable take on a positive value. Given that it is impossible for both saturation limits to be simultaneously active, the slack variables cannot both be non-zero at the same time instance. The conditional statements in Eq. (3.7) are therefore expressed as

$$\hat{\mathbf{u}}_j^{\mathbf{DRTO}} = \hat{\boldsymbol{u}}_j^{\mathbf{MPC}} + \boldsymbol{\eta}_j^1 - \boldsymbol{\eta}_j^2 \tag{3.9a}$$

$$\mathbf{0} = \boldsymbol{\eta}_j^1 \left(\hat{\mathbf{u}}_j^{\mathbf{DRTO}} - \mathbf{u}_{\min} \right) \tag{3.9b}$$

$$\mathbf{0} = \boldsymbol{\eta}_j^2 \left(\mathbf{u}_{\max} - \hat{\mathbf{u}}_j^{\mathbf{DRTO}} \right) \tag{3.9c}$$

$$\mathbf{u}_{\min} \leq \hat{\mathbf{u}}_j^{\mathbf{DRTO}} \leq \mathbf{u}_{\max} \tag{3.9d}$$

$$\mathbf{0} \leq \left(\boldsymbol{\eta}_j^1,\ \boldsymbol{\eta}_j^2 \right) \tag{3.9e}$$

Input constraint Eq. (3.9d) is subsequently transformed to equality constraints using slack variables by defining

$$\boldsymbol{\mu}_j^1 = \hat{\mathbf{u}}_j^{\mathbf{DRTO}} - \mathbf{u}_{\min}$$
$$\boldsymbol{\mu}_j^2 = \mathbf{u}_{\max} - \hat{\mathbf{u}}_j^{\mathbf{DRTO}}$$

This allows reformulation of the input saturation mechanism Eqs. (3.9a)-(3.9e) to a set of linear and complementarity constraints:

$$\begin{aligned}
\hat{\mathbf{u}}_j^{\mathbf{DRTO}} &= \hat{\boldsymbol{u}}_j^{\mathbf{MPC}} + \boldsymbol{\eta}_j^1 - \boldsymbol{\eta}_j^2 \\
\mathbf{0} &= \hat{\mathbf{u}}_j^{\mathbf{DRTO}} - \mathbf{u}_{\min} - \boldsymbol{\mu}_j^1 \\
\mathbf{0} &= \mathbf{u}_{\max} - \hat{\mathbf{u}}_j^{\mathbf{DRTO}} - \boldsymbol{\mu}_j^2 \\
\mathbf{0} &= \boldsymbol{\eta}_j^i \boldsymbol{\mu}_j^i, \quad i = 1,2 \\
\mathbf{0} &\leq \left(\boldsymbol{\eta}_j^i,\ \boldsymbol{\mu}_j^i \right), \quad i = 1,2
\end{aligned} \tag{3.10}$$

This construct for the input saturation mechanism can be readily embedded into the primary DRTO

optimization problem. The CL-DRTO formulation given below is based on the rigorous closed-loop prediction with the unconstrained MPC optimization subproblems repeated at each DRTO prediction step $j \in [0, \ldots, N-1]$, as represented by Eq. (3.11c). Although the general formulation given here is based on the rigorous closed-loop prediction, the input clipping approach is also applicable to the hybrid and bilevel CL-DRTO formulations. For the rigorous closed-loop prediction, input clipping is applied only to the first elements of the control trajectories of the corresponding MPC subproblems. Input clipping is applied to the entire control horizon of the final MPC optimization subproblem at time step $j = n$ in the hybrid formulation, and of the MPC optimization subproblem in the bilevel formulation.

$$
\begin{aligned}
&\min_{\mathbf{y}^{\mathbf{Ref}},\, \mathbf{u}^{\mathbf{Ref}}} \ \Phi^{\text{Econ}}(\hat{\mathbf{x}}^{\mathbf{DRTO}},\ \hat{\mathbf{y}}^{\mathbf{DRTO}},\ \hat{\mathbf{u}}^{\mathbf{DRTO}}) \\
\text{s.t.}\quad & \hat{\mathbf{x}}^{\mathbf{DRTO}}_{j+1} = \mathbf{f}^{\mathbf{DRTO}}(\hat{\mathbf{x}}^{\mathbf{DRTO}}_{j},\ \hat{\mathbf{u}}^{\mathbf{DRTO}}_{j}), \quad j = 0, \ldots, N-1 \\
& \hat{\mathbf{y}}^{\mathbf{DRTO}}_{j} = \mathbf{h}^{\mathbf{DRTO}}(\hat{\mathbf{x}}^{\mathbf{DRTO}}_{j}), \quad j = 1, \ldots, N \\
& \mathbf{0} \leq \mathbf{g}^{\mathbf{DRTO}}(\hat{\mathbf{x}}^{\mathbf{DRTO}}_{j},\ \hat{\mathbf{y}}^{\mathbf{DRTO}}_{j}), \quad j = 1, \ldots, N \qquad (3.11a) \\
& \mathbf{0} = \mathbf{h}^{\mathbf{Ref}}(\mathbf{y}^{\mathbf{Ref}},\ \mathbf{u}^{\mathbf{Ref}},\ \mathbf{y}^{\mathbf{SP}},\ \mathbf{u}^{\mathbf{SP}}) \\
& \mathbf{0} \leq \mathbf{g}^{\mathbf{Ref}}(\mathbf{y}^{\mathbf{Ref}}_{j+1},\ \mathbf{u}^{\mathbf{Ref}}_{j}), \quad j = 0, \ldots, N-1 \\
& \hat{\mathbf{d}}_{0,k} = \mathbf{y}^{\mathbf{m}}_{j^*} - C\hat{\mathbf{x}}_{j^*-1,1}, \quad k = 1, \ldots, p \\
& \hat{\mathbf{d}}_{j,k} = \hat{\mathbf{y}}^{\mathbf{DRTO}}_{j} - C\hat{\mathbf{x}}_{j-1,1}, \quad j = 1, \ldots, N-1, \quad k = 1, \ldots, p \\
& \left.\begin{aligned}
\hat{\mathbf{u}}^{\mathbf{DRTO}}_{j} &= \hat{\boldsymbol{u}}^{\mathbf{MPC}}_{j} + \boldsymbol{\eta}^1_j - \boldsymbol{\eta}^2_j, \quad j = 0, \ldots, N-1 \\
\mathbf{0} &= \hat{\mathbf{u}}^{\mathbf{DRTO}}_{j} - \mathbf{u}_{\min} - \boldsymbol{\mu}^1_j, \quad j = 0, \ldots, N-1 \\
\mathbf{0} &= \mathbf{u}_{\max} - \hat{\mathbf{u}}^{\mathbf{DRTO}}_{j} - \boldsymbol{\mu}^2_j, \quad j = 0, \ldots, N-1 \\
\mathbf{0} &= \boldsymbol{\eta}^i_j \boldsymbol{\mu}^i_j \qquad \forall i \in I, \quad j = 0, \ldots, N-1 \\
\mathbf{0} &\leq \left(\boldsymbol{\eta}^i_j,\ \boldsymbol{\mu}^i_j\right) \qquad \forall i \in I, \quad j = 0, \ldots, N-1
\end{aligned}\right\} \text{Input saturation mechanism} \qquad (3.11b) \\
& \hat{\boldsymbol{u}}^{\mathbf{MPC}}_{j} = \hat{\boldsymbol{u}}_{j,0}, \quad j = 0, \ldots, N-1 \\
& \left.\begin{aligned}
\hat{\mathbf{u}}_{j,0} \in \arg \min_{\hat{\mathbf{u}}_{j,k}} \ & \phi_j := \textstyle\sum_{k=1}^{p} (\hat{\mathbf{y}}_{j,k} - \mathbf{y}^{\mathbf{SP}}_{j,k})^{\mathrm{T}} Q (\hat{\mathbf{y}}_{j,k} - \mathbf{y}^{\mathbf{SP}}_{j,k}) + \textstyle\sum_{k=0}^{m-1} \boldsymbol{\Delta}\hat{\mathbf{u}}^{\mathrm{T}}_{j,k} R \boldsymbol{\Delta}\hat{\mathbf{u}}_{j,k} \\
& \qquad + \textstyle\sum_{k=0}^{m-1} (\hat{\mathbf{u}}_{j,k} - \mathbf{u}^{\mathbf{SP}}_{j,k})^{\mathrm{T}} S (\hat{\mathbf{u}}_{j,k} - \mathbf{u}^{\mathbf{SP}}_{j,k}) \\
s.t. \quad & \hat{\mathbf{x}}_{j,k+1} = A\hat{\mathbf{x}}_{j,k} + B\hat{\mathbf{u}}_{j,k}, \quad k = 0, \ldots, m-1 \\
& \hat{\mathbf{x}}_{j,k+1} = A\hat{\mathbf{x}}_{j,k} + B\hat{\mathbf{u}}_{j,m-1}, \quad k = m, \ldots, p-1 \\
& \hat{\mathbf{y}}_{j,k} = C\hat{\mathbf{x}}_{j,k} + \hat{\mathbf{d}}_{j,k}, \quad k = 1, \ldots, p \\
& \boldsymbol{\Delta}\hat{\mathbf{u}}_{j,k} = \hat{\mathbf{u}}_{j,k} - \hat{\mathbf{u}}_{j,k-1}, \quad k = 0, \ldots, m-1
\end{aligned}\right\} \begin{array}{c}\text{Unconstrained} \\ \text{MPC} \\ \text{subproblems,} \\ j = 0, \ldots, N-1\end{array} \qquad (3.11c)
\end{aligned}
$$

3.2.6 Solution Strategy

In this study, we employ a simultaneous solution approach by transforming the constrained MPC optimization subproblems to algebraic equations using their first-order, Karush-Kuhn-Tucker (KKT) optimality conditions. For a constrained MPC problem formulated as a convex quadratic programming (QP) problem as considered in this study, such a transformation is valid as the KKT conditions are necessary and sufficient for optimality. The MPC subproblem at each DRTO prediction step may be represented as a QP of the form:

$$\begin{aligned} \min_{\mathbf{z}} \ & \frac{1}{2}\mathbf{z}^{\mathrm{T}} H\mathbf{z} + \mathbf{g}^{\mathrm{T}}\mathbf{z} \\ \text{s.t.} \quad & A\mathbf{z} = \mathbf{b} \\ & \mathbf{z} \geq \mathbf{0} \end{aligned} \tag{3.12}$$

with the corresponding KKT conditions given by

$$\begin{aligned} H\mathbf{z} + \mathbf{g} - A^{\mathrm{T}}\boldsymbol{\lambda} - \boldsymbol{\nu} &= \mathbf{0} \\ A\mathbf{z} - \mathbf{b} &= \mathbf{0} \\ z_i\nu_i = 0, \quad i &= 1, ..., I \\ (\mathbf{z},\ \boldsymbol{\nu}) &\geq \mathbf{0} \end{aligned} \tag{3.13}$$

A detailed derivation of the KKT conditions corresponding to the MPC optimization subproblem related to this study can be found in Baker and Swartz [30]. Replacement of the MPC optimization subproblems with the KKT conditions gives rise to a single-level mathematical program with complementarity constraints (MPCC).

The presence of complementarity constraints, which take the form $z_i\nu_i = 0$, generally poses difficulties for standard NLP formulations due to violation of constraint qualifications [31]. Effective handling of complementarity constraints requires reformulation of the MPCC, or an alternative NLP algorithm that internally treats the complementarity constraints. In this study, an exact penalty formulation [32] is applied, in which the complementarity constraints are moved from the constraint set of the original MPCC problem to the objective function as an additional penalty term with a penalty parameter ρ of the form $\rho\sum_i^I z_i\nu_i$, with the resulting problem posed to a standard NLP solver.

3.2.7 Economic Objective Function

Our case studies consider product grade transition, a common operating practice in the polymerization industry that typically involves a sequence of product grade changeovers over a predetermined production schedule. Revenue is assumed to accrue only when the product quality lies within a given specification band. The times at which the product quality enters or leaves the band are not known a priori; adherence to the specification limits is captured through continuous hyperbolic tangent function approximations to discrete switching functions, as proposed by Tousain [33]. This is illustrated in Figure 3.6, in which an output y is driven from y^{initial} to y^{target}, where it is allowed to vary within a strict tolerance of $\pm\delta y^{\text{target}}$. Revenue accrues only when y lies in the intersection of regions $y \geq y^{\text{target}} - \delta y^{\text{target}}$ and $y \leq y^{\text{target}} + \delta y^{\text{target}}$, with associated switching functions defined by R^1 and R^2:

$$R^1 = \frac{1}{2}\tanh\left[\gamma(y - y^{\text{target}} + \delta y^{\text{target}})\right] + \frac{1}{2} \approx \begin{cases} 0, & y < y^{\text{target}} - \delta y^{\text{target}} \\ 1, & y > y^{\text{target}} - \delta y^{\text{target}} \end{cases}$$

$$R^2 = \frac{1}{2}\tanh\left[\gamma(y^{\text{target}} + \delta y^{\text{target}} - y)\right] + \frac{1}{2} \approx \begin{cases} 0, & y > y^{\text{target}} + \delta y^{\text{target}} \\ 1, & y < y^{\text{target}} + \delta y^{\text{target}} \end{cases}$$

where γ is a weighting parameter used to define the steepness of the switching function. In the optimization formulation, the product revenue expression is multiplied by R^1R^2, which is approximately 1 when the product is within the specification limits, and zero otherwise.

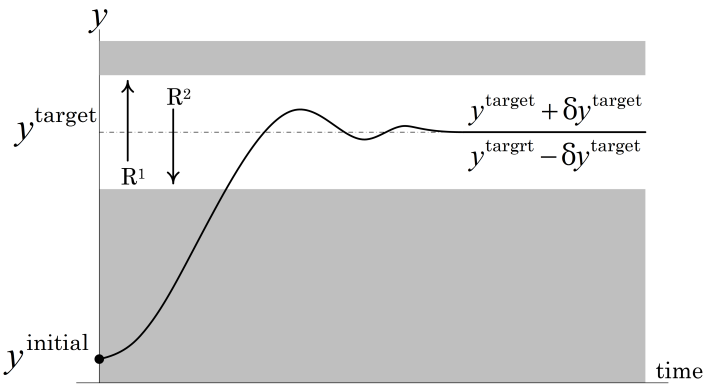

Figure 3.6: Tracking dynamic economics using hyperbolic tangent function.

3.3 Case Studies

In Section 3.3.1, the performance of the proposed closed-loop approximation approaches is analyzed using a case study involving a linear dynamic system. In the Section 3.3.2, the approximation ap-

proaches are applied to to a nonlinear dynamic model of a polystyrene production reactor system with consideration of plant-model mismatch and a disturbance. In all case studies, steady-state transitions are considered with the objective of maximizing profit. Dynamic models describing the systems' behaviour are discretized to state-space models in MATLAB based on the controller sample time for implementation in the MPC and DRTO formulations.

Real-time implementation of the two-level DRTO/MPC configuration in the case studies follows the schematic diagram illustrated in Figure 3.7. At each time step t_{j^*}, the DRTO receives feedback information and performs economic optimization to compute the set-point trajectories, $\mathbf{y}_j^{\mathbf{SP}}$ and $\mathbf{u}_j^{\mathbf{SP}}$, to be prescribed to the MPC level. Economic optimization is computed based on the aforementioned closed-loop approximation approaches, as well as the rigorous DRTO formulation as a performance benchmark. DRTO calculations are performed periodically based on a predetermined optimization interval of Δt_{DRTO}. The MPC tracks the reference trajectories at a sampling interval of Δt_{MPC}, which is smaller than that of the DRTO. It computes the optimal control inputs, $\hat{\mathbf{u}}_j$, for plant implementation. The plant level generally consists of continuous process operation, which may also include local PID controllers. Output feedback $\mathbf{y}_j^{\mathbf{m}}$ is used to compute a disturbance bias update in the DRTO and MPC formulations.

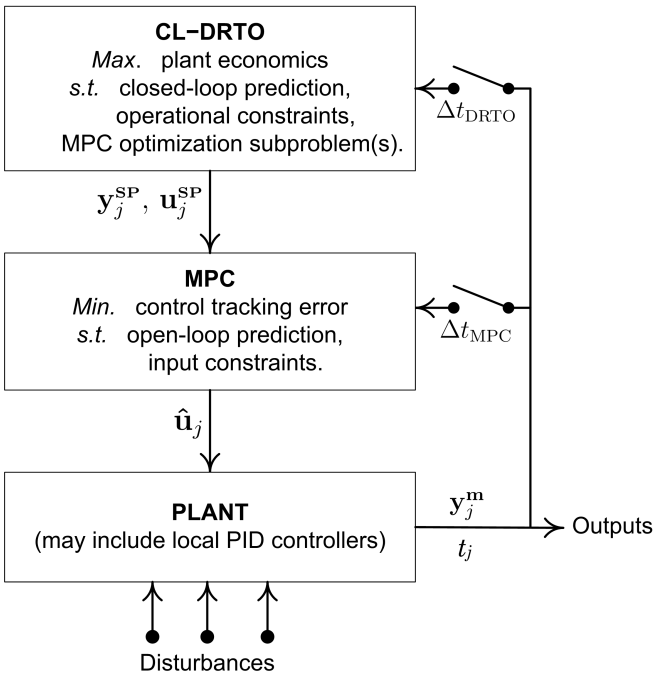

Figure 3.7: Real-time implementation of the two-level DRTO/MPC configuration.

In this work, MATLAB R2012b is chosen as a supervisory computational platform to solve the MPC problem using the `quadprog` solver and also to perform process simulation, while the DRTO problem is modelled in AMPL and solved using `IPOPT 3.12.0` [34] utilizing the linear solver `ma27`. An in-house

interface developed in PYTHON to allow communication between MATLAB and AMPL is used. All case studies are solved using a 3.4GHz INTEL CORE-i7 with 8GB RAM running Windows 7.

3.3.1 Performance Analysis

The case study considered here is a nonsquare system with two manipulated inputs and a single output (MISO), described as

$$y(s) = \frac{1}{750s^2 + 65s + 1}u_1(s) + \frac{1}{400s^2 + 40s + 1}u_2(s)$$

Output y responds faster to input u_2, and the cost of input u_2 is higher than that of input u_1. Since input u_2 has a significant impact on the transition dynamics and the overall process economics, we include it as a manipulated variable with a set-point trajectory, in addition to the set-point for output y. The economic objective and problem constraints are

$$\begin{aligned} \min \quad & \Delta t_{\text{MPC}} \sum_{j=0}^{N-1} \left(2u_{1,j} + 10u_{2,j} - 100R^1_{j+1}R^2_{j+1}\right) \\ & 0 \leq y,\ y^{\text{Ref}} \leq 1.1 \\ & 0 \leq u_1,\ u_2,\ u_2^{\text{Ref}} \leq 1.5 \end{aligned} \tag{3.14}$$

The system is discretized based on an MPC sample time of 2 min. The nominal MPC design parameters are as follows: prediction horizon $p = 30$, control horizon $m = 3$, output tracking weight $Q = 1$, move suppression weight $R = \text{diag}(1, 1)$, and control tracking weight $S = \text{diag}(0, 1)$. A DRTO sample time of 20 min is used, with a DRTO prediction horizon of 300 min (i.e. $N = 150$). A penalty parameter value of 80 is used for the complementarity constraints. The system is brought from the initial steady-state to the desired target of 1.0 ± 0.1 in output y. R^1 and R^2 are outputs of hyperbolic tangent switching function approximations described earlier.

Table 3.1 compares the performance of the proposed closed-loop approximation approaches relative to the rigorous formulation. In this case study, the rigorous formulation involves 57,743 optimization variables with an average solution time of 5.6 CPU(s) per DRTO execution. The hybrid formulation, applied with constrained and unconstrained MPC optimization subproblems (the latter with input clipping), reduces the dimension of the closed-loop prediction by a factor of approximately seven, while retaining up to 99.7% of the economic return obtained with the rigorous closed-loop formulation, i.e. 0.3% loss in the economics. The hybrid formulations contain ten MPC optimization subproblems within the first DRTO interval for rigorous closed-loop prediction, which is given by $n = \Delta t_{\text{DRTO}}/\Delta t_{\text{MPC}}$,

and also an additional extended horizon MPC optimization subproblem for approximate closed-loop prediction. This results in 9,079 and 8,198 optimization variables for the hybrid formulation that utilizes a constrained and unconstrained MPC algorithm, respectively. A substantial reduction in of problem size can be be achieved, particularly if the MPC formulation has a long control horizon. We note here that the input clipping approach can also be applied to the rigorous multilevel and bilevel CL-DRTO formulations.

The bilevel formulation approximates the closed-loop prediction with only 5,077 optimization variables, thus having the smallest problem size in comparison to the other CL-DRTO formulations. The bilevel formulation has an economic loss of 3.23% relative to the rigorous multilevel formulation, which is still very small compared that of an open-loop DRTO strategy, which has a relative economic offset of 16.45%. The substantial reduction in computation time achievable with the closed-loop approximation techniques increases the potential application of the closed-loop DRTO strategy to larger and more complex problems. We observe an average solution time of approximately 1.0 CPU(s) per DRTO calculation for all closed-loop approximation approaches as well as the implementation of OL-DRTO formulation.

Table 3.1: Performance comparison of DRTO formulations in MISO case study.

DRTO formulation	# var.	Ave. CPU(s)	Economics ($)	Loss (%)
Rigorous formulation	57,743	5.6	7,371	–
Hybrid formulation	9,079	1.0	7,348	0.31
Hybrid formulation with clipping	8,198	0.9	7,346	0.34
Bilevel formulation	5,077	0.8	7,133	3.23
Open-loop formulation	1,039	0.9	6,158	16.45

We next explore the effect of the approximation formulations on the number of complementarity variables. The complementarities arise from the KKT conditions of the embedded MPC optimization subproblem(s), and the reformulation of the clipping constraint logical conditions. Figure 3.8 illustrates the growth in the number of complementarity variables with control horizon, m. For the rigorous formulation, the number of complementarity variables grows dramatically with an increase in the MPC control horizon. We also note here that an increase in the length of DRTO prediction horizon increases the number of MPC optimization subproblems which results in a growing number of complementarity constraints. The hybrid formulation largely reduces the number of complementarity constraints due to a significant reduction in the number of MPC optimization subproblems applied over the DRTO optimization horizon. The advantage of the bilevel formulation and input clipping approach is that they are insensitive to the length of MPC control horizon, and dependent only on the length of DRTO prediction horizon. The input clipping approach eliminates the complementarity constraints needed to

handle input constraints in the embedded MPC optimization subproblems because an unconstrained MPC algorithm is utilized as an approximation to the actual input-constrained MPC implemented at the lower level. However, the input saturation mechanism considered at the primary optimization problem still makes use of complementarity constraints applied to the DRTO input trajectory, instead of to the input trajectory of each MPC subproblem. Therefore, the same number of complementarity variables is needed to formulate the saturation mechanism in the input clipping approach regardless of its application to either the rigorous, hybrid or bilevel formulation.

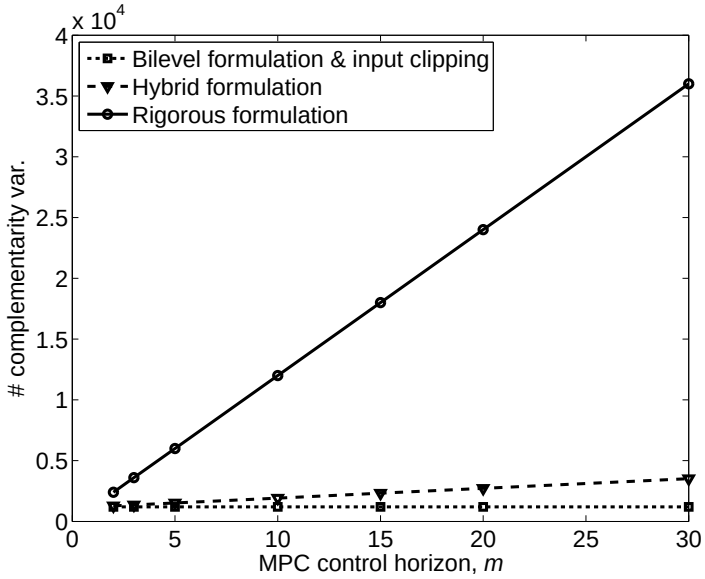

Figure 3.8: Scaling of complementarity variables with control move horizon.

System output dynamics and output set-points of the proposed closed-loop approximation approaches exhibit similar behavior, as illustrated in Figure 3.9. Input dynamics and input set-points for the hybrid formulations (applied with constrained and unconstrained MPC optimization subproblems) follow the same pattern as that of the rigorous formulation, as depicted in Figure 3.10. A slight difference is observed for the case of the bilevel formulation. The set-point trajectories shown correspond to the first portion of the DRTO reference trajectories (of length Δt_{DRTO}) computed at each DRTO execution. Overall, excellent approximation of the closed-loop prediction is obtained from all approaches. Significant reduction in problem size and solution time are achieved in comparison to the rigorous formulation, while the economics are largely retained. Although the economic performance of the hybrid formulations exceeds that of the bilevel programming approach, the later could be useful for modeling of large-scale systems.

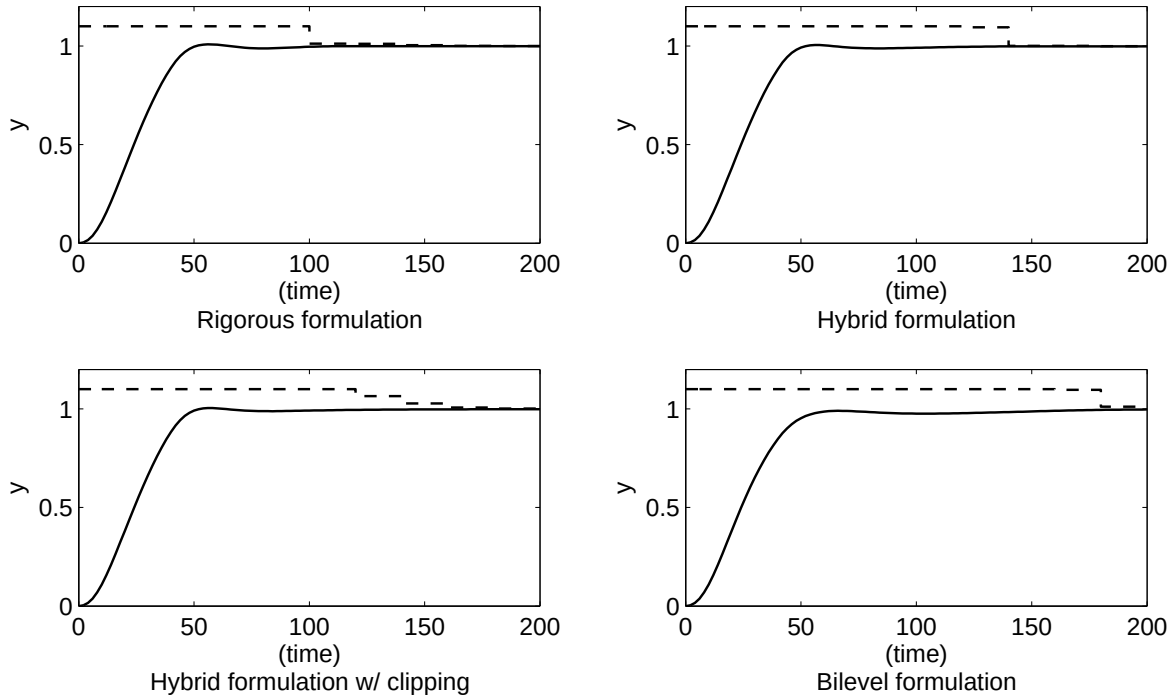

Figure 3.9: Closed-loop response dynamics of the MISO case study.
Legend: *solid lines* = output trajectories, *dashed lines* = set-point trajectories.

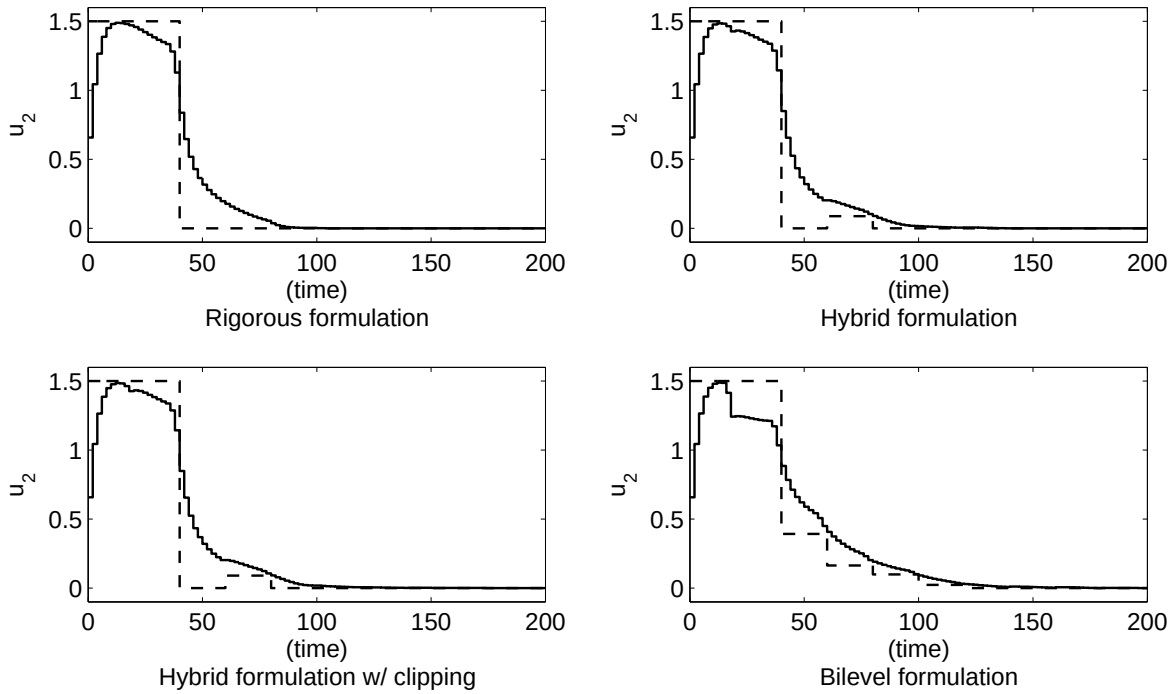

Figure 3.10: Closed-loop response dynamics of the MISO case study.
Legend: *solid lines* = input trajectories, *dashed lines* = set-point trajectories.

3.3.2 Application to Polymer Grade Transition

We consider in this section a polystyrene grade transition case study to which the proposed closed-loop approximation approaches are applied. It involves the polymerization of styrene in a constant-volume CSTR, as depicted in Figure 3.11, that requires three main ingredients comprising styrene monomer, azobisisobutyronitrile (AIBN) initiator and isopropyle benzene solvent. Sufficient solvent supply to the reactor is essential to avoid the "gel" effect, a phenomenon that describes a rapid increase in the viscosity of the polymerization mixture which alters the desired polymer characteristics and potentially leads to process runaway.

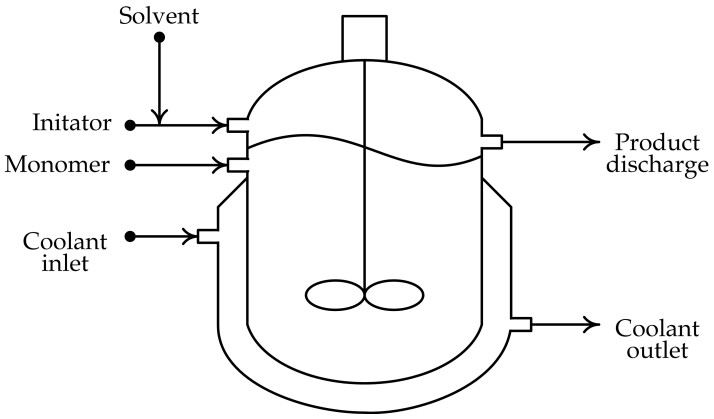

Figure 3.11: Polystyrene reactor.

The dynamic model used in this case study is taken from Maner et al. [35], and based on the original work by Hidalgo and Brosilow [36]. The model is scaled as described in Russo and Bequette [37] to avoid potential numerical problems in the optimization and simulation studies. Model equations, nominal simulation data and scaling parameters used in this case study are provided in Appendix A. A linearized polystyrene model is utilized in the DRTO and MPC formulations, and the nonlinear model is used to perform process simulation. This indirectly introduces plant-model mismatch in our case study simulations. Linearization of the continuous DAE system at the nominal operating point is carried out in MATLAB by computing state-space model matrices using a complex-step differentiation, and the linearized model is subsequently discretized based on the controller sample time.

In this polymerization system, production load mainly depends on the monomer fed into the reactor while an appropriate adjustment of initiator flow rate controls the specified polymer grade, which is commonly characterized by the number average molecular weight (NAMW). The polymerization reaction is highly exothermic, and therefore efficient temperature control is vital for economic and safety reasons. A summary of the chosen manipulated inputs and controlled outputs, and optimization problem parameters are reported in Table 3.2. Tracking set-points are provided for the polymer NAMW,

Table 3.2: Polystyrene case study data.

Variables	Parameters	
	MPC	DRTO
Manipulated inputs:	$p = 15$	$N = 50$
Initiator feed, Q_i (L/hr)	$m = 3$	$\rho = 0.5$
Monomer feed, Q_m (L/hr)	$Q = \text{diag}(1.5, 3)$	$\gamma = 5$
Coolant supply, Q_c (L/hr)	$R = \text{diag}(50, 20, 2)$	$\Delta t_{\text{DRTO}} = 5$ hr
Controlled outputs:	$S = \text{diag}(0, 2, 0)$	
Polymer grade, $NAMW$ (kg/mol)	$\Delta t_{\text{MPC}} = 1$ hr	
Reactor temperature, T (K)		

reactor temperature and monomer feed flow rate in order to maintain the desired polymer grade specifications, to ensure smooth and safe operation, and to help maintain high reactor productivity. We also assume that there is a sufficient solvent-monomer feed ratio to prevent the "gel" effect in the operation, and therefore the solvent feed flow rate is kept constant.

The production profit takes into account the revenue of polymer product that is within the specified grade tolerance, as well as the costs of raw materials and cooling supply. Accordingly, the DRTO economic objective function is written as follows:

$$\min \Phi = \Delta t_{\text{MPC}} \sum_{j=0}^{N-1} \left(C_i Q_{i,j} + C_m Q_{m,j} + C_c Q_{c,j} - P_p Q_{t,j+1} R^1_{j+1} R^2_{j+1} \right) \tag{3.15}$$

where C_i is the cost of the initiator (\$0.1/L), C_m is the cost of the monomer (\$0.50/L), C_c is the cost of the cooling supply (\$0.01/L), and Q_t is an inferred estimate of the process throughput with P_p being the price of the desired polymer product (\$20/L) that is assumed constant for all polymer grades. R^1 and R^2 are hyperbolic tangent switching functions that indicate the economically feasible grade tolerances for the polymer produced. The solvent is also assumed to be recovered and recycled, and the related operation cost is not considered in this study. Constraints on the inputs, outputs and reference trajectories are applied as follows:

$$0 \leq Q_i \leq 300$$
$$0 \leq Q_m,\ Q_m^{\text{Ref}} \leq 400$$
$$0 \leq Q_c \leq 700$$
$$46 \leq NAMW,\ NAMW^{\text{Ref}} \leq 71$$
$$315 \leq T,\ T^{\text{Ref}} \leq 325$$

with units as indicated in Table 3.2. An end-point constraint is also enforced at the DRTO level to ensure that the DRTO reference trajectory of the polymer NAMW meets the desired specification at the

end of the optimization horizon. The desired polymer grades are allowed to vary within a tolerance of $\pm 3\%$. It is desirable that the DRTO reoptimization interval be smaller than the process settling time to allow appropriate adjustments be made to the reference trajectories during the course of grade transition. Since the settling time of the system can be up to 20 hr, an optimization interval of 5 hr is chosen for the DRTO calculations.

The polymer reactor runs two production campaigns over a 100 hr simulation time frame. The process transitions from the nominal operating condition to Grade A (NAMW of 58 kg/mol) at the initial simulation time, and then to Grade B (NAMW of 69 kg/mol) at time 50 hr. We also consider a disturbance scenario involving a pulse disturbance change in the reactor feed temperature of $\Delta T_f = -1$ K from the initial steady-state of 330 K, which occurs during the course of grade transition between time 40 and 75 hrs.

Table 3.3 summarizes the problem size and solution statistics of the implemented closed-loop DRTO approaches. The rigorous formulation contains 19,839 optimization variables with an average solution time of 6.3 CPU(s) per DRTO calculation. The hybrid and bilevel formulations reduce the original problem size by factors of approximately four and seven, respectively, with average solution times decreased by a factor of six. On the economics aspect, the hybrid formulation gives an excellent approximation to the rigorous closed-loop formulation by retaining 99.75% of the economic return. The bilevel formulation demonstrates good performance with only 2.98% of economic loss relative to the rigorous approach.

Table 3.3: Problem dimension and results of the polystyrene case study.

Nominal case study	# var.	Ave. CPU(s)	Economics ($)	Loss (%)
Rigorous formulation	19,839	6.3	15,816	—
Hybrid formulation	4,760	1.0	15,776	0.25
Bilevel formulation	2,787	1.3	15,345	2.98

Overall, the optimal polymer grade transitions based on the implemented closed-loop approximation approaches are consistent with results generated by the rigorous formulation, as illustrated in Figures 3.12 to 3.14. Updating the set-point trajectories at every DRTO interval drives the polymer grade transitions in a cost-optimal fashion, and also helps to maintain the polymer grades within the specified product quality bands. On the other hand, the reactor operating temperature is mostly driven to the upper limit, which implies a lower cooling cost. Appropriate adjustments are made to the set-point point trajectories to minimize the degree of violation of product and constraint specifications in the presence of plant-model mismatch and a disturbance in the reactor feed temperature.

Smooth transition from the initial steady-state to polymer Grade A is obtained for all cases, with

minimal constraint violation in the polymer NAMW occuring during transition from Grade A to Grade B. An implicit backoff mechanism functions to move the set-point trajectories away from the upper bound tolerance of the polymer Grade B during the course of transition, as indicated between time 60 and 65 hrs in all cases, hence minimizing the magnitude of off-specification polymer productivity. The monomer feed is enforced to the maximum limit for much of the simulation time frame to allow a high reactor productivity, whereas initiator feed is the key manipulated input used to keep the polymer grades within the desired specifications. However, both the initiator and monomer feeds are simultaneously adjusted when a disturbance in the reactor feed temperature enters the system. The monomer concentration in the polystyrene reactor is low for the lower molecular weight polymer, and vice versa.

A drop in the reactor feed temperature between time 40 and 75 hrs causes the reactor temperature to fluctuate slightly around its upper bound within a magnitude of $\pm 0.6^{\circ}$C, hence affecting the rate of polymerization and the polymer grades. The temperature set-point trajectories of all approaches are adjusted appropriately to minimize the impact of such a disturbance, resulting in a substantial manipulation of the coolant flow rates within the prescribed constraint limits.

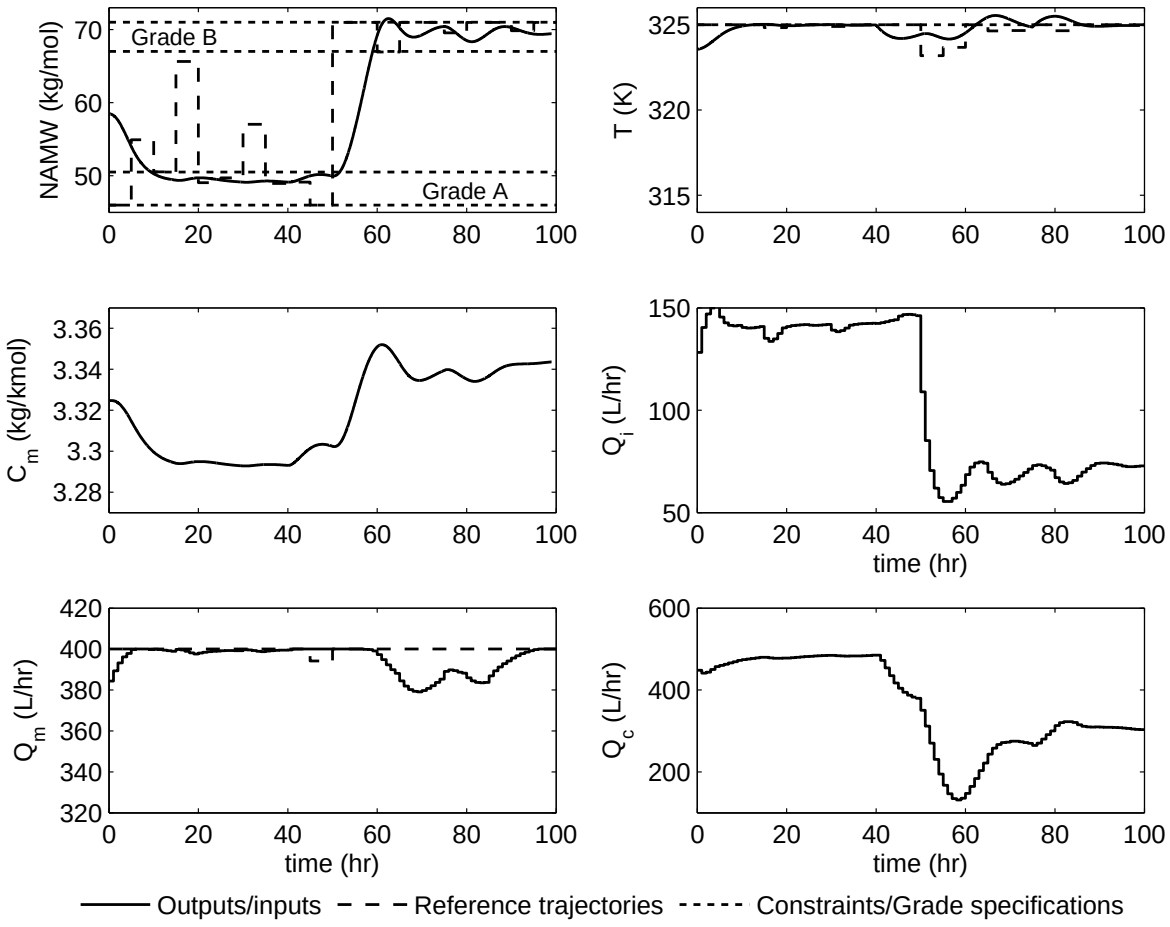

Figure 3.12: Optimal polymer grade transitions based on the rigorous DRTO formulation.

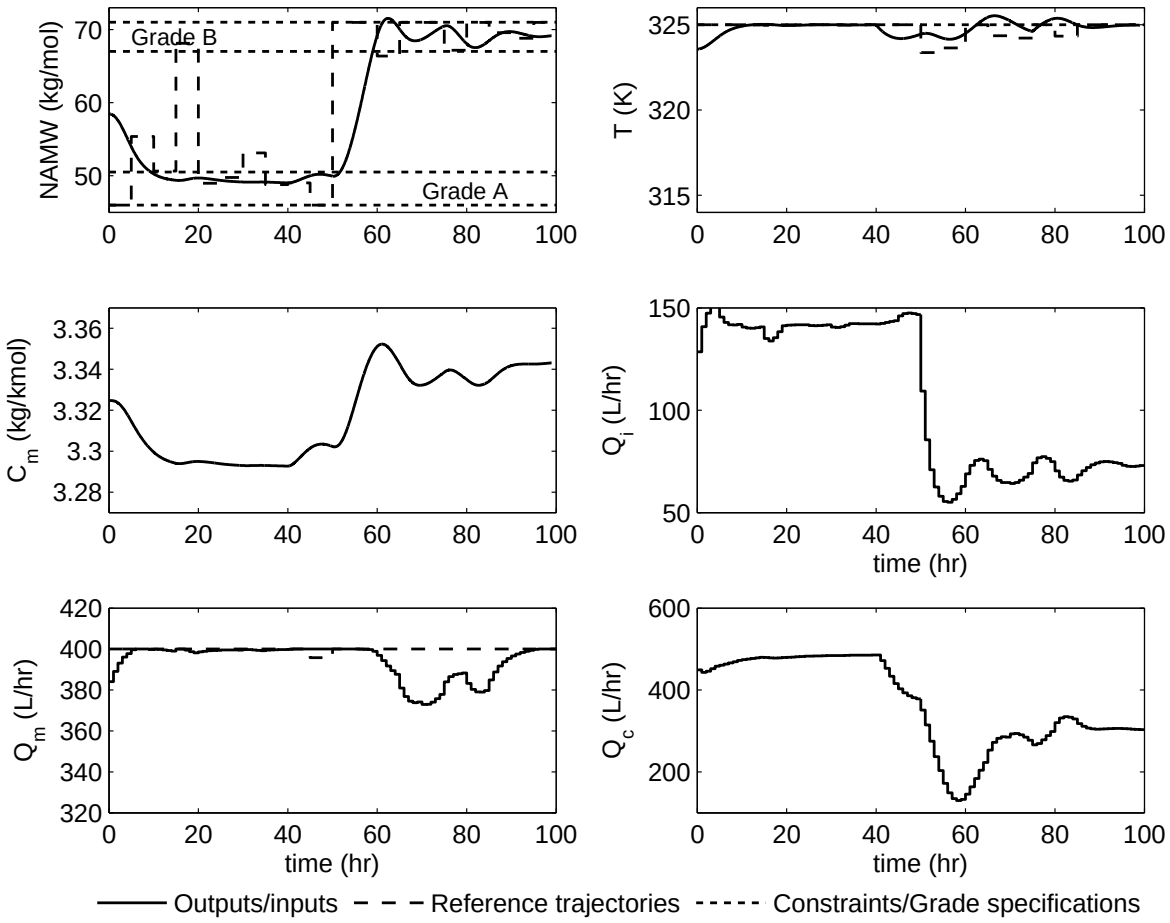

Figure 3.13: Optimal polymer grade transitions based on the hybrid DRTO formulation.

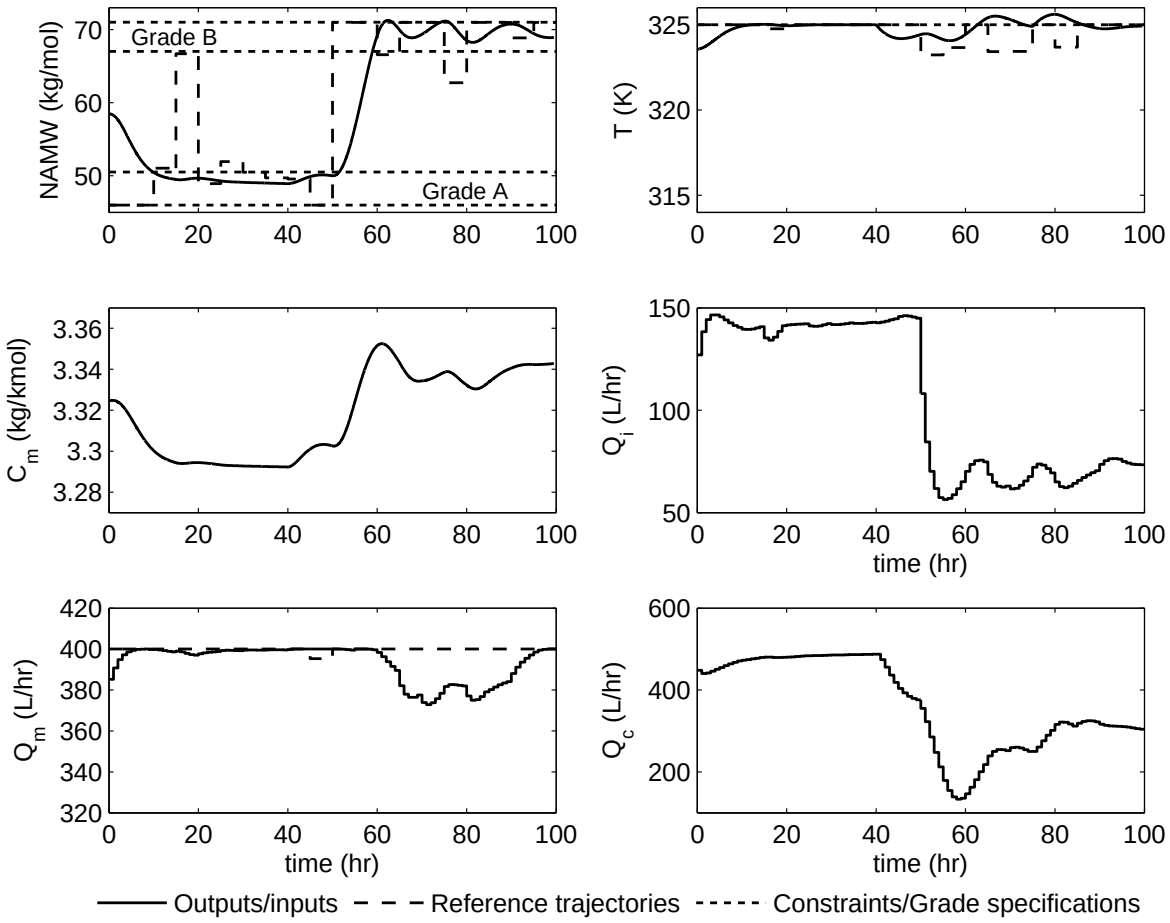

Figure 3.14: Optimal polymer grade transitions based on the bilevel DRTO formulation.

3.4 Conclusion

In this work, we consider CL-DRTO formulations based on the predicted closed-loop response dynamics of processes regulated under input-constrained MPC. Our previously proposed rigorous CL-DRTO formulation demonstrates excellent performance at the expense of a relatively large problem size. In this study, we present multiple closed-loop approximation approaches to perform the closed-loop prediction: (i) a hybrid formulation, (ii) a bilevel formulation, and (iii) an input clipping formulation with application of an unconstrained MPC algorithm in the CL-DRTO problem. The proposed approaches substantially reduce the complexity of the rigorous closed-loop DRTO formulation. Performance analysis on a MISO system demonstrates that the proposed approximation approaches provide accurate results at greatly reduced the problem size and faster solution times in comparison to the rigorous CL-DRTO formulation.

The rigorous, hybrid and bilevel CL-DRTO formulations were subsequently applied to optimal grade transition of polystyrene production in a jacketed CSTR. The objective was to maximize the economics of producing the specified polymer grades in the presence of plant model-mismatch and a disturbance. Simulation results showed the implemented closed-loop approximation approaches to successfully assist the grade transitions in a cost optimal fashion, and also maintain the polymer productivity within the desired grade tolerances.

In the next chapter, we will utilize the bilevel approximation approach to formulate a CL-DRTO prediction based on a nonlinear dynamic plant model.

3.A Case Study 2 Data

The polystyrene reactor model presented in this chapter is based on the adaptation of Hidalgo and Brosilow [36] model given in Maner et al. [35]. The process model consists of six ordinary differential equations: component balances of monomer (C_m) and initiator (C_i), energy balances of the reactor temperature (T) and coolant temperature (T_c), and population balances of the polymer zero (D_0) and first (D_1) moments; and six algebraic equations: polymer radical (C_{gp}), polymerization kinetics (k_i), reactor discharge flow (Q_t) and polymer NAMW (P_{NAMW}). The model equations are written as

$$\frac{dC_i}{dt} = \frac{Q_i C_{if} - Q_t C_i}{V} - k_d C_i \tag{A-1}$$

$$\frac{dC_m}{dt} = \frac{Q_m C_{mf} - Q_t C_m}{V} - k_p C_m C_{gp} \tag{A-2}$$

$$\frac{dT}{dt} = \frac{Q_t(T_f - T)}{V} + \frac{(-\Delta H_r)}{\rho c_p} k_p C_m C_{gp} - \frac{UA}{\rho c_p V}(T - T_c) \tag{A-3}$$

$$\frac{dT_c}{dt} = \frac{Q_c(T_{cf} - T_c)}{V_c} + \frac{UA}{\rho_c c_{pc} V_c}(T - T_c) \tag{A-4}$$

$$\frac{dD_0}{dt} = 0.5 k_t C_{gp}^2 - \frac{Q_t D_0}{V} \tag{A-5}$$

$$\frac{dD_1}{dt} = k_p C_m C_{gp} - \frac{Q_t D_1}{V} \tag{A-6}$$

where

$$C_{gp} = \left[\frac{2 f k_d C_i}{k_t}\right]^{0.5} \tag{A-7}$$

$$k_i = k_{0i} exp(-E_i/T), \quad i = d,\ p,\ t \tag{A-8}$$

$$Q_t = Q_i + Q_m + Q_s \tag{A-9}$$

and the polymer NAMW is calculated as

$$P_{NAMW} = \frac{D_1}{D_0} \mathrm{MW_m} \tag{A-10}$$

Model parameters and nominal simulation data are given in Table A-1. The dimensionless model parameters and variables needed to transform the original model equations to dimensionless form are given in Table A-2. The resulting dimensionless model equations are given in Eqs. (A-11)-(A-17).

$$\frac{dx_1}{dt} = q_i x_{1f} - q_t x_1 - \phi_d K_d(x_3) x_1 \tag{A-11}$$

$$\frac{dx_2}{dt} = q_m x_{2f} - q_t x_2 - \phi_p K_p(x_3) x_2 x_{gp} \tag{A-12}$$

$$\frac{dx_3}{dt} = q_t(x_{3f} - x_3) + \beta\phi_p K_p(x_3) x_2 x_{gp} - \delta(x_3 - x_4) \tag{A-13}$$

$$\frac{dx_4}{dt} = \delta_1 \left[q_c(x_{4f} - x_4) + \delta\delta_2(x_3 - x_4) \right] \tag{A-14}$$

$$\frac{dx_5}{dt} = 0.5\phi_t K_t(x_3) x_{gp}^2 - q_t x_5 \tag{A-15}$$

$$\frac{dx_6}{dt} = \phi_p K_p(x_3) x_2 x_{gp} - q_t x_6 \tag{A-16}$$

$$p_{namw} = \frac{x_6}{x_5} \tag{A-17}$$

Table A-1: List of nominal inputs, model parameters and steady-states [35].

Nominal inputs	Model parameters	Nominal steady-states
$Q_i = 108$ L/hr	$f = 0.6$	$\bar{C}_i = 0.066832$ mol/L
$Q_m = 378$ L/hr	$\mathrm{MW_m} = 104.14$ g/mol	$\bar{C}_m = 3.324541$ mol/L
$Q_s = 459$ L/hr	$V = 3000$ L	$\bar{T} = 323.555818$ K
$Q_c = 471.6$ L/hr	$V_c = 3312.4$ L	$\bar{T}_c = 305.168142$ K
$C_{if} = 0.5888$ mol/L	$-\Delta H_r = 16700$ cal/mol	$\bar{D}_0 = 0.000275$ mol/L
$C_{mf} = 8.6981$ mol/L	$UA = 0.252 \times 10^6$ cal/mol/K	$\bar{D}_1 = 0.154699$ mol/L
$T_f = 330$ K	$\rho c_p = 360$ cal/L/K	$\bar{P}_{NAMW} = 58483.650560$ g/mol
$T_{cf} = 295$ K	$\rho_c c_{p_c} = 966.3$ cal/L/K	
$Q_{t0} = 3000$ L/hr	$k_{d0} = 2.142 \times 10^{17}$ 1/hr	
$C_{mf0} = 1$ mol/L	$k_{p0} = 3.816 \times 10^{10}$ 1/mol/hr	
$T_{f0} = 330$ K	$k_{t0} = 4.500 \times 10^{12}$ 1/mol/hr	
	$E_d = 14897$ K	
	$E_p = 3557$ K	
	$E_t = 843$ K	

Table A-2: List of dimensionless model variables and parameters [37].

$$q_i = \frac{Q_i}{Q_{t0}} \qquad x_{gp} = \frac{C_{gp}}{C_{mf0}}$$

$$q_m = \frac{Q_m}{Q_{t0}} \qquad x_{1f} = \frac{C_{if}}{C_{mf0}}$$

$$q_s = \frac{Q_s}{Q_{t0}} \qquad x_{2f} = \frac{C_{mf}}{C_{mf0}}$$

$$q_c = \frac{Q_c}{Q_{t0}} \qquad x_{3f} = \frac{T_f - T_{f0}}{T_{f0}}\gamma_p$$

$$x_1 = \frac{C_i}{C_{mf0}} \qquad x_{4f} = \frac{T_{cf} - T_{f0}}{T_{f0}}\gamma_p$$

$$x_2 = \frac{C_m}{C_{mf0}} \qquad \tau = t\frac{Q_{t0}}{V}$$

$$x_3 = \frac{T - T_{f0}}{T_{f0}}\gamma_p \qquad \delta = \frac{UA}{\rho c_p Q_{t0}}$$

$$x_4 = \frac{T_c - T_{f0}}{T_{f0}}\gamma_p \qquad \delta_1 = \frac{V}{V_c}$$

$$x_5 = \frac{D_0}{C_{mf0}} \qquad \delta_2 = \frac{\rho c_p}{\rho_c c_{p_c}}$$

$$x_6 = \frac{D_1}{C_{mf0}} \qquad \gamma_d = \frac{E_d}{E_p}$$

$$K_d(x_3) = \exp\left(\frac{\gamma_d x_3}{1 + \frac{x_3}{\gamma_p}}\right) \qquad \gamma_t = \frac{E_t}{E_p}$$

$$K_t(x_3) = \exp\left(\frac{\gamma_t x_3}{1 + \frac{x_3}{\gamma_p}}\right) \qquad \gamma_p = \frac{E_p}{T_{f0}}$$

$$K_p(x_3) = \exp\left(\frac{x_3}{1 + \frac{x_3}{\gamma_p}}\right) \qquad \phi_d = \frac{V}{Q_{t0}} k_{d0} \exp\left(-\gamma_d \gamma_p\right)$$

$$\beta = \frac{(-\Delta H_r) C_{mf0} \gamma_p}{\rho c_p T_{f0}} \qquad \phi_t = \frac{V C_{mf0}}{Q_{t0}} k_{t0} \exp\left(-\gamma_t \gamma_p\right)$$

$$\phi_p = \frac{V C_{mf0}}{Q_{t0}} k_{p0} \exp\left(-\gamma_p\right)$$

References

[1] T. E. Marlin and A. N. Hrymak. "Real-time operations optimization of continuous processes". In: *AIChE Symposium Series: Proceedings of the 5th International Conference on Chemical Process Control*. Ed. by J. C. Kantor, C. E. Garcia, and B. Carnahan. Vol. 93. 316. AIChE and CACHE, 1997, pp. 156 –164.

[2] M. L. Darby, M. Nikolaou, J. Jones, and D. Nicholson. "RTO: An overview and assessment of current practice". In: *J Process Control* 21.6 (2011), pp. 874 –884.

[3] S. J. Qin and T. A. Badgwell. "A survey of industrial model predictive control technology". In: *Control Eng Pract* 11.7 (2003), pp. 733 –764.

[4] M. L. Darby and M. Nikolaou. "MPC: Current practice and challenges". In: *Control Eng Pract* 20.4 (2012), pp. 328 –342.

[5] C.-M. Ying and B. Joseph. "Performance and stability analysis of LP-MPC and QP-MPC cascade control systems". In: *AIChE J* 45.7 (1999), pp. 1521–1534.

[6] A. Nikandrov and C. L. E. Swartz. "Sensitivity analysis of LP-MPC cascade control systems". In: *J Process Control* 19.1 (2009), pp. 16 –24.

[7] T. Tosukhowong, J. M. Lee, J. H. Lee, and J. Lu. "An introduction to a dynamic plant-wide optimization strategy for an integrated plant". In: *Comput Chem Eng* 29.1 (2004), pp. 199 –208.

[8] J. Kadam, M. Schlegel, W. Marquardt, R. Tousain, D. van Hessem, J. van den Berg, and O. Bosgra. "A two-level strategy of integrated dynamic optimization and control of industrial processes – a case study". In: *European Symposium on Computer Aided Process Engineering-12*. Ed. by J. Grievink and J. van Schijndel. Vol. 10. Computer Aided Chemical Engineering. Elsevier, 2002, pp. 511 –516.

[9] L. Würth, R. Hannemann, and W. Marquardt. "A two-layer architecture for economically optimal process control and operation". In: *J Process Control* 21.3 (2011), pp. 311 –321.

[10] I. J. Wolf, D. A. Muñoz, and W. Marquardt. "Consistent hierarchical economic NMPC for a class of hybrid systems using neighboring-extremal updates". In: *J Process Control* 24.2 (2014), pp. 389 –398.

[11] A. Zanin, M. T. de GouvÃła, and D. Odloak. "Integrating real-time optimization into the model predictive controller of the FCC system". In: *Control Eng Pract* 10.8 (2002), pp. 819 –831.

[12] R. Amrit, J. B. Rawlings, and D. Angeli. "Economic optimization using model predictive control with a terminal cost". In: *Annual Reviews in Control* 35.2 (2011), pp. 178 –186.

[13] M. Heidarinejad, J. Liu, and P. D. Christofides. "Economic model predictive control of nonlinear process systems using Lyapunov techniques". In: *AIChE J* 58.3 (2012), pp. 855–870.

[14] A. Gopalakrishnan and L. T. Biegler. "Economic Nonlinear Model Predictive Control for periodic optimal operation of gas pipeline networks". In: *Comput Chem Eng* 52 (2013), pp. 90 –99.

[15] Z. Chong and C. L. E. Swartz. "Optimal operation of process plants under partial shutdown conditions". In: *AIChE J* 59.11 (2013), pp. 4151–4168.

[16] R. Amrit, J. B. Rawlings, and L. T. Biegler. "Optimizing process economics online using model predictive control". In: *Comput Chem Eng* 58.0 (2013), pp. 334 –343.

[17] V. M. Zavala and L. T. Biegler. "The advanced-step NMPC controller: Optimality, stability and robustness". In: *Automatica* 45.1 (2009), pp. 86 –93.

[18] R. Huang, V. M. Zavala, and L. T. Biegler. "Advanced step nonlinear model predictive control for air separation units". In: *J Process Control* 19 (2009), pp. 678 –685.

[19] L. T. Biegler. "10th IFAC International Symposium on Dynamics and Control of Process Systems (DYCOPS): A Survey on Sensitivity-based Nonlinear Model Predictive Control". In: *IFAC Proceedings Volumes* 46.32 (2013), pp. 499 –510.

[20] P. Tatjewski. "Advanced control and on-line process optimization in multilayer structures". In: *Annual Reviews in Control* 32.1 (2008), pp. 71 –85.

[21] R. Scattolini. "Architectures for distributed and hierarchical Model Predictive Control A review". In: *J Process Control* 19.5 (2009), pp. 723 –731.

[22] M. Ellis, H. Durand, and P. D. Christofides. "A tutorial review of economic model predictive control methods". In: *J Process Control* 24.8 (2014), pp. 1156 –1178.

[23] M. Z. Jamaludin and C. L. E. Swartz. "Effects of closed-loop dynamics in dynamic real-time optimization". In: *AIChE Annual Meeting*. Atlanta, GA, USA, 2014.

[24] J. M. Maciejowski. *Predictive Control with Constraints*. Essex, England: Prentice Hall, 2002.

[25] C. R. Cutler and B. L. Ramaker. "Dynamic Matrix Control - a computer control algorithm". In: *AIChE 86th National Meeting*. Houston, TX, USA, 1979.

[26] C. E. Garcia and A. M. Morshedi. "Quadratic programming solution of dynamic matrix control (QDMC)". In: *Chem Eng Commun* 46.1-3 (1986), pp. 73–87.

[27] D. Mayne, J. Rawlings, C. Rao, and P. Scokaert. "Constrained model predictive control: Stability and optimality". In: *Automatica* 36.6 (2000), pp. 789 –814.

[28] E. Zafiriou and A. L. Marchal. "Stability of SISO quadratic dynamic matrix control with hard output constraints". In: *AIChE J* 37.10 (1991), pp. 1550–1560.

[29] R. Baker and C. L. E. Swartz. "Simultaneous Solution Strategies for Inclusion of Input Saturation in the Optimal Design of Dynamically Operable Plants". In: *Optimization and Engineering* 5.1 (2004), pp. 5–24.

[30] R. Baker and C. L. E. Swartz. "Interior point solution of multilevel quadratic programming problems in constrained model predictive control applications". In: *Ind Eng Chem Res* 47.1 (2008), pp. 81–91.

[31] B. Baumrucker, J. Renfro, and L. Biegler. "MPEC problem formulations and solution strategies with chemical engineering applications". In: *Comput Chem Eng* 32.12 (2008), pp. 2903 –2913.

[32] D. Ralph and S. J. Wright. "Some properties of regularization and penalization schemes for MPECs". In: *Optimization Methods and Software* 19.5 (2004), pp. 527–556.

[33] R. L. Tousain. "Dynamic Optimization in Business-Wide Process Control". Ph.D. Thesis. Delft University of Technology, Delft, The Netherlands, 2002.

[34] A. Wächter and L. T. Biegler. "On the implementation of an interior-point filter line-search algorithm for large-scale nonlinear programming". In: *Math Prog* 106.1 (2006), pp. 25–57.

[35] B. R. Maner, F. J. Doyle III, B. A. Ogunnaike, and R. K. Pearson. "Nonlinear model predictive control of a simulated multivariable polymerization reactor using second-order Volterra models". In: *Automatica* 32.9 (1996), pp. 1285 –1301.

[36] P. Hidalgo and C. Brosilow. "Nonlinear model predictive control of styrene polymerization at unstable operating points". In: *Comput Chem Eng* 14.4/5 (1990), pp. 481 –494.

[37] L. P. Russo and B. Bequette. "Operability of chemical reactors: multiplicity behavior of a jacketed styrene polymerization reactor". In: *Chem Eng Sci* 53.1 (1998), pp. 27 –45.

Chapter 4

Formulation of Nonlinear Dynamic Real-time Optimization

The formulations and results in this chapter have been published and presented in:

[1] M.Z. Jamaludin and C.L.E. Swartz. "IFAC International Symposium on Dynamics and Control of Process Systems, including Biosystems (DYCOPS-CAB): Closed-loop formulation for nonlinear dynamic real-time optimization". *IFAC-PapersOnLine* 49-7 (2016), pp 406-411.

4.1 Introduction

Process plants operate in an ever increasing environment of uncertainty and changing conditions, driven by factors such as increased global competition, variation in utility costs, restrictive environmental regulations, changing raw material prices, varying product quality specifications, and volatile market demands. Real-time optimization (RTO) is a closed-loop economic optimizer in the process automation architecture that computes set-point targets for the lower level regulatory control systems [1]. The traditional RTO strategy is designed based on a steady-state model, which suffers from a limited execution frequency resulting in suboptimal operation for processes with frequent transitions and long transient dynamics. Recent advances have transformed the steady-state RTO to dynamic real-time optimization (DRTO) based on a dynamic prediction model, hence allowing process transient economics be evaluated at a substantially higher frequency.

Proposed DRTO strategies that follow a two-layer architecture generally perform economic optimization in an open-loop fashion without taking into account the presence of the plant control system, which we denote here as an open-loop DRTO strategy. In this approach, the set-points prescribed to the underlying control system are based on the optimal open-loop trajectories under an expectation that the closed-loop response dynamics at the plant level will follow the economically optimal trajectories obtained at the DRTO level. Tosukhowong et al. [2] design the DRTO framework based on a linear(ized) process model while Würth et al. [3] utilize a nonlinear dynamic model. An alternative to the multilevel configuration is a single-level, economic model predictive control (EMPC) approach that optimizes the plant economics at the controller sampling frequency. Such a strategy aims to address the issues of model inconsistency and conflicting objectives between the traditional RTO system and the MPC control layer, and is usually designed based on the nonlinear dynamic model describing the process behavior. In this case, the objective function could be based purely on economics [4], or a hybrid between cost and control performance [5].

In previous work, we proposed a closed-loop DRTO strategy with a rigorous inclusion of the future MPC control calculations, which for constrained MPC cannot be expressed as an explicit continuous function to be readily included in the optimization problem. The overall closed-loop DRTO problem structure is in the form of a multilevel dynamic optimization problem with embedded MPC optimization subproblems, as illustrated in Figure 4.1. It optimizes the closed-loop response dynamics of the process where the optimal control inputs are computed by a sequence of inner MPC optimization subproblems. This scheme computes the MPC set-point trajectories that determine the best economics of the predicted closed-loop response, under the assumption that the process follows the trajectory calculated by MPC until the next DRTO execution. The closed-loop DRTO formulation may be viewed as an EMPC approach due to explicit consideration of control performance while making economic

decisions. However, it has the flexibility to be implemented less frequently at the supervisory level because controller set-point trajectories are the primary decision variables of the economic optimization problem. This allows the existing plant automation architecture to remain unaltered, and the higher frequency control calculation remains less complex and computationally inexpensive.

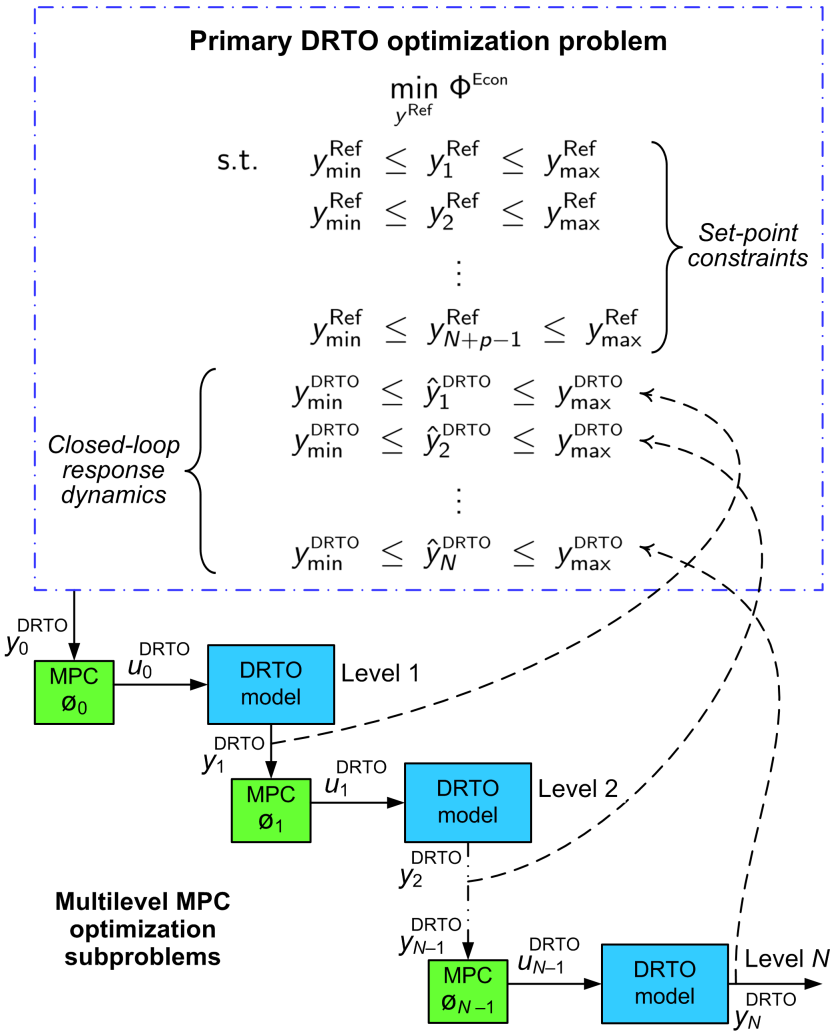

Figure 4.1: Illustration of the multilevel dynamic optimization formulation of the closed-loop DRTO problem.

Our prior analysis based on a linear dynamic system demonstrated that the closed-loop DRTO strategy outperforms the traditional open-loop counterpart under control performance limitations where the controller has to be detuned [6, 7]. Despite its advantages, the multilevel programming formulation significantly increases the size and solution time of the DRTO problem. In a recent study [8], we proposed a closed-loop DRTO strategy in the form of a bilevel programming problem in which only a single MPC calculation is embedded over the DRTO optimization horizon as an approximation of the rigorous closed-loop response dynamics.

This chapter extends the application of the closed-loop DRTO strategy to a nonlinear dynamic system formulated as a bilevel program. We consider implementation of linear MPC on a nonlinear dynamic plant model. The following sections describe the closed-loop formulation of the nonlinear DRTO problem, followed by the solution approach adopted for the resulting dynamic optimization problem. A technique to handle complementary constraints arising from reformulation of the MPC optimization subproblem to its KKT conditions, and formulation of an economic objective function, are also be presented. A comparative study of the closed-loop DRTO performance based on the nonlinear and linear embedded dynamic plant model is conducted using a polystyrene grade transition case study in the presence of plant-model mismatch and a disturbance.

4.2 Problem Formulation

4.2.1 Dynamic Optimization

For clarity of exposition, we first describe the conversion of a nonlinear continuous dynamic model to its discrete representation, which will later be used with the embedded MPC optimization subproblem. Here we consider process dynamic behavior described by a nonlinear differential algebraic equation (DAE) system of the form:

$$\begin{aligned}
\dot{\hat{\mathbf{x}}}^{\mathbf{DRTO}}(t) &= \mathbf{f}^{\mathbf{DRTO}}(\hat{\mathbf{x}}^{\mathbf{DRTO}}(t),\ \hat{\mathbf{z}}^{\mathbf{DRTO}}(t),\ \hat{\mathbf{u}}^{\mathbf{DRTO}}(t)) \\
0 &= \mathbf{h}^{\mathbf{DRTO}}(\hat{\mathbf{x}}^{\mathbf{DRTO}}(t),\ \hat{\mathbf{z}}^{\mathbf{DRTO}}(t),\ \hat{\mathbf{u}}^{\mathbf{DRTO}}(t)) \\
0 &\leq \mathbf{g}^{\mathbf{DRTO}}(\hat{\mathbf{x}}^{\mathbf{DRTO}}(t),\ \hat{\mathbf{z}}^{\mathbf{DRTO}}(t),\ \hat{\mathbf{u}}^{\mathbf{DRTO}}(t)) \\
\hat{\mathbf{x}}^{\mathbf{DRTO}}(0) &= \mathbf{x}_0 \\
t &\in [0,\ t_f]
\end{aligned}$$

where $\hat{\mathbf{x}}^{\mathbf{DRTO}}(t) \in \mathbb{R}^{n_x}$ = differential state vector, $\hat{\mathbf{x}}^{\mathbf{DRTO}}(0)$ = initial state vector, $\hat{\mathbf{z}}^{\mathbf{DRTO}}(t) \in \mathbb{R}^{n_z}$ = algebraic state vector, $\hat{\mathbf{u}}^{\mathbf{DRTO}}(t) \in \mathbb{R}^{n_u}$ = control input vector, and t_f = final time in prediction/optimization horizon. To solve the DAE system using an optimization (specifically, a nonlinear programming [NLP]) framework, the differential-algebraic equations are discretized in the time coordinate using a Backward Euler approximation, as follows:

$$
\begin{aligned}
\frac{\hat{\mathbf{x}}_j^{\mathbf{DRTO}} - \hat{\mathbf{x}}_{j-1}^{\mathbf{DRTO}}}{\Delta t_j} &= \mathbf{f}^{\mathbf{DRTO}}(\hat{\mathbf{x}}_j^{\mathbf{DRTO}}, \hat{\mathbf{z}}_j^{\mathbf{DRTO}}, \hat{\mathbf{u}}_{j-1}^{\mathbf{DRTO}}), \\
& \qquad\qquad k = 1, \ldots, N \\
\mathbf{h}^{\mathbf{DRTO}}(\hat{\mathbf{x}}_j^{\mathbf{DRTO}}, \hat{\mathbf{z}}_j^{\mathbf{DRTO}}, \hat{\mathbf{u}}_j^{\mathbf{DRTO}}) &= \mathbf{0}, \qquad k = 0, \ldots, N \\
\mathbf{g}^{\mathbf{DRTO}}(\hat{\mathbf{x}}_j^{\mathbf{DRTO}}, \hat{\mathbf{z}}_j^{\mathbf{DRTO}}, \hat{\mathbf{u}}_j^{\mathbf{DRTO}}) &\geq \mathbf{0}, \qquad k = 0, \ldots, N \\
\hat{\mathbf{x}}_0^{\mathbf{DRTO}} &= \mathbf{x}_0
\end{aligned}
$$

We assume that the controller sampling interval is the same duration as the finite element interval Δt_j partitioned over the optimization horizon, and thus piecewise constant inputs (i.e. zero-order hold) can be conveniently placed at every finite element. There are also other nonlinear discretization approaches such as orthogonal collocation on finite elements (which corresponds to an implicit Runge-Kutta method), should a more precise integration procedure be desired. The resulting set of equations is posed as constraints in the optimization problem. In our case, the resulting sparse structured NLP is modeled using a specialized in-house modeling software package, a Modeling Language for Dynamic Optimization (MLDO) [9], which generates AMPL code, permitting solution by means of large-scale NLP solvers.

The bilevel closed-loop DRTO formulation consists of a primary DRTO optimization problem Eq. (4.1a) based on the nonlinear dynamic system to predict the closed-loop response dynamics, and an inner MPC optimization subproblem based on the linear(ized) dynamic system to calculate the optimal control input trajectories Eq. (4.1b). The controller set-point trajectories $\tilde{\mathbf{y}}^{\mathbf{SP}}$ are the decision variables for the outer problem, whereas the control input trajectories $\tilde{\mathbf{u}}$ are the decision variables for the inner subproblem.

The MPC optimization subproblem Eq. (4.1b) utilizes the state-space formulation of a standard input-constrained MPC controller with a quadratic objective function; further detailed of the algorithm which can be found in [10]. In the bilevel formulation, only a single MPC optimization subproblem is required within the DRTO calculation where the prediction and control horizons are extended to match the DRTO optimization horizon, such that $p = m = N$. Weighting parameters Q and R for penalization of output tracking error and control move suppression, respectively, are exactly the same as the MPC controller implemented at the lower level. ϕ is a quadratic MPC cost function. $\tilde{\mathbf{x}} \in \mathbb{R}^{n_x}$ is a vector of MPC model states, $\tilde{\mathbf{y}} \in \mathbb{R}^{n_y}$ is a corresponding vector of MPC model outputs, and $\tilde{\mathbf{u}} \in \mathbb{R}^{n_u}$ is a vector of MPC inputs at each prediction step k. $\tilde{\mathbf{y}}^{\mathbf{SP}} \in \mathbb{R}^{N.n_y}$ is a composite vector of MPC set-point trajectories for the controlled outputs over the the DRTO optimization horizon N.

$$
\begin{aligned}
& \min_{\tilde{\mathbf{y}}^{\mathbf{SP}}} \Phi^{\text{Econ}}(\hat{\mathbf{x}}_j^{\mathbf{DRTO}},\ \hat{\mathbf{z}}_j^{\mathbf{DRTO}},\ \hat{\mathbf{u}}_j^{\mathbf{DRTO}}) \\
s.t. \quad & \hat{\mathbf{x}}_{j+1}^{\mathbf{DRTO}} = \check{\mathbf{f}}^{\mathbf{DRTO}}(\hat{\mathbf{x}}_j^{\mathbf{DRTO}},\ \hat{\mathbf{z}}_j^{\mathbf{DRTO}},\ \hat{\mathbf{u}}_j^{\mathbf{DRTO}}), \quad j = 0, \ldots, N-1 \\
& \mathbf{0} = \mathbf{h}^{\mathbf{DRTO}}(\hat{\mathbf{x}}_j^{\mathbf{DRTO}},\ \hat{\mathbf{z}}_j^{\mathbf{DRTO}},\ \hat{\mathbf{u}}_j^{\mathbf{DRTO}}), \quad j = 1, \ldots, N \\
& \mathbf{0} \leq \mathbf{g}^{\mathbf{DRTO}}(\hat{\mathbf{x}}_j^{\mathbf{DRTO}},\ \hat{\mathbf{z}}_j^{\mathbf{DRTO}}), \quad j = 1, \ldots, N \\
& \mathbf{0} = \mathbf{h}^{\mathbf{Ref}}(\tilde{\mathbf{y}}^{\mathbf{SP}}) \\
& \mathbf{0} \leq \mathbf{g}^{\mathbf{Ref}}(\tilde{\mathbf{y}}^{\mathbf{SP}})
\end{aligned}
\tag{4.1a}
$$

$$
\left.
\begin{aligned}
(\hat{\mathbf{u}}^{\mathbf{DRTO}} - \hat{\mathbf{u}}^{\mathbf{ss}}) = \arg \min_{\tilde{\mathbf{u}}} \ & \phi := \textstyle\sum_{k=1}^{N} (\tilde{\mathbf{y}}_k - \tilde{\mathbf{y}}_k^{\mathbf{SP}})^{\mathrm{T}} Q (\tilde{\mathbf{y}}_k - \tilde{\mathbf{y}}_k^{\mathbf{SP}}) + \textstyle\sum_{k=0}^{N-1} \boldsymbol{\Delta}\tilde{\mathbf{u}}_k^{\mathrm{T}} R \boldsymbol{\Delta}\tilde{\mathbf{u}}_k \\
s.t. \quad & \tilde{\mathbf{x}}_{k+1} = A\tilde{\mathbf{x}}_k + B\tilde{\mathbf{u}}_k, \quad k = 0, \ldots, N-1 \\
& \tilde{\mathbf{y}}_k = C\tilde{\mathbf{x}}_k + \tilde{\mathbf{d}}_k, \quad k = 1, \ldots, N \\
& \boldsymbol{\Delta}\tilde{\mathbf{u}}_k = \tilde{\mathbf{u}}_k - \tilde{\mathbf{u}}_{k-1}, \quad k = 0, \ldots, N-1 \\
& \mathbf{u}_{\min} \leq \tilde{\mathbf{u}}_k \leq \mathbf{u}_{\max}, \quad k = 0, \ldots, N-1
\end{aligned}
\right\} \text{MPC subproblem}
\tag{4.1b}
$$

We also note that referring to the notation of the previous section, we have:

$$
\tilde{\mathbf{u}} = \left[(\tilde{\mathbf{u}}_0)^{\mathrm{T}},\ (\tilde{\mathbf{u}}_1)^{\mathrm{T}}, \ldots, (\tilde{\mathbf{u}}_{N-1})^{\mathrm{T}} \right]^{\mathrm{T}}
$$

that is a composite vector comprising all the MPC inputs over the MPC horizon. $\hat{\mathbf{u}}^{\mathbf{DRTO}}$ and $\tilde{\mathbf{y}}^{\mathbf{SP}}$ are analogously defined. The inputs to the DRTO plant model correspond to the optimal input trajectory of the MPC optimization subproblem, added to the nominal steady-state inputs (since the MPC formulation utilizes deviation variables). We note that $\hat{\mathbf{u}}^{\mathbf{ss}}$ is a composite vector of the steady-state inputs repeated for each step of the DRTO prediction horizon for compatibility with $\hat{\mathbf{u}}^{\mathbf{DRTO}}$.

For comparison, we also apply a linear(ized) DRTO model to generate the closed-loop response dynamics at the primary optimization problem. In this case, the function $\check{\mathbf{f}}^{\mathbf{DRTO}}$ represents the linear dynamic model utilized for DRTO prediction at time step $j \in [0, \ldots, N-1]$, which can be consistent with the MPC state-space model. The closed-loop DRTO strategy optimizes the set-point trajectories directly to be prescribed to the MPC controller at the lower level. At the lower level, these set-point trajectories are shifted in time to account for the moving horizon of the MPC controller.

4.2.2 Simultaneous Solution Approach

One way to solve the bilevel closed-loop DRTO problem is to apply a sequential approach by iteratively solving the primary DRTO problem and the inner MPC subproblem until convergence to an optimum. However, we avoid this approach as it may encounter numerical difficulty in the DRTO optimization problem posed by derivative discontinuities induced by control input saturation at the inner MPC optimization subproblem.

In this study, we employ a simultaneous solution approach by transforming the MPC optimization subproblem to a set of algebraic equations using its first-order, Karush-Kuhn-Tucker (KKT) optimality conditions. For a constrained MPC problem formulated as a convex quadratic programming (QP) problem as considered in this study, such a transformation is valid as the KKT conditions are necessary and sufficient for optimality. The MPC subproblem at each DRTO prediction step may be represented as a QP of the form:

$$\begin{aligned} \min_{\mathbf{u}} \ & \frac{1}{2}\mathbf{u}^T H \mathbf{u} + \mathbf{g}^T \mathbf{u} \\ s.t. \quad & A\mathbf{u} = \mathbf{b} \\ & \mathbf{u} \geq \mathbf{0} \end{aligned} \tag{4.2}$$

with the corresponding KKT conditions are given by:

$$\begin{aligned} H\mathbf{u} + \mathbf{g} - A^T \boldsymbol{\lambda} - \boldsymbol{\nu} &= \mathbf{0} \\ A\mathbf{u} &= \mathbf{b} \\ u_i \nu_i &= 0 \quad \forall i \in I \\ (\mathbf{u},\ \boldsymbol{\nu}) &\geq \mathbf{0} \end{aligned} \tag{4.3}$$

Details of the KKT conditions as applied to the MPC (QP) subproblem can be found in Baker and Swartz [11].

4.2.3 Handling complementarity constraints

Complementarity constraints, which take the form $u_i \nu_i = 0$, are generally hard to solve due to violation of constraint qualifications in the nonlinear programming (NLP) problem [12]. Handling complementarity constraints requires reformulation of the MPCC, or an alternative NLP algorithm that internally treats the complementarity constraints.

In this study, the complementarity constraints are handled using an exact penalty formulation [13]. They are moved from the constraint set of the original MPCC problem to the objective function as an additional penalty term with a penalty parameter ρ, as represented in Eq. (4.4), with the resulting problem posed to a standard NLP solver. Tuning of the complementarity penalty parameter ρ starts from a small value, roughly of the same order of magnitude as the decision variables, and increased until it exceeds a critical value, i.e. $\rho > \rho_c$, at which point the original complementarity constraints will be approximately satisfied. However, choosing too large a penalty parameter may lead to scaling issues and longer solution times.

$$\begin{aligned} \min_{\mathbf{u},\mathbf{z},\boldsymbol{\nu}} \; & \Phi^{\text{Econ}}(\mathbf{u},\mathbf{z}) + \rho \sum_{i=1}^{I} u_i \nu_i \\ s.t. \quad & \mathbf{h}(\mathbf{u},\mathbf{z}) = \mathbf{0} \\ & \mathbf{g}(\mathbf{u},\mathbf{z}) \geq \mathbf{0} \\ & H\mathbf{u} + \mathbf{g} - A^T\boldsymbol{\lambda} - \boldsymbol{\nu} = \mathbf{0} \\ & A\mathbf{u} = \mathbf{b} \\ & (\mathbf{u},\ \boldsymbol{\nu}) \geq \mathbf{0} \end{aligned} \tag{4.4}$$

We use a single penalty parameter for all complementarity constraints, although different parameter assignments can be used. At the optimum, the value of the complementarity penalty function will be close to zero, and the optimal solution recovers the original objective function of the MPCC problem due to the negligible contribution of the penalty term.

4.2.4 Economic Objective Function

In general, any appropriate economic objective function suitable for process optimization may be used. However, our case study is specifically motivated by product grade transition problems, such as those arising in the polymer and bioprocess industries. The DRTO objective function is formulated to minimize the input cost while at the same time taking into account the revenue when the product quality is within the desired target tolerance. The revenue is continuously tracked using a hyperbolic tangent function,

$$R(x) = \frac{1}{2}\tanh(\gamma x) + \frac{1}{2} \approx \begin{cases} 0, & x < 0 \\ 1, & x > 0 \end{cases} \tag{4.5}$$

where γ is a weighting parameter used to define the steepness of the switching function that produces

a function value either smoothly or sharply approaching 0 or 1. The function is used as a continuous approximation of a switching function constructed to indicate when the variable enters a specification tolerance band. These may be used in combination to capture specification bands with upper and lower limits around a desired target, and included in the objective function in order for revenue to apply only when the product quality falls within specification limits.

Consider a transition of an output from an initial specification (y^{init}) to a new target (y^{target}) where the output is allowed to vary within a strict tolerance, for example $\pm\delta\%$. The economic objective function is formulated to take into account the revenue when the output is within the specification limits. Thus, the tolerances of the desired output target may be written as Eq. (4.6) and Eq. (4.7).

- Region 1 (lower bound):

$$R^1(y) = \frac{1}{2}\tanh\left[\gamma(y - y^{\text{target}} + \delta y^{\text{target}})\right] + \frac{1}{2} \tag{4.6}$$

  where $R^1 \approx 0$ if $y < y^{\text{target}} - \delta y^{\text{target}}$ and $R^1 \approx 1$ if $y > y^{\text{target}} - \delta y^{\text{target}}$.

- Region 2 (upper bound):

$$R^2(y) = \frac{1}{2}\tanh\left[\gamma(y^{\text{target}} + \delta y^{\text{target}} - y)\right] + \frac{1}{2} \tag{4.7}$$

  where $R^2 \approx 0$ if $y > y^{\text{target}} + \delta y^{\text{target}}$ and $R^2 \approx 1$ if $y < y^{\text{target}} + \delta y^{\text{target}}$.

Therefore $R_1 R_2 \approx 1$ if y lies in Region 1 and 2 of the target tolerance and is approximately zero otherwise. This construct of tracking the dynamic economics of the output will be applied in following case study.

4.3 Case Study

In this case study, we implement the bilevel DRTO formulations for optimal polymer grade transitions of a free-radical solution polymerization of styrene in a jacketed CSTR [14], as depicted in Figure 4.2.

Two manipulated inputs and two controlled outputs are selected to design an input-constrained MPC controller, given in Table 4.1. Initiator is mainly used to control the specified polymer grades, and cooling supply is used to absorb the heat of polymerization. We assume sufficient solvent feed ratio to the monomer feed to keep the viscosity of the reaction mixture low, and therefore both flowrates are kept constant at their nominal values. For the nonlinear DRTO application, the polystyrene reactor DAE system is discretized using the Backward Euler method as described in Section 4.2.1. The model

is also linearized at the nominal steady-state operating points to a state-space formulation for the MPC calculation as well as linear DRTO application. Linearization is carried out in MATLAB by computing the Jacobian of the reactor model using a complex-step differentiation to generate the continuous state-space model, which is subsequently discretized based on the MPC sample time of 1 hr. The original DAE models are utilized to perform plant simulations.

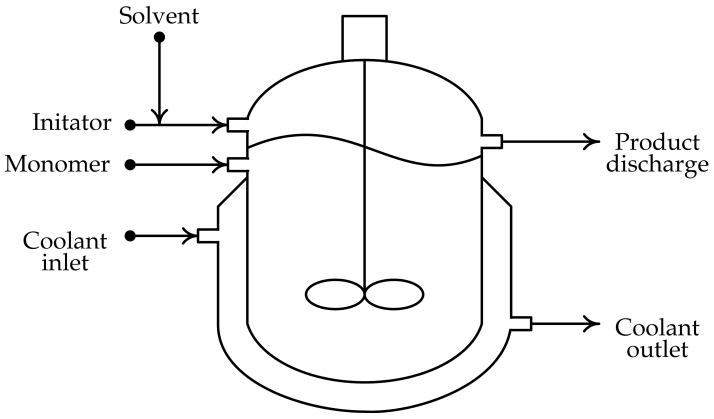

Figure 4.2: Polystyrene reactor.

Table 4.1: Polystyrene case study data.

Manipulated inputs	*Controlled outputs*
Initiator feed, Q_i	Polymer grade, $NAMW$
Coolant supply, Q_c	Reactor temperature, T
DRTO parameters	*MPC parameters*
$N = p^* = m^* = 50$	$p = 15,\ m = 3$
$\rho = 5$	$Q = \text{diag}(0.5,1)$
$\gamma = 8$	$R = \text{diag}(50,20)$
$\Delta t_{\text{DRTO}} = 5$ hr	$\Delta t_{\text{MPC}} = 1$ hr

*Extended MPC horizons for bilevel formulation

The economics of the polymer grade transition problem are formulated to maximize the economic return over the simulation horizon of producing the specified polymer grades, which is characterized by the polymer number average molecular weight (NAMW). The reactor discharge flowrate is used as an inferred estimate of the polymer production rate. The economic objective function is formulated as:

$$\min \Phi = \sum_{j=0}^{N-1} \Delta t_j \left(C_i Q_{i,j} + C_c Q_{c,j} - P_p Q_{t,j+1} R^1_{j+1} R^2_{j+1} \right)$$

where C_i is the cost of the initiator (\$0.2/L/hr), C_c is the cost of the cooling supply (\$0.1/L/hr), P_p is the price of the desired polymer product (\$10/L/hr), and R_1 and R_2 are outputs of hyperbolic tangent switching function approximations that indicate satisfaction of the lower and upper bounds of the polymer grade specification tolerances. The solvent and unreacted monomer are assumed to be recovered and recycled, and their effects on the transition cost are not taken into account. Constraints on the inputs, outputs and set-points are applied as follows:

$$
\begin{aligned}
0 \leq Q_i \leq 300 \quad \text{L/hr} \\
0 \leq Q_c \leq 700 \quad \text{L/hr} \\
56 \leq NAMW,\ NAMW^{\text{SP}} \leq 71 \quad \text{kg/mol} \\
315 \leq T,\ T^{\text{SP}} \leq 325 \quad \text{K}
\end{aligned}
$$

In this study, MATLAB R2012b is chosen as a supervisory computing platform to solve the MPC problem using the `quadprog` solver, and also to perform the plant simulation using an `ode15s`. The DRTO problem, which is larger in size than the MPC problem, is modelled in AMPL and is solved using `IPOPT` (version 3.12.0) with an embedded linear solver `ma27`. The solution from an open-loop simulation is used as an initial guess for DRTO calculation at the start of simulation time, and initializations at the subsequent DRTO calculations are provided using the previously computed optimal solutions. Computation is performed using a 3.4GHz INTEL CORE-i7 with 8GB RAM running Windows 7.

In the following simulations, the polystyrene production is sought from a lower NAMW of 58.5 kg/mol to 68.9 kg/mol with a $\pm 3\%$ of grade tolerance over a 50 hr simulation horizon. Although the target for the NAMW is specified (usually based on product demand, planning and scheduling), the set-point trajectory for the reaction temperature is a degree-of-freedom (DOF) for the economic optimization. We also introduce an unmeasured disturbance of a 5% step increase in the initiator feed concentration at time 31 hr. The polymerization system is known to be sensitive to the initiator feed supply, for instance, slight changes in the initiator feed concentration will significantly alter the polymer NAMW. In addition, discretization of the nonlinear DAE system indirectly introduces mismatch between the nonlinear DRTO model predictions and the actual plant dynamics.

The optimal input, output and set-point trajectories for the nonlinear DRTO application are plotted in Figure 4.3, in which dotted lines represent grade tolerances/output constraints, and dashed lines represent set-point trajectories computed at the initial simulation time. The DRTO is able to keep the polymer NAMW within the acceptable grade tolerance through appropriate adjustment of the set-point trajectories. The reactor is operated near its temperature upper limit which accounts for less utilization of cooling cost, and the constraint is satisfied for the entire simulation run. Figure 4.3 also shows that there are steady-state offsets between the set-point trajectories computed from the

first DRTO execution at time 0 hr and the actual plant dynamics. However, the closed-loop DRTO calculation has an adaptive mechanism to update the set-point trajectories at the subsequent DRTO calculations using current feedback information, which eventually eliminate the offsets. The DRTO problem based on the nonlinear prediction model comprises 2797 optimization variables and the average solution time is 2.8 CPU(s). It generates an economic return of $7925.

In the rigorous multilevel DRTO formulation, there are feedback bias updates at every prediction step generated from a sequence of MPC optimization subproblems embedded over the DRTO optimization horizon in which they provide integral action to the overall closed-loop predictions. Hence, final steady-state offsets can be eliminated based on the set-point trajectories computed at the initial DRTO calculation, assuming a perfect model of the process is available for optimization. Unlike the multilevel DRTO formulation, approximation of closed-loop dynamics using the bilevel formulation does not provide integral action to the closed-loop predictions to eliminate these offsets because the MPC feedback bias update is not available at every DRTO prediction step. Nevertheless, the bilevel formulation has the ability to recognize the future model mismatch between the nonlinear DRTO and linear MPC predictions, and therefore adjusts the set-point trajectories in such a way that the closed-loop predictions will return the best economics. This is a similar idea to the backoff mechanism that moves the set-points away from constraints to allow the process to remain feasible in the face of disturbances and plant-model mismatch.

Simulation results from the application of a linear DRTO plant model are depicted in Figure 4.4. The polymer NAMW violates the specified grade tolerance due to an overshoot during the grade transition and after a disturbance enters the system at time 31 hr, whereas the reactor temperature satisfies the prescribed constraint limit. Although the closed-loop predictions provide a backoff mechanism to prevent constraint violation at the plant level, it does not address model mismatch of implementing a linear MPC controller on a nonlinear process, and therefore the magnitude of the backoff may not be sufficient. Steady-state offsets also occur in this case because the set-point trajectories are optimized based the closed-loop response dynamics of a linear plant model, while the process behavior is nonlinear; such offsets will not be eliminated because the the DRTO assumes linear process behavior. We also observe that the input and output dynamics are not as smooth as compared to the dynamics generated by implementation of the nonlinear DRTO model, even though they finally settle at the same region of steady-states. The DRTO problem based on the linear prediction model comprises 2097 optimization variables and the average solution time is 1.3 CPU(s). The overall simulation results in an economic return of $3475, which is 56% lower than that of the nonlinear model.

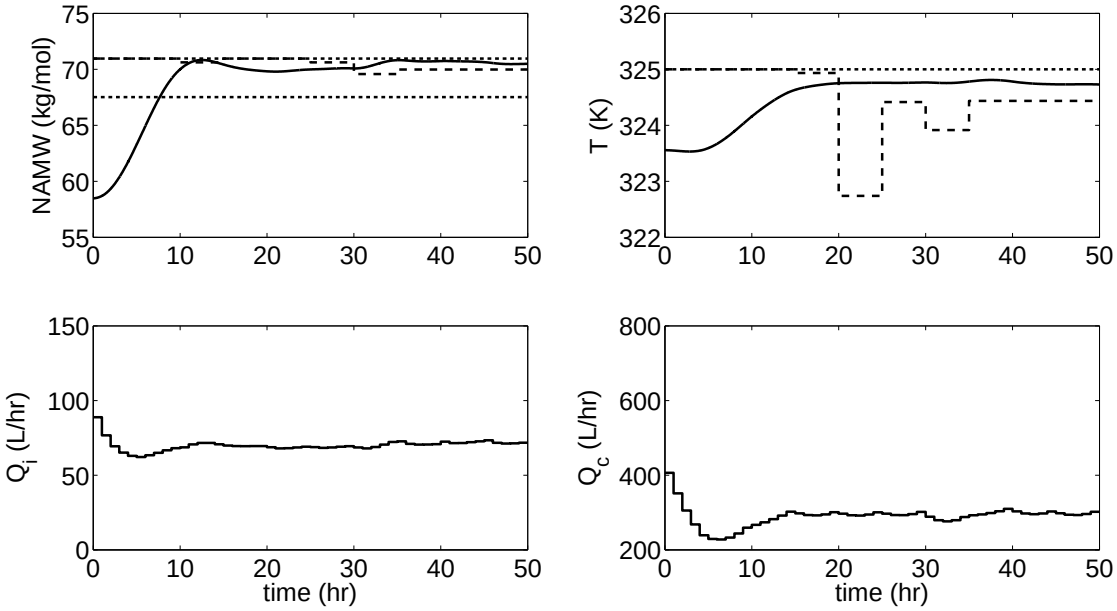

Figure 4.3: Closed-loop DRTO calculations based on closed-loop dynamics and a nonlinear plant model.

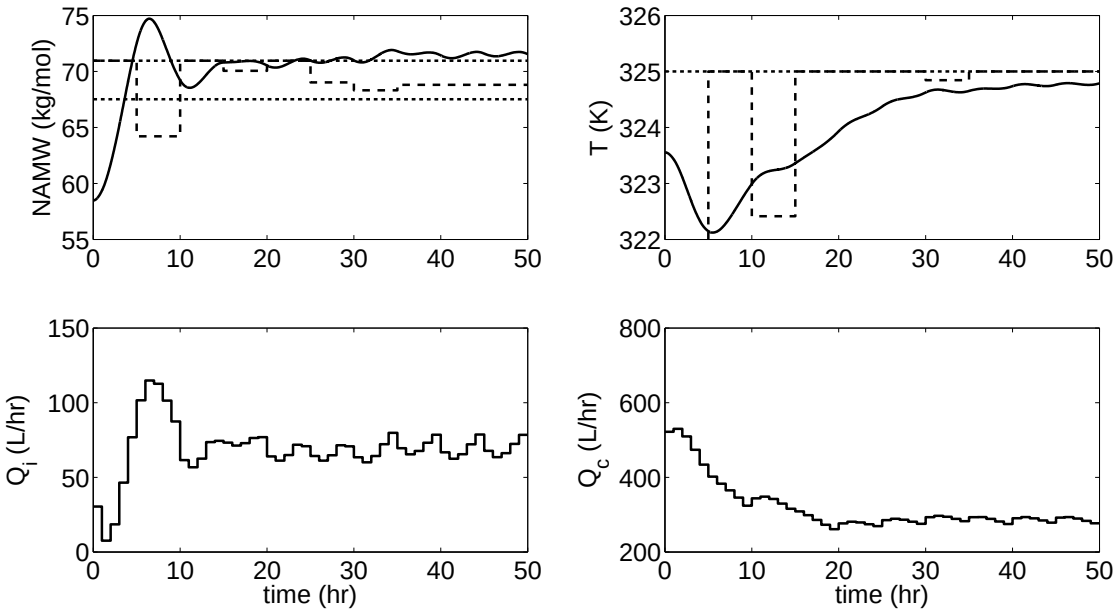

Figure 4.4: Closed-loop DRTO calculations based on closed-loop dynamics and a linear plant model.

4.4 Conclusion

This chapter compares the performance of a closed-loop DRTO strategy based on nonlinear and linear plant model predictions. Approximation of the rigorous DRTO closed-loop prediction is performed using a bilevel programming formulation with an embedded linear MPC optimization subproblem. We demonstrate that implementation of a nonlinear DRTO model in the bilevel programming approximation to predict the closed-loop response dynamics helps to achieve superior economics and control performance to that obtained using a linear model for the plant response determination, while the problem size remains manageable.

In the next chapter, we will utilize the bilevel closed-loop prediction to formulate a DRTO coordination strategy for application in a distributed MPC environment.

References

[1] M. L. Darby, M. Nikolaou, J. Jones, and D. Nicholson. "RTO: An overview and assessment of current practice". In: *J Process Control* 21.6 (2011), pp. 874 –884.

[2] T. Tosukhowong, J. M. Lee, J. H. Lee, and J. Lu. "An introduction to a dynamic plant-wide optimization strategy for an integrated plant". In: *Comput Chem Eng* 29.1 (2004), pp. 199 –208.

[3] L. Würth, R. Hannemann, and W. Marquardt. "A two-layer architecture for economically optimal process control and operation". In: *J Process Control* 21.3 (2011), pp. 311 –321.

[4] R. Amrit, J. B. Rawlings, and L. T. Biegler. "Optimizing process economics online using model predictive control". In: *Comput Chem Eng* 58.0 (2013), pp. 334 –343.

[5] M. Ellis and P. D. Christofides. "Economic model predictive control with time-varying objective function for nonlinear process systems". In: *AIChE J* 60.2 (2014), pp. 507–519.

[6] M. Z. Jamaludin and C. L. E. Swartz. "Effects of closed-loop dynamics in dynamic real-time optimization". In: *AIChE Annual Meeting*. Atlanta, GA, USA, 2014.

[7] M. Z. Jamaludin and C. L. E. Swartz. "Performance analysis of closed-loop dynamic real-time optimization". In: *CSChE Conference*. Calgary, AB, Canada, 2015.

[8] M. Z. Jamaludin and C. L. Swartz. "IFAC Symposium on Advanced Control of Chemical Processes (ADCHEM): A Bilevel Programming Formulation for Dynamic Real-time Optimization". In: *IFAC-PapersOnLine* 48.8 (2015), pp. 906 –911.

[9] Z. Chong and C. L. E. Swartz. "A Modelling Language for Dynamic Optimization (MLDO)". In: *CSChE Conference*. Sherbrooke, QC, Canada, 2006.

[10] J. M. Maciejowski. *Predictive Control with Constraints*. Essex, England: Prentice Hall, 2002.

[11] R. Baker and C. L. E. Swartz. "Interior point solution of multilevel quadratic programming problems in constrained model predictive control applications". In: *Ind Eng Chem Res* 47.1 (2008), pp. 81–91.

[12] B. Baumrucker, J. Renfro, and L. Biegler. "MPEC problem formulations and solution strategies with chemical engineering applications". In: *Comput Chem Eng* 32.12 (2008), pp. 2903 –2913.

[13] D. Ralph and S. J. Wright. "Some properties of regularization and penalization schemes for MPECs". In: *Optimization Methods and Software* 19.5 (2004), pp. 527–556.

[14] B. R. Maner, F. J. Doyle III, B. A. Ogunnaike, and R. K. Pearson. "Nonlinear model predictive control of a simulated multivariable polymerization reactor using second-order Volterra models". In: *Automatica* 32.9 (1996), pp. 1285 –1301.

Chapter 5

Coordination of Distributed Model Predictive Control

The formulations and results in this chapter will be presented in, and submitted to:

[1] M.Z. Jamaludin and C.L.E. Swartz. "Dynamic Real-Time Optimization of Distributed MPC Systems". *Accepted in AIChE Annual Meeting* (2016). San Francisco, CA, USA.

[2] M.Z. Jamaludin and C.L.E. Swartz. "Coordination of distributed model predictive control via closed-loop dynamic real-time optimization". *In preparation for journal publication submission*.

5.1 Introduction

Real-time optimization (RTO) is a supervisory process automation strategy that computes set-points for an underlying regulatory control system based on optimizing the plant economics. Industrial RTO systems typically utilize a steady-state model of the process, and are executed every few hours in order to track the economic optimum, as parameters affecting the plant conditions and process economics change [1, 2]. The limited execution frequency of steady-state RTO systems poses a drawback for application to processes that exhibit frequent transitions or slowly varying dynamics, which has prompted the development of dynamic RTO (DRTO) strategies. Two key control architectures for addressing plant economics within a dynamic setting are (i) a hierarchical structure, similar to the way that current industrial RTO systems are implemented, but with a dynamic model used instead of a steady-state model, and (ii) a single-level control structure in which the economic objective is incorporated within the MPC controller formulation [3, 4, 5]. The present work follows the former approach due to its compatibility with existing industrial control systems, and builds on recent advances that have considered DRTO in conjunction with a single MPC system.

Previously proposed DRTO strategies that follow a two-layer architecture typically perform economic optimization in an open-loop fashion without taking into account the presence of the plant control system. In this so-called open-loop DRTO (OL-DRTO) approach, the set-points prescribed to the underlying control system are based on the optimal open-loop trajectories under an expectation that the closed-loop response dynamics at the plant level will follow the economically optimal trajectories obtained at the DRTO level. In Tosukhowong et al. [6], the DRTO framework is designed based on a linear(ized) process model, while Würth et al. [7] utilize a nonlinear dynamic model. In an earlier study, we proposed the use of a dynamic model at the DRTO level that considers the effects of the underlying MPC system on the plant dynamics [8]. The resulting closed-loop DRTO (CL-DRTO) formulation computes controller set-point trajectories that lead to the best economics of process operation while satisfying the prevailing constraints based on the predicted closed-loop response dynamics. Neglecting the effect of the control system in the DRTO optimization tacitly assumes perfect control, which is not achievable in practice and leads to suboptimal economic performance. However, this new formulation results in a more complex problem, since each MPC control calculation over the future DRTO prediction horizon is itself defined by an optimization problem. This is handled by replacing the MPC optimization subproblems by their equivalent first-order Karush-Kuhn-Tucker (KKT) optimality conditions, and including the resulting algebraic equations as equality constraints in the DRTO economic optimization problem. In Jamaludin and Swartz [9], the rigorous closed-loop prediction problem was approximated as a bilevel rather than a multilevel optimization problem, resulting in significantly reduced computation times with modest loss in economic performance.

An overall optimal process operation can be achieved via utilization of a centralized model predictive control (MPC) system in which all control inputs are computed simultaneously from a single optimization problem, as illustrated in Figure 5.1(a). However, large scale systems, such as refineries, manufacturing plants and power generation networks, typically have a collection of MPC controllers, with each controlling a subsystem of the process plant [10], as depicted in Figure 5.1(b). Key considerations in the selection of distributed MPC systems are process scale and complexity, computational tractability, and geographic footprint. Distributed MPC architectures are designed to meet performance specifications that are relatively equivalent to the centralized MPC system, but retaining the modularity, reliability and maintainability of each controller [11]. Comprehensive reviews on distributed MPC architectures can be found in Rawlings and Stewart [12], Scattolini [13] and Christofides et al. [14]. A variety of approaches to achieve high performance distributed MPC systems has been proposed in the literature in which the control structure either involves a coordination scheme, or a direct communication between the controllers.

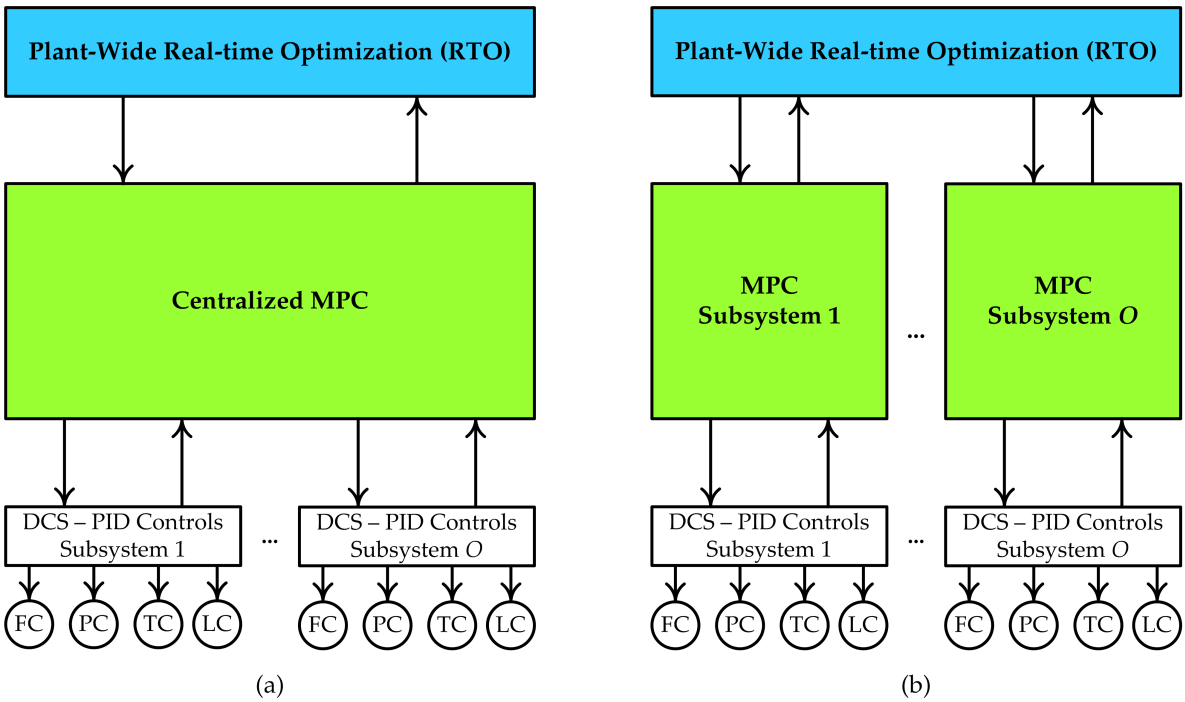

Figure 5.1: DRTO/MPC configurations in the process automation architecture: (a) centralized MPC system and (b) distributed MPC system.

Coordination of the distributed MPC systems usually involves an additional process automation scheme that supervises the interaction between MPC subsystems. Tosukhowong et al. [6] design a DRTO strategy for integrated process networks regulated under multiple local MPC controllers. A least-squares coordination layer is placed between the DRTO and MPC layers whose function is to ensure feasibility of the set-point trajectories at the end of the MPC prediction horizon. Cheng et al.

[15] propose a price-driven coordination scheme based on Newton's method in which it identifies linking constraints between MPC subsystems to compute steady-state targets for the controllers using a quadratic objection function. In a related study, Cheng et al. [16] apply Dantzig-Wolfe decomposition to the steady-state target calculation for the underlying MPC controllers based on a linear objective function. Aske et al. [17] design an MPC coordination strategy, formulated as a linear program (LP), to compute feed flows that maximize manufacturing throughput by requiring information on the available unit capacities. Shao and Cinar [18] formulate a hierarchical MPC coordination scheme in the form of a centralized supervisory control problem in which it minimizes the summation of cost functions of all MPC controllers based on integrated subsystem model matrices and input trajectories, without the inclusion of process constraints. The coordinator subsequently decomposes and distributes the anticipated control actions of all controllers to each MPC subsystem to be considered in its control calculation.

Direct communication between MPC subsystems, on the other hand, requires design of a process control network that allows information exchange between the local controllers. Camponogara et al. [19] propose a cooperative iteration MPC strategy in which each controller solves its local control problem by assuming solutions from the other subsystem controllers, and then resolves the control problem after solutions are exchanged between the controllers. Sun and El-Farra [20] design a model-based, state feedback control strategy for implementation in interconnected process networks. Control formulation of each process subsystem integrates dynamic prediction model and control law of all neighbouring subsystems to provide an estimate of the overall process interactions. The study also analyzes stability properties of the proposed control strategy, and determines an appropriate model update period that minimizes cross communication between process subsystems. Liu et al. [21] introduces a hierarchical architecture of a distributed MPC system for nonlinear dynamic systems by adding a networked control system on top of a locally stabilizing, decentralized control system, in which both of them are designed based on a Lyapunov model predictive control (LMPC) approach. The networked controller computes input trajectories for all control subsystems by embedding an approximate behavior of the local controller, and then provides its optimal input trajectory to the local controller which computes the local input trajectory. Venkat et al. [22] and Stewart et al. [23] develop an iterative, cooperation-based MPC algorithm with guaranteed feasibility and stability properties of linear system dynamics for application in a distributed control environment. Such an algorithm entails a control calculation of each MPC subsystem using a composite model of all the process subsystems to generate full system dynamics. All MPC controllers run in parallel and each optimizes a plantwide objective function formulated as a summation of the weighted cost functions of all local controllers, hence avoiding the need for of an additional coordinating scheme. The control algorithm also has the flexibility of implementing a suboptimal solution while still satisfying input constraints and stability conditions, allowing the optimization problem to be terminated at any iterate

before convergence. An extension to nonlinear system dynamics is studied in Stewart et al. [24]. Scheu and Marquardt [25] introduce a sensitivity-driven distributed MPC system in which a parallel coordination mechanism is achieved through extension of the local controller objective functions with linear approximations of objective functions of the neighbouring local controllers. In a case study, they demonstrate computational efficiency of the proposed strategy as an optimal control sequence can be achieved after only several iterations. In a recent study, Razzanelli and Pannocchia [26] present cooperative MPC algorithms for tracking piecewise constant operating targets in a distributed control environment with an application to linear system dynamics. The proposed cooperative algorithms optimize the augmented model of each MPC subsystem developed based on graph theory.

In this study, we consider a hierarchical DRTO/MPC configuration that fits well within the industrial process automation architecture in which the DRTO system optimizes the process operation at the supervisory level and provides set-point trajectories for the lower level MPC controllers. We utilize the aforementioned CL-DRTO strategy formulated as a bilevel programming problem [9] to develop a coordination scheme for application in a distributed MPC environment. The coordination scheme proposed in this study has a unique feature because interaction between the MPC subsystems and their effects to the overall plantwide dynamics are naturally taken into account through a closed-loop prediction that embeds the lower level MPC optimization algorithms. We will explore two alternatives of the CL-DRTO coordination scheme that are based on economic and target tracking objective functions. The remainder of this chapter is organized as follows. In Section 5.2, we will describe mathematical formulations of the dynamic optimization problems, and followed by a solution strategy to the bilevel programming problem. In Section 5.3, we will illustrate the performance of the proposed coordination schemes via case study simulations involving two continuous stirred-tank reactors (CSTRs) in series. Finally, this chapter is concluded in Section 5.4.

5.2 Problem Formulations

5.2.1 MPC Formulation

In this work, we consider an input-constrained MPC based on a state-space formulation [10, 27], with the general optimization problem solved at each sample time j taking the form:

$$\begin{aligned}
\min_{\hat{\mathbf{u}}_{j,k}} \phi_j := & \sum_{k=1}^{p} (\hat{\mathbf{y}}_{j,k} - \mathbf{y}^{\mathbf{SP}}_{j,k})^{\mathrm{T}} Q (\hat{\mathbf{y}}_{j,k} - \mathbf{y}^{\mathbf{SP}}_{j,k}) + \sum_{k=0}^{m-1} \Delta\hat{\mathbf{u}}^{\mathrm{T}}_{j,k} R \Delta\hat{\mathbf{u}}_{j,k} \\
& + \sum_{k=0}^{m-1} (\hat{\mathbf{u}}_{j,k} - \mathbf{u}^{\mathbf{SP}}_{j,k})^{\mathrm{T}} S (\hat{\mathbf{u}}_{j,k} - \mathbf{u}^{\mathbf{SP}}_{j,k}) \\
s.t. \quad & \hat{\mathbf{x}}_{j,k+1} = A\hat{\mathbf{x}}_{j,k} + B\hat{\mathbf{u}}_{j,k}, \quad k = 0, \ldots, m-1 \\
& \hat{\mathbf{x}}_{j,k+1} = A\hat{\mathbf{x}}_{j,k} + B\hat{\mathbf{u}}_{j,m-1}, \quad k = m, \ldots, p-1 \\
& \hat{\mathbf{y}}_{j,k} = C\hat{\mathbf{x}}_{j,k} + \hat{\mathbf{d}}_{j,k}, \quad k = 1, \ldots, p \\
& \Delta\hat{\mathbf{u}}_{j,k} = \hat{\mathbf{u}}_{j,k} - \hat{\mathbf{u}}_{j,k-1}, \quad k = 0, \ldots, m-1 \\
& \mathbf{u}_{\min} \leq \hat{\mathbf{u}}_{j,k} \leq \mathbf{u}_{\max}, \quad k = 0, \ldots, m-1
\end{aligned} \tag{5.1}$$

where $\hat{\mathbf{x}} \in \Re^{n_x}$ is a vector of predicted states and $\hat{\mathbf{y}} \in \Re^{n_y}$ is a corresponding vector of the predicted outputs over a prediction horizon p; $\hat{\mathbf{u}} \in \Re^{n_u}$ is a vector of predicted inputs over a control horizon m; $\hat{\mathbf{d}} \in \Re^{n_y}$ is a vector of disturbance estimates for output correction; $\mathbf{y}^{\mathbf{SP}} \in \Re^{n_y}$ and $\mathbf{u}^{\mathbf{SP}} \in \Re^{n_u}$ are vectors of set-point trajectories for the controlled outputs and manipulated inputs; and Q, R and S are diagonal positive semidefinite weighting matrices on the output tracking, move suppression penalty, and control tracking in the objective function, respectively. $A \in \Re^{n_x \times n_x}$, $B \in \Re^{n_x \times n_u}$ and $C \in \Re^{n_y \times n_x}$ are linear(ized), discrete-time, state-space matrices; and $\mathbf{u}_{\min}$ and $\mathbf{u}_{\max}$ are lower and upper bounds on the manipulated inputs, respectively. $\hat{\mathbf{y}}_{j,k}$ represents the predicted value of the outputs over horizon $k \in [1, \ldots, p]$ based on information available at sample time j. Although the MPC calculation results in a sequence of optimal inputs, only inputs corresponding to the first time interval are utilized for plant implementation. The optimization problem is solved iteratively at each controller sample time, constituting a moving horizon approach.

The disturbance estimate, as proposed in the original DMC and QDMC algorithms [28, 29], is computed as the difference between the current measured outputs and predicted outputs based on the information available at the previous sample time, and is assumed constant over the prediction horizon. The corresponding equations are:

$$\hat{\mathbf{d}}_j = \mathbf{y}_j^{\mathbf{m}} - C\hat{\mathbf{x}}_{j-1,1}$$
$$\hat{\mathbf{d}}_{j,k} = \hat{\mathbf{d}}_j, \quad k = 1, \ldots, p$$

where $\mathbf{y}_j^{\mathbf{m}}$ is the set of measured outputs at current time step j. To compute $\boldsymbol{\Delta}\hat{\mathbf{u}}_{j,0}$, the previously implemented manipulated input vector $\hat{\mathbf{u}}_{j-1}$ is written in the above formulation as $\hat{\mathbf{u}}_{j,-1}$ and given by:

$$\hat{\mathbf{u}}_{j,-1} = \hat{\mathbf{u}}_{j-1,0}$$

The predicted states at sampling instance j may be obtained from:

$$\begin{aligned}\hat{\mathbf{x}}_{j,0} &= \hat{\mathbf{x}}_{j-1,1} \\ &= A\hat{\mathbf{x}}_{j-1,0} + B\hat{\mathbf{u}}_{j-1,0}\end{aligned}$$

We remark here that MPC formulations, such as the variations discussed in Qin and Badgwell [10], are readily accommodated into the DRTO coordination strategy proposed in this study by tailoring the corresponding MPC optimization subproblems to the solution approach presented later. Also, the input tracking term in the MPC cost function Eq. (5.1) is not needed for square systems, in which the number of manipulated inputs is equal to the number of controlled outputs, as imposing such a term could result in offset in the face of plant-model mismatch and disturbances [30]. However, the input tracking term is useful for nonsquare systems with more manipulated inputs than the outputs to control where the corresponding input set-points $\mathbf{u}^{\mathbf{sp}}$ are typically obtained from the solution of an economic optimization problem. To maintain robustness of the control regulation, we do not include output constraints in the MPC formulation as this could lead to infeasibility and/or instability in the control calculations [10, 31]. Instead, the output constraints are considered at the upper level DRTO formulation and are applied indirectly to the regulatory level through appropriate adjustment of the set-point trajectories. The MPC formulation (5.1) represents application to a centralized control system, and extension of the formulation to a distributed MPC environment is direct. This can be done by adding a superscript of each MPC subsystem $i \in \mathcal{O}$ (with set $\mathcal{O}$ containing all the MPC subsystems $[1, ..., n_s]$), to the predicted variables, state-space matrices, prediction horizons and weighting matrices in the objective function, such as, $\hat{\mathbf{x}}_{j,k}^{(i)}$, $A^{(i)}$, $p^{(i)}$ and $Q^{(i)}$, respectively.

5.2.2 CL-DRTO with a Centralized MPC System

For clarity of exposition, we first describe the CL-DRTO formulation for a process under regulation of a centralized MPC system. The CL-DRTO problem formulated as a bilevel program presented here

utilizes only a single MPC optimization subproblem, as illustrated in Figure 5.2.

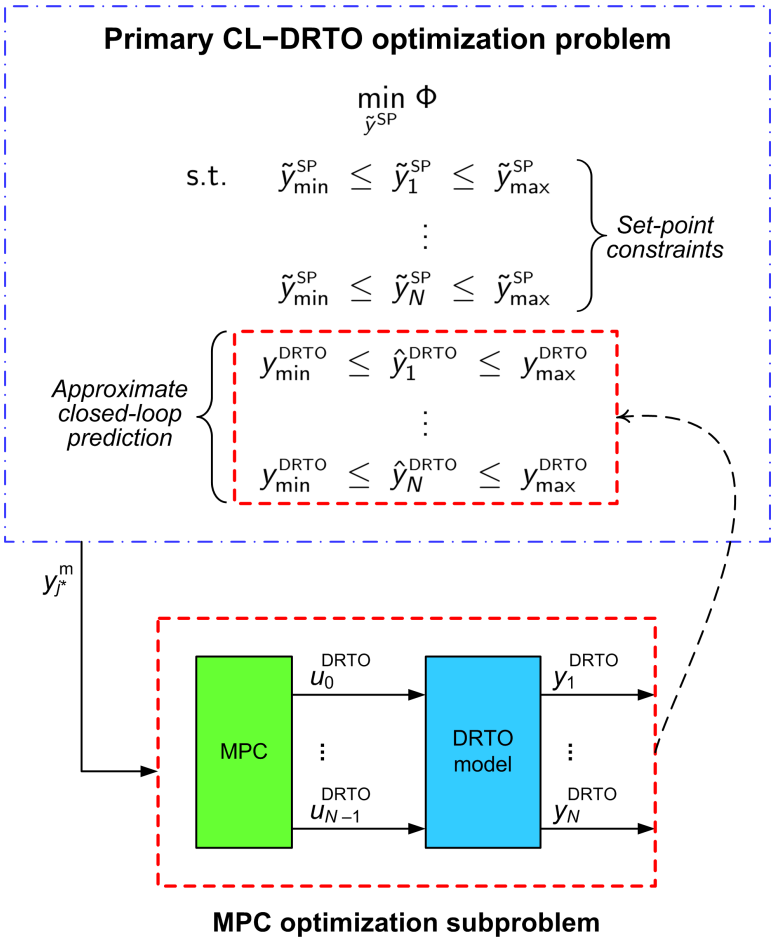

Figure 5.2: Illustration of the bilevel closed-loop prediction for a single, centralized MPC system.

The bilevel formulation is an approximation to the rigorous multilevel dynamic optimization problem that is cognizant of the future plant closed-loop behaviour involving execution of a sequence of MPC calculations. In the bilevel formulation, the MPC prediction and control horizons are extended to match the DRTO optimization horizon such that $\tilde{p} = \tilde{m} = N$, while other controller tuning parameters are exactly the same as the actual MPC controller implemented at the lower level as given in Eq. (5.1). Mathematically, we have a primary DRTO optimization problem Eq. (5.2a) and an MPC optimization subproblem Eq. (5.2b). The control trajectory from the MPC subproblem is assumed to be fully implemented to generate closed-loop prediction at the primary problem. The closed-loop optimization formulation computes set-point trajectories of the embedded MPC subproblem that minimizes (or maximizes) an objective function, usually defined by an economic criterion, based on the predicted

closed-loop response dynamics. The formulation is written as follows:

$$
\begin{aligned}
&\min_{\tilde{\mathbf{y}}^{\mathbf{SP}},\,\tilde{\mathbf{u}}^{\mathbf{SP}}} \Phi\big(\hat{\mathbf{x}}_j^{\mathbf{DRTO}},\ \hat{\mathbf{y}}_j^{\mathbf{DRTO}},\ \hat{\mathbf{u}}_j^{\mathbf{DRTO}}\big) \\
s.t.\quad \hat{\mathbf{x}}_{j+1}^{\mathbf{DRTO}} &= \mathbf{f}^{\mathbf{DRTO}}\big(\hat{\mathbf{x}}_j^{\mathbf{DRTO}},\ \hat{\mathbf{u}}_j^{\mathbf{DRTO}}\big), \qquad j = 0,\ldots,N-1 \\
\hat{\mathbf{y}}_j^{\mathbf{DRTO}} &= \mathbf{h}^{\mathbf{DRTO}}\big(\hat{\mathbf{x}}_j^{\mathbf{DRTO}}\big), \qquad j = 1,\ldots,N \\
\mathbf{0} &\le \mathbf{g}^{\mathbf{DRTO}}\big(\hat{\mathbf{x}}_j^{\mathbf{DRTO}},\ \hat{\mathbf{y}}_j^{\mathbf{DRTO}}\big), \qquad j = 1,\ldots,N \\
\mathbf{0} &= \mathbf{h}^{\mathbf{SP}}\big(\tilde{\mathbf{y}}^{\mathbf{SP}},\ \tilde{\mathbf{u}}^{\mathbf{SP}}\big) \\
\mathbf{0} &\le \mathbf{g}^{\mathbf{SP}}\big(\tilde{\mathbf{y}}_{j+1}^{\mathbf{SP}},\ \tilde{\mathbf{u}}_j^{\mathbf{SP}}\big), \qquad j = 0,\ldots,N-1 \\
\tilde{\mathbf{d}}_j &= \mathbf{y}_{j^*}^{\mathbf{m}} - C\hat{\mathbf{x}}_{j^*-1,1}, \qquad j = 1,\ldots,N
\end{aligned}
\tag{5.2a}
$$

$$
\left.
\begin{aligned}
\hat{\mathbf{u}}^{\mathbf{DRTO}} = \arg\ \min_{\tilde{\mathbf{u}}}\ & \phi := \textstyle\sum_{j=1}^{N}\big(\tilde{\mathbf{y}}_j - \tilde{\mathbf{y}}_j^{\mathbf{SP}}\big)^{\mathrm{T}} Q\big(\tilde{\mathbf{y}}_j - \tilde{\mathbf{y}}_j^{\mathbf{SP}}\big) + \textstyle\sum_{j=0}^{N-1} \boldsymbol{\Delta}\tilde{\mathbf{u}}_j^{\mathrm{T}} R\boldsymbol{\Delta}\tilde{\mathbf{u}}_j \\
& \qquad + \textstyle\sum_{k=0}^{N-1}\big(\tilde{\mathbf{u}}_j - \tilde{\mathbf{u}}_j^{\mathbf{SP}}\big)^{\mathrm{T}} S\big(\tilde{\mathbf{u}}_j - \tilde{\mathbf{u}}_j^{\mathbf{SP}}\big) \\
s.t.\quad \tilde{\mathbf{x}}_{j+1} &= A\tilde{\mathbf{x}}_j + B\tilde{\mathbf{u}}_j, \quad j = 0,\ldots,N-1 \\
\tilde{\mathbf{y}}_j &= C\tilde{\mathbf{x}}_j + \tilde{\mathbf{d}}_j, \quad j = 1,\ldots,N \\
\boldsymbol{\Delta}\tilde{\mathbf{u}}_j &= \tilde{\mathbf{u}}_j - \tilde{\mathbf{u}}_{j-1}, \quad j = 0,\ldots,N-1 \\
\mathbf{u}_{\min} \le \tilde{\mathbf{u}}_j &\le \mathbf{u}_{\max}, \quad j = 0,\ldots,N-1
\end{aligned}
\right\} \text{MPC subproblem}
\tag{5.2b}
$$

where $\hat{\mathbf{x}}_j^{\mathbf{DRTO}} \in \Re^{n_x}$ is a vector of DRTO model states, $\hat{\mathbf{y}}_j^{\mathbf{DRTO}} \in \Re^{n_y}$ is a corresponding vector of DRTO model outputs, and $\hat{\mathbf{u}}_j^{\mathbf{DRTO}} \in \Re^{n_u}$ is a vector of DRTO inputs. $\hat{\mathbf{u}}^{\mathbf{DRTO}}$, $\hat{\mathbf{x}}^{\mathbf{DRTO}}$ and $\hat{\mathbf{y}}^{\mathbf{DRTO}}$ are composite vectors comprising all the DRTO inputs, states and outputs over the optimization horizon $j \in [0,\ldots,N-1]$:

$$
\begin{aligned}
\hat{\mathbf{u}}^{\mathbf{DRTO}} &= \left[\big(\hat{\mathbf{u}}_0^{\mathbf{DRTO}}\big)^{\mathrm{T}},\ \big(\hat{\mathbf{u}}_1^{\mathbf{DRTO}}\big)^{\mathrm{T}},\ldots,\big(\hat{\mathbf{u}}_{N-1}^{\mathbf{DRTO}}\big)^{\mathrm{T}}\right]^{\mathrm{T}} \\
\hat{\mathbf{x}}^{\mathbf{DRTO}} &= \left[\big(\hat{\mathbf{x}}_1^{\mathbf{DRTO}}\big)^{\mathrm{T}},\ \big(\hat{\mathbf{x}}_2^{\mathbf{DRTO}}\big)^{\mathrm{T}},\ldots,\big(\hat{\mathbf{x}}_N^{\mathbf{DRTO}}\big)^{\mathrm{T}}\right]^{\mathrm{T}} \\
\hat{\mathbf{y}}^{\mathbf{DRTO}} &= \left[\big(\hat{\mathbf{y}}_1^{\mathbf{DRTO}}\big)^{\mathrm{T}},\ \big(\hat{\mathbf{y}}_2^{\mathbf{DRTO}}\big)^{\mathrm{T}},\ldots,\big(\hat{\mathbf{y}}_N^{\mathbf{DRTO}}\big)^{\mathrm{T}}\right]^{\mathrm{T}}
\end{aligned}
\tag{5.3}
$$

with $\tilde{\mathbf{u}}^{\mathbf{SP}}$ and $\tilde{\mathbf{y}}^{\mathbf{SP}}$ analogously defined. Φ is typically an economic objective function used to optimize plant operation, $\mathbf{f}^{\mathbf{DRTO}}$ represents the dynamic model utilized for DRTO prediction, $\mathbf{h}^{\mathbf{DRTO}}$ are equality constraints that relate the states to the outputs, and $\mathbf{g}^{\mathbf{DRTO}}$ comprises inequality constraints on the outputs and possibly some of the states. The time index j also corresponds to the MPC sampling instances over the DRTO optimization horizon. Equality $\mathbf{h}^{\mathbf{SP}}$ enforces the set-point trajectories to be constant for every DRTO interval within the optimization horizon, which is useful to dampen

aggressive changes in the set-points in the corresponding trajectories. Inequality $\mathbf{g}^{\mathbf{SP}}$ is used to impose upper and lower bounds on the set-point trajectories. $\tilde{\mathbf{d}}_j$ defines the disturbance estimate for the MPC subproblem, which is computed based on the current plant output measurement ($\mathbf{y}^{\mathbf{m}}_{j^*}$) and the output prediction at the previous controller sampling instance, given by $C\hat{\mathbf{x}}_{j^*-1,1}$.

MPC optimization subproblem Eq. (5.2b) follows the algorithm described in Eq. (5.1), with a subscript j used to indicate prediction steps over the optimization horizon. ϕ is a quadratic MPC cost function, $\tilde{\mathbf{x}} \in \Re^{n_x}$ is a vector of MPC model states, $\tilde{\mathbf{y}} \in \Re^{n_y}$ is a corresponding vector of MPC model outputs, $\tilde{\mathbf{u}} \in \Re^{n_u}$ is a vector of MPC inputs at each prediction step j, and $\tilde{\mathbf{y}}_j$ represents the predicted value of the outputs over a prediction horizon $j \in [1, \ldots, N]$. $\tilde{\mathbf{y}}^{\mathbf{SP}} \in \Re^{n_y}$ and $\tilde{\mathbf{u}}^{\mathbf{SP}} \in \Re^{n_u}$ are vectors of tracking set-points for the outputs and inputs, respectively. In this formulation, there is a direct correspondence between the DRTO variables $\hat{\mathbf{x}}^{\mathbf{DRTO}}_j$, $\hat{\mathbf{y}}^{\mathbf{DRTO}}_j$, and $\hat{\mathbf{u}}^{\mathbf{DRTO}}_j$ with the MPC variables $\tilde{\mathbf{x}}_j$, $\tilde{\mathbf{y}}_j$, and $\tilde{\mathbf{u}}_j$, respectively. However, we utilize notation that differentiates between the DRTO variables in the primary problem and the MPC variables in the optimization subproblem because such a direct correspondence does not carry over to the CL-DRTO formulation with an embedded distributed MPC system that we will describe next.

5.2.3 CL-DRTO with a Distributed MPC System

Application of the CL-DRTO approach for coordination of a distributed MPC system computes optimal set-point trajectories for all MPC controllers simultaneously. The DRTO plant model represents the overall plantwide dynamics whereas the MPC models represent the local dynamics of process subsystems. The plant model used within the DRTO module is consistent with the dynamic models used in the MPC controllers, but with the interactions between the process subsystems captured through appropriate linking relationships, such as material flows. The response of the plant under the action of the MPC subsystems is computed by taking into account the actions of all the controllers, as well as the process interactions between the subsystems. As depicted in Figure 5.3, the CL-DRTO coordination scheme consists of a primary optimization problem Eq. (5.4a) that supervises all MPC subsystems functioning in the plant. The coordinator predicts the plant closed-loop response dynamics based on the control input trajectories computed by the local MPC optimization subproblems Eq. (5.4b) of $i \in \mathcal{O}$ with superscript i defining each MPC subsystem. The objective function of the coordinator Φ implemented via this CL-DRTO strategy can be based purely on economics or target tracking; we will explore both alternatives in the case study section.

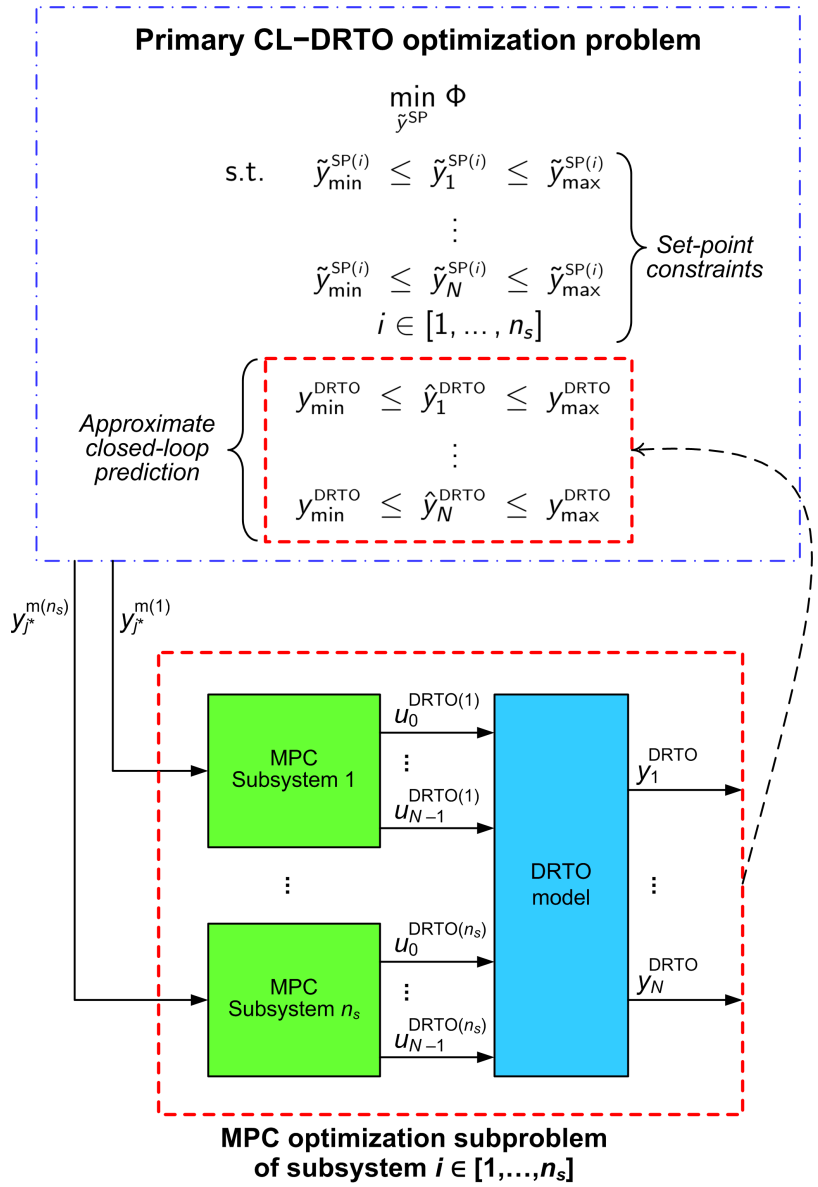

Figure 5.3: Illustration of the bilevel closed-loop prediction for a distributed MPC system.

The CL-DRTO coordination formulation is written as follows:

$$\min_{\tilde{\mathbf{y}}^{\mathbf{SP}},\, \tilde{\mathbf{u}}^{\mathbf{SP}},\, \tilde{\mathbf{d}}^{\mathbf{DRTO}}} \Phi\big(\hat{\mathbf{x}}_j^{\mathbf{DRTO}},\, \hat{\mathbf{y}}_j^{\mathbf{DRTO}},\, \hat{\mathbf{u}}_j^{\mathbf{DRTO}}\big)$$

$$\begin{aligned}
s.t.\quad \hat{\mathbf{x}}_{j+1}^{\mathbf{DRTO}} &= \mathbf{f}^{\mathbf{DRTO}}\big(\hat{\mathbf{x}}_j^{\mathbf{DRTO}},\, \hat{\mathbf{u}}_j^{\mathbf{DRTO}}\big), \qquad j = 0,\ldots,N-1 \\
\hat{\mathbf{y}}_j^{\mathbf{DRTO}} &= \mathbf{h}^{\mathbf{DRTO}}\big(\hat{\mathbf{x}}_j^{\mathbf{DRTO}}\big), \qquad j = 1,\ldots,N \\
\mathbf{0} &\leq \mathbf{g}^{\mathbf{DRTO}}\big(\hat{\mathbf{x}}_j^{\mathbf{DRTO}},\, \hat{\mathbf{y}}_j^{\mathbf{DRTO}}\big), \qquad j = 1,\ldots,N \\
\mathbf{0} &= \mathbf{h}^{\mathbf{SP}}\big(\tilde{\mathbf{y}}^{\mathbf{SP}(i)},\, \tilde{\mathbf{u}}^{\mathbf{SP}(i)}\big), \qquad \forall i \in \mathcal{O} \\
\mathbf{0} &\leq \mathbf{g}^{\mathbf{SP}}\big(\tilde{\mathbf{y}}_{j+1}^{\mathbf{SP}(i)},\, \tilde{\mathbf{u}}_j^{\mathbf{SP}(i)}\big), \qquad \forall i \in \mathcal{O}, \quad j = 0,\ldots,N-1 \\
\tilde{\mathbf{d}}_1^{(i)} &= \mathbf{y}_{j^*}^{\mathbf{m}(i)} - C^{(i)}\hat{\mathbf{x}}_{j^*-1,1}^{(i)}, \qquad \forall i \in \mathcal{O} \\
\tilde{\mathbf{d}}_j^{(i)} &= \mathbf{y}_{j^*}^{\mathbf{m}(i)} - C^{(i)}\hat{\mathbf{x}}_{j^*-1,1}^{(i)} + \tilde{\mathbf{d}}_j^{\mathbf{DRTO}(i)}, \qquad \forall i \in \mathcal{O}, \qquad j = 2,\ldots,N \\
\mathbf{0} &= \mathbf{h}^{\mathbf{FIX}}(\hat{\mathbf{y}}_j^{\mathbf{DRTO}},\, \tilde{\mathbf{y}}_j), \qquad j = 2,\ldots,N
\end{aligned} \tag{5.4a}$$

$$\left.\begin{aligned}
\hat{\mathbf{u}}^{\mathbf{DRTO}} = \ \arg\ \min_{\tilde{\mathbf{u}}^{(i)}}\ & \phi^{(i)} := \textstyle\sum_{k=1}^{N} \big(\tilde{\mathbf{y}}_j^{(i)} - \tilde{\mathbf{y}}_j^{\mathbf{SP}(i)}\big)^{\mathrm{T}} Q^{(i)} \big(\tilde{\mathbf{y}}_j^{(i)} - \tilde{\mathbf{y}}_j^{\mathbf{SP}(i)}\big) \\
& \qquad + \textstyle\sum_{k=0}^{N-1} \big(\boldsymbol{\Delta}\tilde{\mathbf{u}}_j^{(i)}\big)^{\mathrm{T}} R^{(i)} \big(\boldsymbol{\Delta}\tilde{\mathbf{u}}_j^{(i)}\big) \\
& \qquad + \textstyle\sum_{k=0}^{N-1} \big(\tilde{\mathbf{u}}_j^{(i)} - \tilde{\mathbf{u}}_j^{\mathbf{SP}(i)}\big)^{\mathrm{T}} S^{(i)} \big(\tilde{\mathbf{u}}_j^{(i)} - \tilde{\mathbf{u}}_j^{\mathbf{SP}(i)}\big) \\
s.t.\quad & \tilde{\mathbf{x}}_{j+1}^{(i)} = A^{(i)}\tilde{\mathbf{x}}_j^{(i)} + B^{(i)}\tilde{\mathbf{u}}_j^{(i)}, \quad j = 0,\ldots,N-1 \\
& \tilde{\mathbf{y}}_j^{(i)} = C^{(i)}\tilde{\mathbf{x}}_j^{(i)} + \tilde{\mathbf{d}}_j^{(i)}, \quad j = 1,\ldots,N \\
& \boldsymbol{\Delta}\tilde{\mathbf{u}}_j^{(i)} = \tilde{\mathbf{u}}_j^{(i)} - \tilde{\mathbf{u}}_{j-1}^{(i)}, \quad j = 0,\ldots,N-1 \\
& \mathbf{u}_{\min}^{(i)} \leq \tilde{\mathbf{u}}_j^{(i)} \leq \mathbf{u}_{\max}^{(i)}, \quad j = 0,\ldots,N-1
\end{aligned}\right\} \begin{array}{l}\text{MPC} \\ \text{subproblem} \\ \text{of} \\ \text{subsystem } i \in \mathcal{O}\end{array} \tag{5.4b}$$

Model equations $\mathbf{f}^{\mathbf{DRTO}}$ and $\mathbf{h}^{\mathbf{DRTO}}$, inequality constraint $\mathbf{g}^{\mathbf{DRTO}}$, and composite vectors $\hat{\mathbf{x}}^{\mathbf{DRTO}}$ and $\hat{\mathbf{y}}^{\mathbf{DRTO}}$ follow the definition given in Section 5.2.2. On the other hand, composite vector $\hat{\mathbf{u}}^{\mathbf{DRTO}}$ comprises input trajectories from all MPC subsystems $\mathcal{O}$ as written below:

$$\hat{\mathbf{u}}^{\mathbf{DRTO}} = \left[\big(\hat{\mathbf{u}}_0^{\mathbf{DRTO}}\big)^{\mathrm{T}},\ \big(\hat{\mathbf{u}}_1^{\mathbf{DRTO}}\big)^{\mathrm{T}}, \ldots,\ \big(\hat{\mathbf{u}}_{N-1}^{\mathbf{DRTO}}\big)^{\mathrm{T}}\right]^{\mathrm{T}}$$

where

$$\hat{\mathbf{u}}_j^{\mathbf{DRTO}} = \left[\big(\hat{\mathbf{u}}_j^{(1)}\big)^{\mathrm{T}},\ \big(\hat{\mathbf{u}}_j^{(2)}\big)^{\mathrm{T}}, \ldots,\ \big(\hat{\mathbf{u}}_j^{(n_s)}\big)^{\mathrm{T}}\right]^{\mathrm{T}}$$

with $\tilde{\mathbf{y}}^{\mathbf{SP}}$ and $\tilde{\mathbf{u}}^{\mathbf{SP}}$ analogously defined. Equality constraint $\mathbf{h}^{\mathbf{SP}}$ enforces the set-point trajectories of

each MPC subsystem i to be constant for every DRTO interval within the optimization horizon, and inequality constraint $\mathbf{g}^{\mathbf{SP}}$ defines the upper and lower bounds of the corresponding set-point trajectories.

Disturbance estimate $\tilde{\mathbf{d}}_1^{(i)}$ is computed based on the current output measurement $\mathbf{y}_{j^*}^{\mathbf{m}(i)}$ and the output prediction at the previous controller sampling instance of each MPC subsystem i. The subsequent disturbance estimate $\tilde{\mathbf{d}}_j^{(i)}$ of $j \in [2, \ldots, N]$ is augmented with an additional vector of optimization variable $\tilde{\mathbf{d}}_j^{\mathbf{DRTO}(i)}$ to indirectly take into account output feedback from the DRTO plant model to the future MPC calculations that is not considered in the bilevel formulation. Consequently, we impose an equality constraint $\mathbf{h}^{\mathbf{FIX}}$ to ensure that the MPC output prediction matches the DRTO output prediction at each time step $j \in [2, \ldots, N]$. Such an equality constraint is also necessary to avoid steady-state offset between the DRTO model prediction and the tracking set-points of the MPC subsystems due to a mismatch between the plantwide model and the subsystem models. $\tilde{\mathbf{y}}_j$ in $\mathbf{h}^{\mathbf{FIX}}$ is a composite vector:

$$\tilde{\mathbf{y}}_j = \left[\left(\tilde{\mathbf{y}}_j^{(1)}\right)^{\mathrm{T}}, \left(\tilde{\mathbf{y}}_j^{(2)}\right)^{\mathrm{T}}, \ldots, \left(\tilde{\mathbf{y}}_j^{(n_s)}\right)^{\mathrm{T}} \right]^{\mathrm{T}}, \quad i \in [2, \ldots, n_s]$$

The definition of MPC optimization subproblem Eq. (5.4b) of each subsystem $i \in \mathcal{O}$ is similar to Eq. (5.2b), except that the prediction variables, state-space model matrices, prediction horizons and weighting matrices in the objective function are accompanied with an additional superscript i to indicate the corresponding subsystem. In this DRTO coordination formulation, we assume that each MPC subsystem has no knowledge of other MPC's actions. However, the effects of inputs from the neighbouring MPC subsystems could be included in the form of feedforward MPC model prediction.

5.2.4 Solution Strategy

The bilevel optimization problem presented in this study is solved following a simultaneous solution approach. This involves replacement of the convex MPC quadratic programming (QP) subproblem(s) with their necessary and sufficient, KKT optimality conditions. The MPC subproblem at each DRTO prediction step may be represented as a QP of the form:

$$\begin{aligned} \min_{\mathbf{z}} \ & \frac{1}{2}\mathbf{z}^{\mathrm{T}} H\mathbf{z} + \mathbf{g}^{\mathrm{T}}\mathbf{z} \\ \text{s.t.} \quad & A\mathbf{z} = \mathbf{b} \\ & \mathbf{z} \geq \mathbf{0} \end{aligned} \tag{5.5}$$

with the corresponding KKT conditions given by the algebraic equations below:

$$\begin{aligned} H\mathbf{z} + \mathbf{g} - A^{\mathrm{T}}\boldsymbol{\lambda} - \boldsymbol{\nu} &= \mathbf{0} \\ A\mathbf{z} - \mathbf{b} &= \mathbf{0} \\ z_i\nu_i = 0, \quad i &= 1, ..., I \\ (\mathbf{z},\ \boldsymbol{\nu}) &\geq \mathbf{0} \end{aligned} \tag{5.6}$$

A detailed derivation of the KKT conditions corresponding to the MPC optimization subproblem related to this study can be found in Baker and Swartz [32]. Reformulation of the bilevel problem results in a single-level mathematical program with complementarity constraints (MPCC).

The complementarity constraints, which take the form $z_i\nu_i = 0$, are a source of difficulty in the solution of nonlinear programming (NLP) problems in which they present due to violation of constraint qualifications [33]. Effective handling of complementarity constraints requires reformulation of the complementarity constraints for solution as typical NLP problems, or an alternative NLP algorithm that internally treats the complementarity constraints. In this study, an exact penalty formulation [34] is applied, in which the complementarity constraints are penalized through a form of $\rho \sum_i^I z_i\nu_i$ in the objective function of the DRTO coordination problem, with the resulting problem posed to a standard NLP solver. The weighting parameter ρ is a tuning parameter for the MPCC problem, obtained by gradually increasing the value from small number until it exceeds a critical value, i.e. $\rho > \rho_c$, at which point the original complementarity constraints will be approximately satisfied, and the optimal solution recovers the original objective function of the MPCC problem due to negligible contribution of the penalty term.

5.2.5 Real-time Implementation

In our coordination framework, we specify that all MPC controllers have the same sampling time of Δt_{MPC}, which is smaller than that of the DRTO, Δt_{DRTO}. This implies that there are multiple MPC calculations within a DRTO optimization interval. The implementation strategy is illustrated in Figure 5.4, and it follows a procedure described here. At every time instance t_{j^*}, output feedback information $\mathbf{y}_{j^*}^{\mathbf{m}(i)}$ is available from measurement of all subsystems $i \in \mathcal{O}$ in the plant. The CL-DRTO

coordination layer receives the feedback information at every optimization interval Δt_{DRTO}, and solves a plantwide dynamic optimization problem to compute DRTO set-point trajectories, $\mathbf{y}_{j^*}^{\mathbf{SP}(i)}$ and $\mathbf{u}_{j^*}^{\mathbf{SP}(i)}$, for the lower level controllers. At the control layer, only a subset of the overall DRTO set-point trajectories will be selected for MPC tracking at a particular time instance. Construction of the tracking set-points is shifted in time by following the MPC moving horizon window until a new update of the DRTO set-point trajectories is issued at the next DRTO calculation. At every sampling time Δt_{MPC}, all MPC controllers receive output feedback information from the plant. Each MPC controller then solves the corresponding local control problem based on the currently prescribed tracking set-points. The resulting optimal control inputs $\mathbf{u}_{j^*}^{(i)}$ are issued to the actuators (or possibly local PID controllers) for plant implementation.

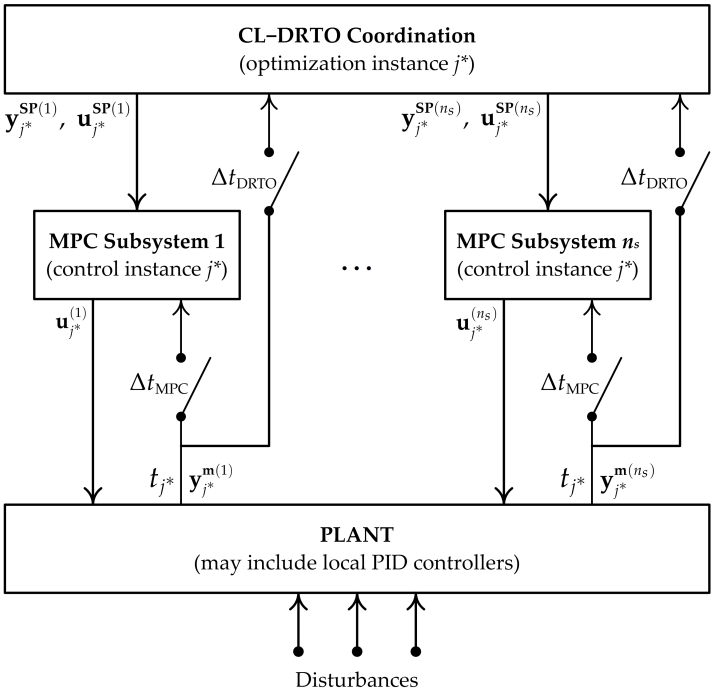

Figure 5.4: Real-time implementation

MATLAB R2012b is chosen as a supervisory computational platform to solve the MPC problem using the `quadprog` solver, and also to perform process simulation. The DRTO problem, the size of which is significantly larger than that of the MPC, is modelled in AMPL and solved using an `IPOPT 3.12.0` [35] utilizing the linear solver `ma27`. Also, a warm-start is provided for the primal variables of the DRTO problems. An in-house interface written in PHYTON allows data transmission between AMPL and MATLAB. All case studies are solved using a 3.4GHz INTEL CORE-i7 with 8GB RAM running Windows 7.

5.3 Illustrative Case Study

The process considered in this case study is depicted in Figure 5.5, which involves two constant-volume continuous stirred-tank reactors (CSTRs) in series with an intermediate mixer introducing the second feed. The system is based on a case study presented in Bahri et al. [36], and Loeblein and Perkins [37]. The reaction taking place in both reactors is a first-order, exothermic, irreversible reaction A $\rightarrow$ B. The model equations describing the dynamic behaviour of the process is derived from first-principles mass and energy balances, with an assumption of negligible dynamics around the mixer. The density and heat capacity of the reactants are assumed constant and are independent of the temperature and concentration of the reactor mixtures. The cooling jackets are assumed to have negligible dynamics. For convenience, the model equations are given below, and a summary of model parameters and nominal simulation data are listed in Table 5.1.

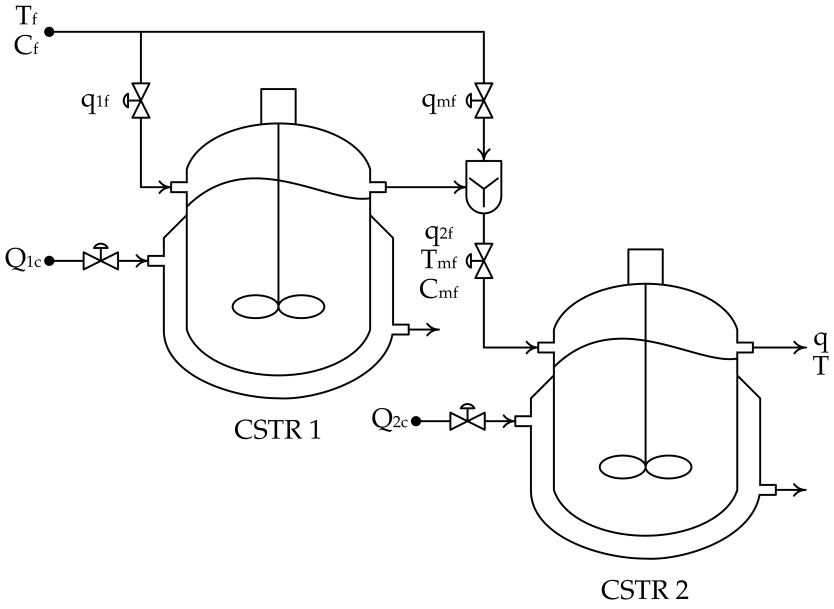

Figure 5.5: Two CSTRs in series with intermediate feed.

- Dynamic model of CSTR 1:

$$\frac{dC_1}{dt} = \frac{1}{V_1}\left(q_{1f}C_{1f} - q_1C_1\right) - k_0 \exp\left[\frac{-E_a}{RT_1}\right] C_1$$
$$\frac{dT_1}{dt} = \frac{1}{V_1}\left(q_{1f}T_{1f} - q_1T_1\right) - \frac{\Delta H}{\rho C_p V_1} k_0 \exp\left[\frac{-E_a}{RT_1}\right] C_1 - \frac{Q_{1c}}{\rho C_p V_1}$$

- Pseudo steady-state model of the mixer:

$$q_{2f} = q_1 + q_{mf}$$

$$q_{2f}C_{2f} = q_1C_1 + q_{mf}C_{mf}$$
$$q_{2f}T_{2f} = q_1T_1 + q_{mf}T_{mf}$$

- Dynamic model of CSTR 2:

$$\frac{dC_2}{dt} = \frac{1}{V_2}\left(q_{2f}C_{2f} - q_2C_2\right) - k_0 \exp\left[\frac{-E_a}{RT_2}\right] C_2$$
$$\frac{dT_2}{dt} = \frac{1}{V_2}\left(q_{2f}T_{2f} - q_2T_2\right) - \frac{\Delta H}{\rho C_p V_2} k_0 \exp\left[\frac{-E_a}{RT_2}\right] C_2 - \frac{Q_{2c}}{\rho C_p V_2}$$

Table 5.1: List of nominal simulation data and model parameters

Nominal inputs [38]	Model parameters [37]
$q_{1f} = 0.6154$ m^3/s	$V_1 = V_2 = 5$ m^3
$q_{mf} = 0.06598$ m^3/s	$\frac{\Delta H}{\rho C_p} = 5$ m^3.K/mol
$Q_{1c} = 30$ W	$\frac{E_a}{R} = 6000$ K
$Q_{2c} = 3.968$ W	$\rho C_p = 1$ J/m^3/K
$T_f = 300$ K	$k_0 = 2.7 \times 10^8$ 1/s
$C_f = 20$ mol/m^3	

In this case study, operational constraints are enforced on the feed flow rates, q_{1f} and q_{mf}, whereas a product demand specification is imposed on C_2. Reactor temperatures T_1 and T_2 are associated with advisory safety limits in the process operation. For this nonsquare system, we include input set-points to generate a unique solution to the control problems. Set-points and the corresponding constraints are applied on the cooling supply to CSTR 1, and also the raw material feed to CSTR 2 as this affects the overall process productivity. The aforementioned constraints are listed as follow:

$$0.05 \leq q_{1f} \leq 0.80540 \quad \text{m}^3/\text{s}$$
$$0.05 \leq q_{mf},\ q_{mf}^{\text{SP}} \leq 0.26098 \quad \text{m}^3/\text{s}$$
$$q_{1f} + q_{mf} \leq 0.8 \quad \text{m}^3/\text{s}$$
$$0 \leq Q_{1c},\ Q_{1c}^{\text{SP}} \leq 30 \quad \text{W}$$
$$0 \leq Q_{2c} \leq 20 \quad \text{W}$$
$$325 \leq T_1,\ T_1^{\text{SP}} \leq 352 \quad \text{K}$$
$$325 \leq T_2,\ T_2^{\text{SP}} \leq 352 \quad \text{K}$$
$$C_2 \leq 0.3 \quad \text{mol/m}^3$$

In order to design a distributed (and decentralized) MPC system, we partition the process into two subsystems by defining the dynamic models of CSTR 1 as the first subsystem and dynamic models of the mixer and CSTR 2 as the second subsystem. The sets of output and input variables for each subsystem are defined by a subscript $i \in [1,\ 2]$ given as follows:

$$x_1 = [C_1,\ T_1]^{\mathrm{T}}, \quad y_1 = T_1, \quad u_1 = [q_{1f},\ Q_{1c}]^{\mathrm{T}}$$
$$x_2 = [C_2,\ T_2]^{\mathrm{T}}, \quad y_2 = T_2, \quad u_2 = [q_{mf},\ Q_{2c}]^{\mathrm{T}}$$

The process model is linearized at the nominal operating point for utilization in the MPC and DRTO formulations, whereas the nonlinear dynamic model is utilized to perform plant simulation. Linearization is carried out in MATLAB by computing the Jacobian of the reactor model at the nominal operating point using a complex-step differentiation to generate the continuous state-space models, which are subsequently discretized based on the MPC sample time of 1 s. Closed-loop simulation is carried out over a time frame of 80 s with a DRTO optimization interval of 4 s. Also, a step decrease of 2 K in the reactor feed temperature is introduced at time 39 s.

5.3.1 Economic Coordination

Here we consider economic coordination of a distributed MPC system based on the CL-DRTO formulation proposed in Section 5.2.3, and compare its performance to implementation of a centralized control environment described in Section 5.2.2. The economics of the process operation takes into account the revenue of the raw material converted to product, as well as the costs of feed and utility supplies. The economic objective function is defined in Eq. (5.7) with the best-performing MPC tuning parameters for the centralized and distributed MPC systems (determined by trial-and-error) given in Table 5.2. A DRTO optimization horizon of 80 s is chosen for closed-loop prediction, and a complementarity penalty parameter of 10 is chosen for penalization of all complementarity constraints.

$$\min \Phi = \Delta t_{\mathrm{MPC}} \sum_{j=0}^{N-1} \left[10 \left(q_{1f,j} C_{1f} + q_{mf,j} C_{mf} - q_{2,j} C_{2,j+1} \right) - 0.1 q_{1f,j} - 0.1 q_{mf,j} - 0.01 Q_{1c,j} - Q_{2c,j} \right] \tag{5.7}$$

Table 5.2: MPC design parameters.

MPC configuration	p	m	Weighting matrices
Centralized MPC	40	2	Q = diag(4.0, 1.0) R = diag(800, 15, 700, 5) S = diag(0, 200, 300, 0)
Coordinated MPC			
MPC CSTR 1	40	2	$Q^{(1)} = 2$, $R^{(1)}$ = diag(800, 15), $S^{(1)}$ = diag(0, 200)
MPC CSTR 2	40	2	$Q^{(2)} = 3$, $R^{(2)}$ = diag(800, 15), $S^{(2)}$ = diag(300, 0)

Figure 5.6 shows plant dynamic response under regulation of a distributed MPC system coordinated using the economic-based CL-DRTO strategy, and Figure 5.7 shows implementation of the CL-DRTO strategy on a centralized MPC environment. Excellent performance is observed for both control configurations, and the results are summarized as follow. The coordinated MPC system generates a profit of \$11,898 with only 0.47% of economic loss relative to \$11,954 for the centralized strategy. The process is operated at the upper bound of temperature safety limits of T_1 and T_2, which accounts for minimum operating cost. The cooling supply Q_{1c} and its corresponding set-point trajectory are enforced at the upper bound to contribute to the lowest operating cost, and therefore feed q_{1f} to CSTR 1 is mainly utilized to control the reactor temperature T_1. In CSTR 2, feed q_{mf} is also adjusted in addition to Q_{2c} for disturbance rejection because the cost of Q_{2c} is ten times larger than that of the q_{mf}. Consequently, such operational behaviour causes the overall production rate to shift after a feed temperature disturbance enters the system at 39 s, due to a reduction in the feed q_{1f} to CSTR 1. The CL-DRTO strategy has an adaptive mechanism to continuously update the set-point trajectories in a cost-optimal fashion at each optimization interval in order to minimize constraint violation at the plant level. Referring to Figure 5.6, temperature set-points of T_1 and T_2 starts off high, then backs off from the constraint limits (i.e. between time 8 and 12 s for T_1^{SP}, and between time 4 and 8 s for T_2^{SP}) to minimize overshoots during process transition at the beginning of the simulation time. The overall set-point trajectories plotted are composed of the first period of the set-point trajectories computed at every DRTO interval, in which significant adjustments (i.e. backoffs) are observed. However, the resulting set-point trajectories from every DRTO calculation converge to certain economically steady-states towards the end of the optimization horizon. The backoff mechanism on the temperature set-points is also observed between time 40 and 44 s after the disturbance enters the system . It also reduces the impact of disturbance propagation from CSTR 1 to CSTR 2. This leads to minimal perturbation in the reactor temperature of less than 0.3 K from the advisory safety limits at the plant level, which is almost negligible from practical standpoint. The sum of constraint violations (SCV), computed as a summation of magnitudes of temperature that exceeds its safety limit at each controller sampling

instance over the simulation horizon, for the distributed and centralized MPC systems are 0.40 and 0.87, respectively.

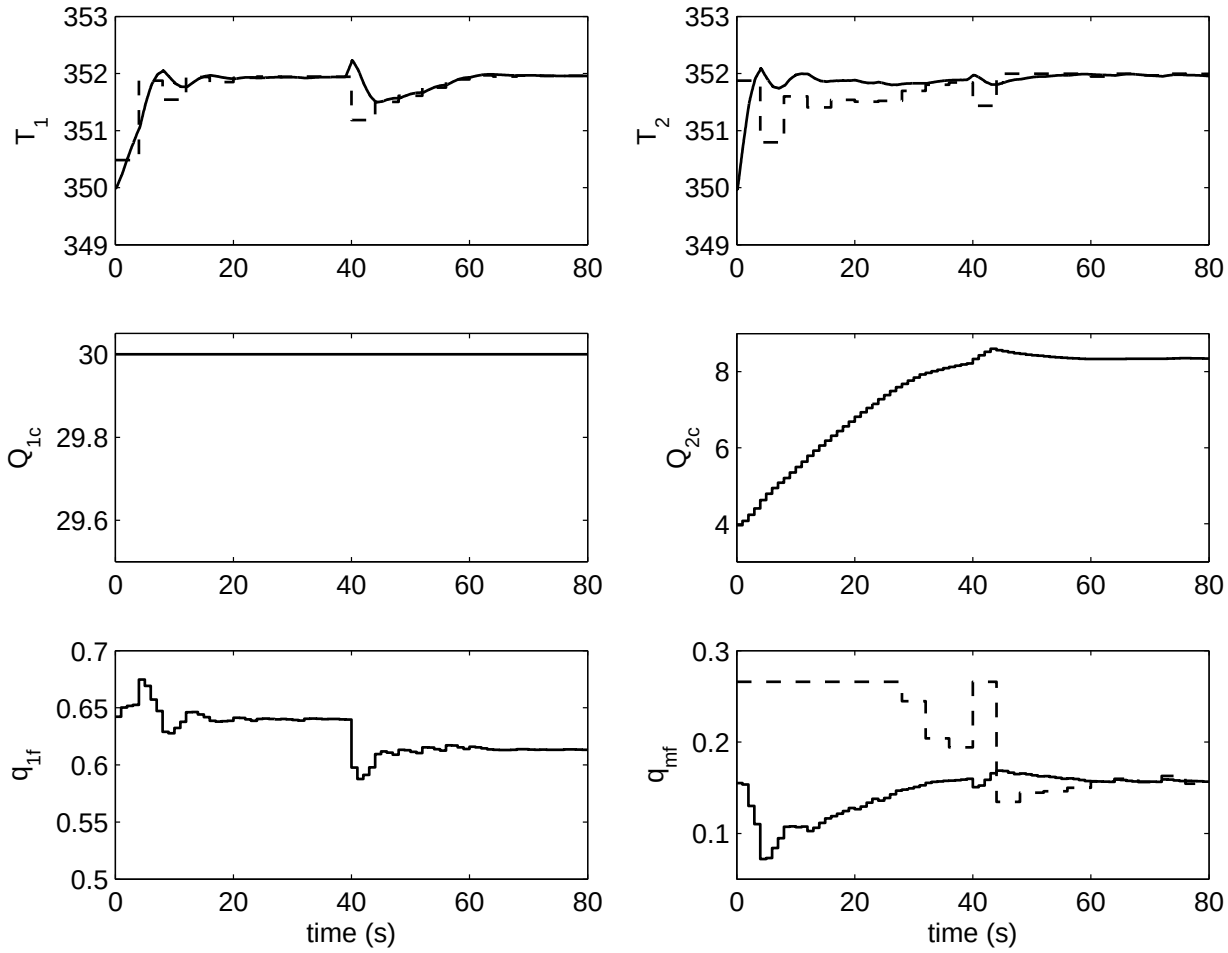

Figure 5.6: CL-DRTO with coordinated MPC, profit = \$11,898.
Legend: *solid lines* = process dynamics, *dashed lines* = set-points.

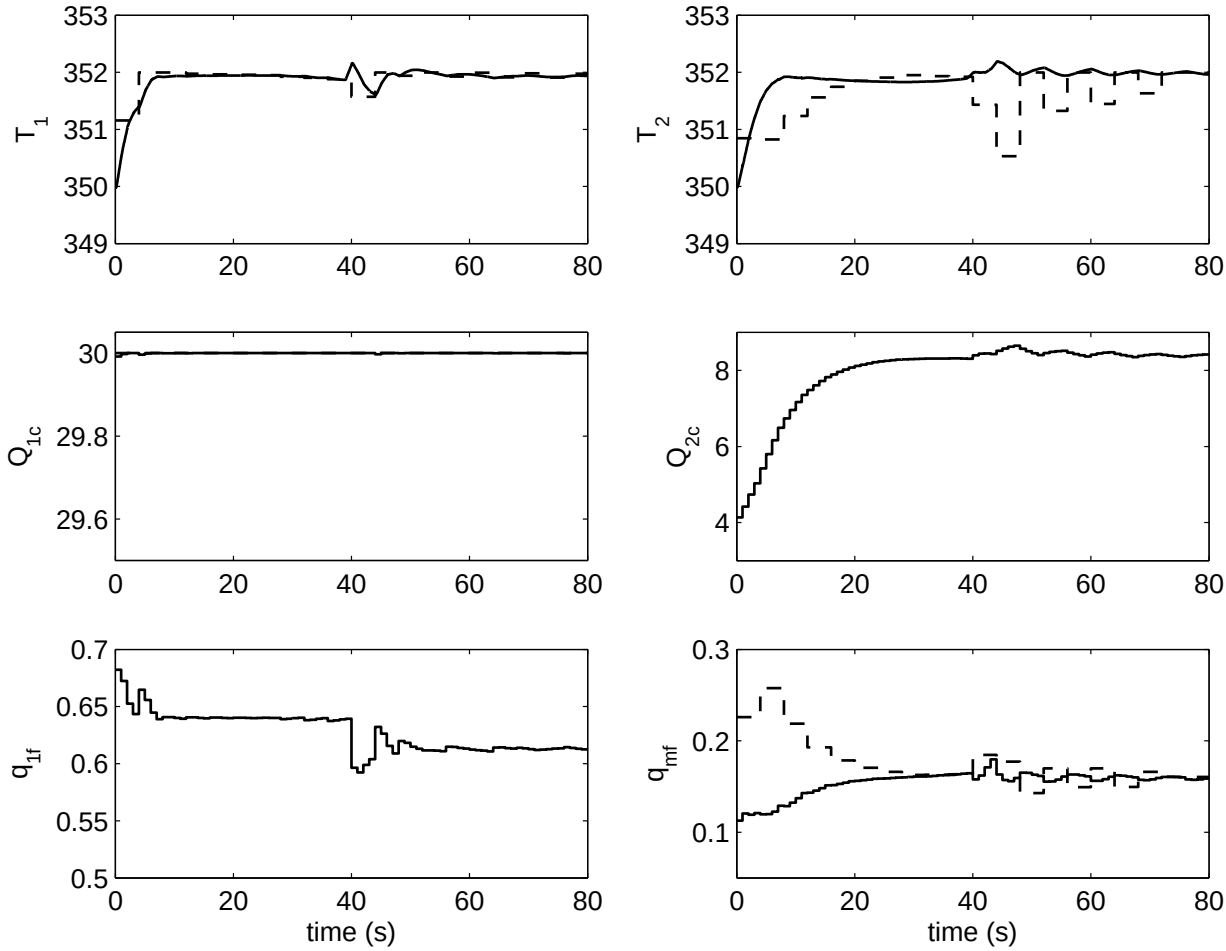

Figure 5.7: CL-DRTO with centralized MPC, profit = $ 11,954.
Legend: *solid lines* = process dynamics, *dashed lines* = set-points.

5.3.2 Target Tracking

In this section, we explore an alternative approach of coordinating a distributed MPC system that is based on a target tracking objective function in the CL-DRTO formulation, with a comparison to regular set-point tracking controllers. Targets (or set-points) for utilization in the CL-DRTO and MPC formulations are obtained from the nominal steady-state set-points of the economic optimization problem in Section 5.3.1, and are given as follow: $T_1^{\text{Target}} = 352$ K, $T_2^{\text{Target}} = 352$ K, $Q_{1c}^{\text{Target}} = 30$ W, $q_{mf}^{\text{Target}} = 0.1603$ m^3/s. The CL-DRTO objective function for the target tracking coordination scheme is written in a quadratic form as given in Eq. (5.8), and the distributed MPC parameters are listed in Table 5.3. A DRTO optimization horizon of 80 s is chosen for closed-loop prediction, and a complementarity penalty parameter of 0.5 is chosen to penalize the summation of complementarity

constraints in the coordinator objective function.

$$\min \Phi = \Delta t_{\text{MPC}} \sum_{j=0}^{N-1} \Bigg[\left(T_{1,j+1} - T_1^{\text{Target}} \right)^2 + \left(T_{2,j+1} - T_2^{\text{Target}} \right)^2 \dots + \left(Q_{1c,j} - Q_{1c}^{\text{Target}} \right)^2 + 1000 \left(q_{mf,j} - q_{mf}^{\text{Target}} \right)^2 \Bigg] \tag{5.8}$$

Table 5.3: Coordinated MPC design parameters.

Parameter	MPC 1	MPC 2
p	40	40
m	2	2
Q	2	3
R	diag(800, 10)	diag(800, 10)
S	diag(0, 200)	diag(300, 0)

Simulation results of coordinating a distributed MPC system using a target tracking CL-DRTO scheme is shown in Figure 5.8. Excellent performance is observed in which the process response dynamics are consistent with the results generated using the economic coordination scheme presented earlier. Both reactor temperature mostly satisfy the safety restriction over the simulation horizon except a slight violation between time 40 and 45 s in which the system is coping with the feed temperature disturbance. Unlike the economic coordination scheme, the target tracking coordination approach does not strictly enforce coolant Q_{1c} to the maximum supply. Also, slower closed-loop response dynamics of the reactor temperature T_1 and T_2 are observed. This is because the weighting parameters for target tracking T_1^{Target}, T_2^{Target} and Q_{1c}^{Target} are set as unity, and a priority of tracking the economics is given to q_{mf}^{Target} with a weighting parameter of 1000 to maintain high process productivity. All manipulated variables are simultaneously adjusted to track the economic optimum defined by the set-point targets and also to reject the disturbance. Referring to Table 5.4, target tracking coordination scheme generates a profit of \$11,883 with only 0.12% economic offset relative to the economic coordination scheme. The resulting sum of squared error (SSE) from the targets is 8.52 and the SCV is 0.94.

Closed-loop performance of the controller tuning parameters from Table 5.3 implemented in a decentralized MPC environment is depicted in Figure 5.9. The economics is 2.3% less than that generated by the target tracking coordination scheme, as shown in Table 5.4. Although the decentralized strategy has slightly lower SSE of 8.47, it has nearly 15 times larger SCV than the coordinated control system. During process operation, the dynamics of CSTR 1 propagate to CSTR 2 as a disturbance and there is no mechanism in the decentralized MPC strategy to mitigate such an impact. The presence of a

feed temperature disturbance after time 40 s also adds more possibility of violating the constraints imposed on the reactor temperatures. This simulation comparison demonstrates the capability of the closed-loop DRTO coordination scheme to supervise the decentralized MPC system, and also to improve the overall process control performance.

Table 5.4: Performance comparison.

MPC configuration	Profit ($)	SSE	SCV
Coordinated MPC‡	11,883	8.52	0.94
Decentralized MPC‡	11,610	8.47	15.35
Decentralized MPC (conservative)	11,082	7.21	9.66
Decentralized MPC (aggressive)	11,898	10.26	16.76

‡Utilizes MPC tuning parameters from Table 5.3.

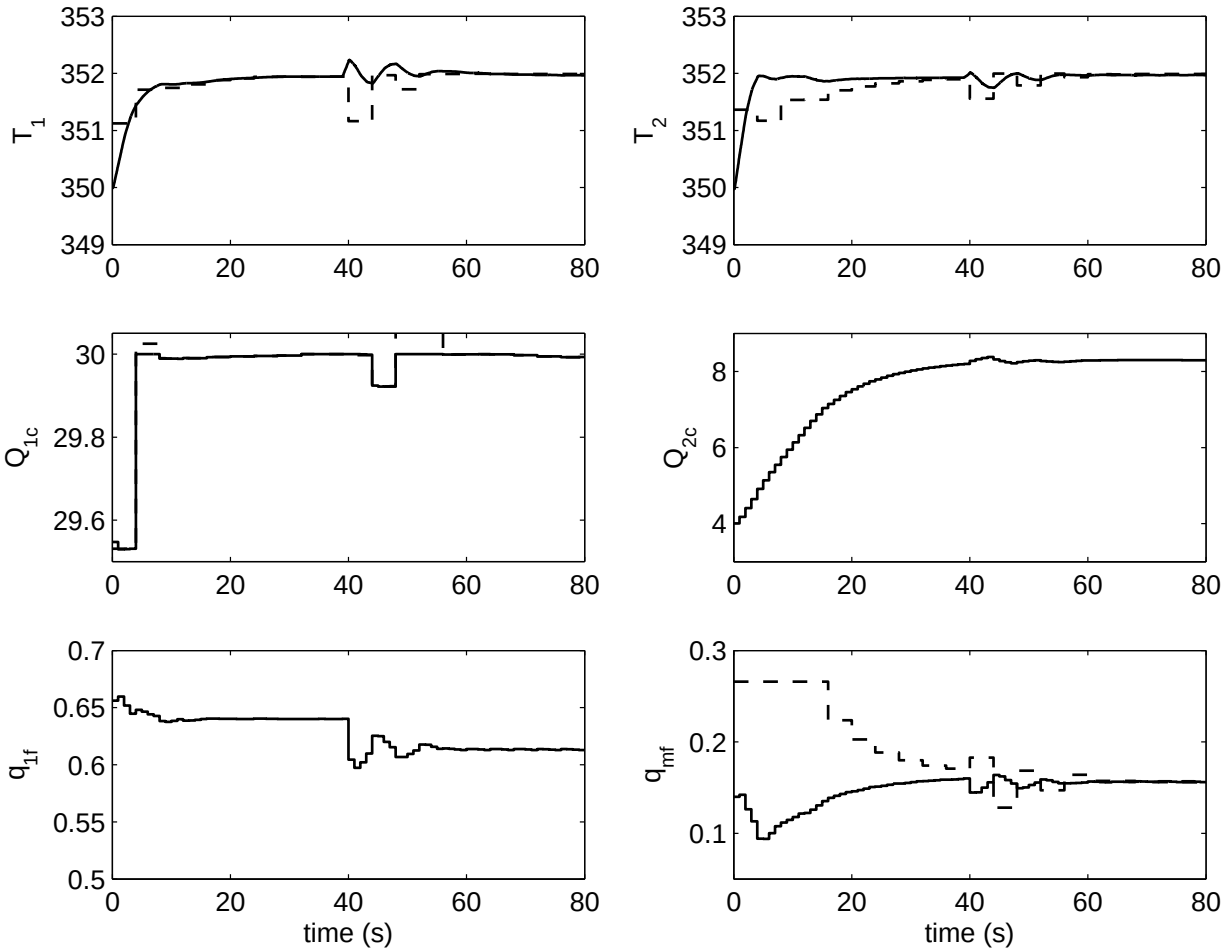

Figure 5.8: Coordinated MPC with target tracking objective, profit = $ 11,883.
Legend: *solid lines* = process dynamics, *dashed lines* = set-points.

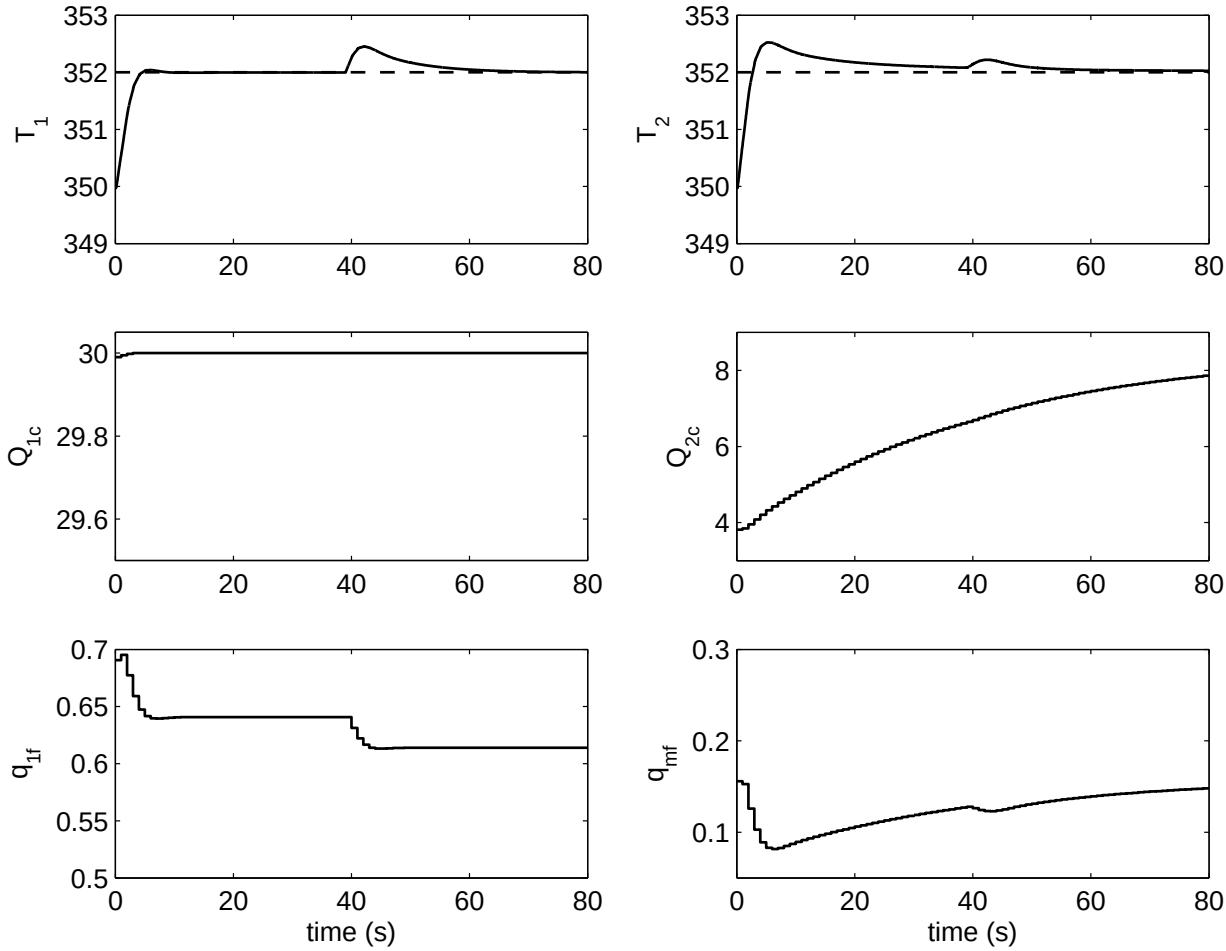

Figure 5.9: Decentralized MPC with tuning parameters from Table 5.3, profit = $ 11,610.
Legend: *solid lines* = process dynamics, *dashed lines* = set-points.

Next, we explore the performance of the decentralized MPC system under conservative and aggressive control settings. For aggressive MPC tuning, the weighting element for q_{mf} in the $S^{(2)}$ matrix (in the MPC cost function of CSTR 2 subsystem) is increased from 300 to 900 to speed up economic tracking of the optimal process productivity, while the parameter is decreased to 30 for the case of conservative tuning. Other controller parameters are taken directly from the coordinated MPC system given in Table 5.3. The aim of conservative MPC tuning in the decentralized control environment is to have minimal temperature constraint violation, at the expense of potentially losing the economics. On the other hand, the aggressive MPC setting is tuned to provide fast tracking of the economic optimum at a risk of violating the temperature limits.

Simulation results of decentralized MPC set-point tracking under conservative and aggressive tunings are shown in Figure 5.10 and Figure 5.11, respectively. A summary of production profit, SSE and SCV of the decentralized control configurations is reported in Table 5.4. Decentralized MPC with aggressive

tuning has faster input dynamics in Q_{2c} and q_{mf} than its conservative counterpart, but input dynamics for Q_{1c} and q_{1f} are similar in both cases. Profits generated by the decentralized MPC system under conservative and aggressive tunings are \$11,082 and \$11,898, respectively.

Although aggressive MPC tuning helps aid fast tracking of the economics, the profit generated is only 0.12% higher than the target tracking coordination scheme, which is an almost negligible difference. Aggressive control actions also lead to the largest SSE and SCV as compared to other cases considered in this section.

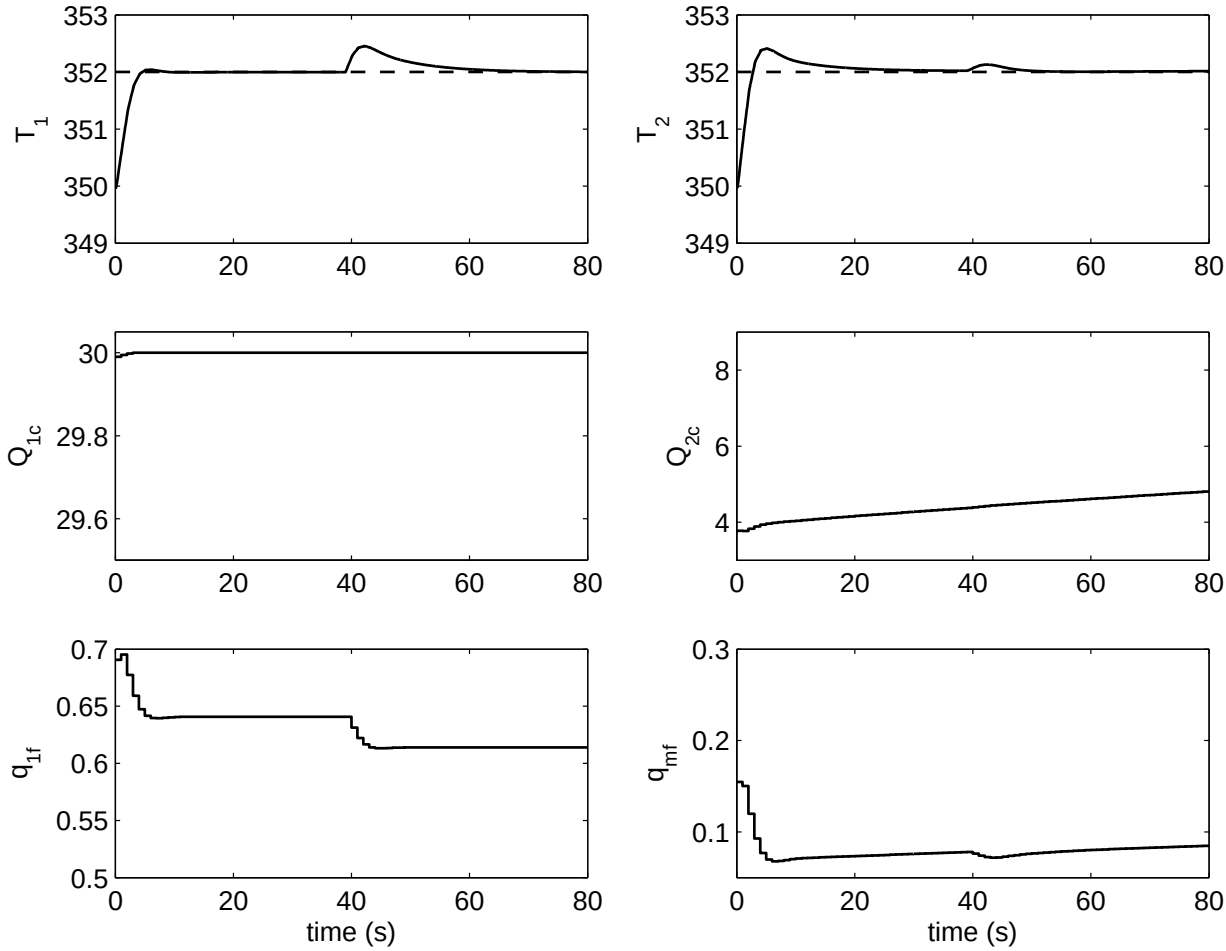

Figure 5.10: Decentralized MPC with conservative tuning, profit = \$ 11,082.
Legend: *solid lines* = process dynamics, *dashed lines* = set-points.

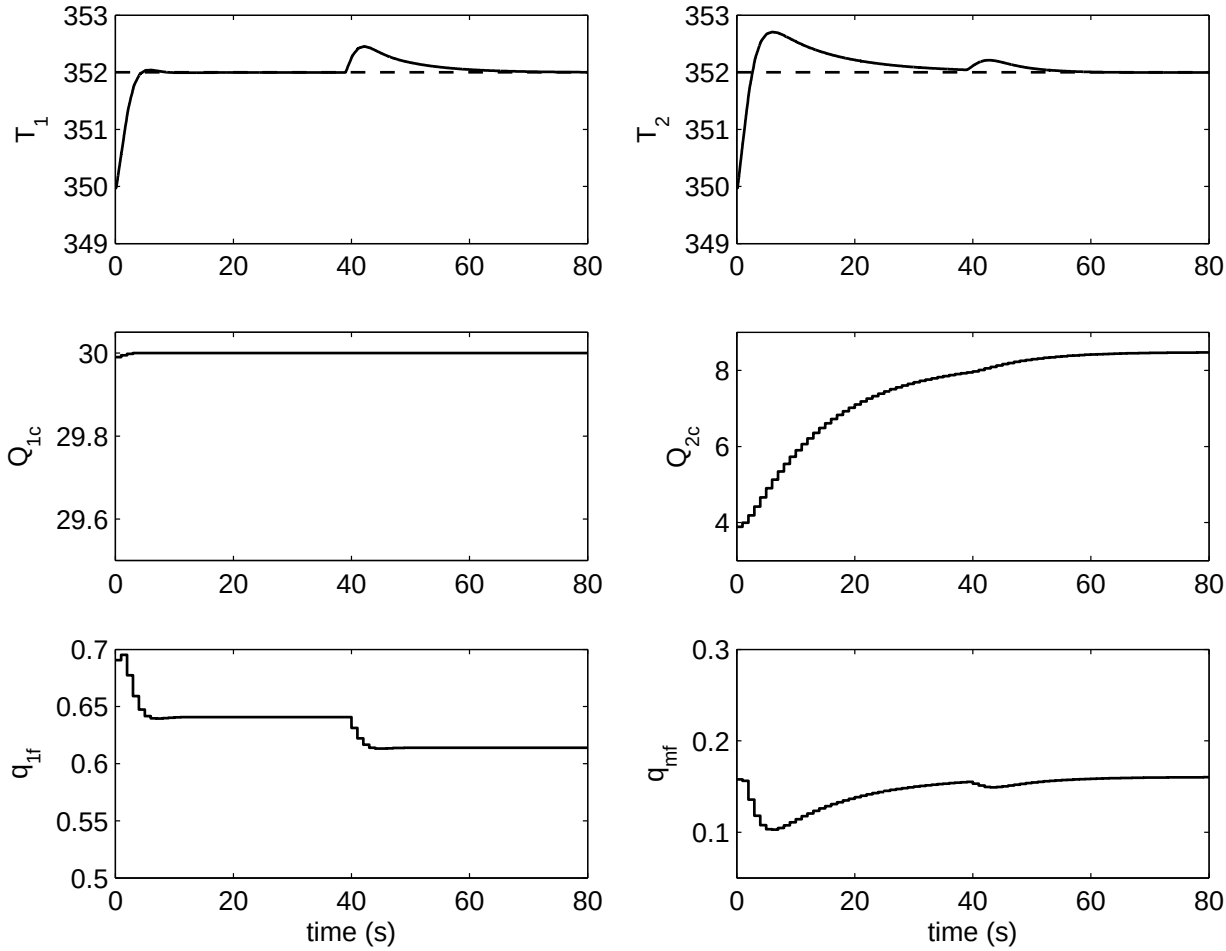

Figure 5.11: Decentralized MPC with aggressive tunings, profit = $ 11,898.
Legend: *solid lines* = process dynamics, *dashed lines* = set-points.

5.4 Conclusion

This chapter proposes coordination of a distributed MPC system via application of closed-loop prediction at the supervisory optimization level in the hierarchical DRTO/MPC configuration. Control coordination is achieved by formulating a CL-DRTO problem as a bilevel program with an embedded optimization subproblem of each MPC functioning in the process, as an approximation to the rigorous multilevel dynamic optimization problem. Interaction between process subsystems is naturally taken into account through the application of control inputs computed by the local MPC optimization subproblems to generate optimal plantwide response dynamics in a closed-loop fashion. The bilevel optimization problem is transformed to a single-level mathematical program with complementarity constraints by replacing all MPC optimization subproblems with the algebraic equations characterizing

their first-order, Karush-Kuhn-Tucker (KKT) optimality conditions, which are subsequently posed as equality constraints in the coordinator optimization problem.

Performance of the proposed CL-DRTO coordination strategy is illustrated using a case study of two CSTRs in series with an intermediate feed regulated using two local MPC controllers. We analyzed coordination schemes based on economic and target tracking objective functions applied in the CL-DRTO formulation, and excellent coordination performance is obtained from both approaches. The CL-DRTO coordination schemes compute optimal set-point trajectories for all MPC controllers simultaneously with an adaptive mechanism to update the tracking set-points at every optimization interval. The closed-loop optimization formulation has the capability to predict the upstream subsystem dynamics and therefore adjust the set-point trajectories to minimize its impact to the downstream subsystem. In addition, having the advantage of adjusting the set-point trajectories also helps to minimize constraint violation at the plant level in the present of plant-model mismatch and disturbances.

References

[1] T. E. Marlin and A. N. Hrymak. "Real-time operations optimization of continuous processes". In: *AIChE Symposium Series: Proceedings of the 5th International Conference on Chemical Process Control*. Ed. by J. C. Kantor, C. E. Garcia, and B. Carnahan. Vol. 93. 316. AIChE and CACHE, 1997, pp. 156 –164.

[2] M. L. Darby, M. Nikolaou, J. Jones, and D. Nicholson. "RTO: An overview and assessment of current practice". In: *J Process Control* 21.6 (2011), pp. 874 –884.

[3] S. Engell. "Feedback control for optimal process operation". In: *J Process Control* 17.3 (2007), pp. 203 –219.

[4] J. B. Rawlings and R. Amrit. "Optimizing process economic performance using model predictive control". In: *Nonlinear Model Predictive Control*. Ed. by L. Magni, D. Raimondo, and F. Allgöwer. Vol. 384. Lecture Notes in Control and Information Sciences. Springer Berlin Heidelberg, 2009, pp. 119–138.

[5] M. Ellis, H. Durand, and P. D. Christofides. "A tutorial review of economic model predictive control methods". In: *J Process Control* 24.8 (2014), pp. 1156 –1178.

[6] T. Tosukhowong, J. M. Lee, J. H. Lee, and J. Lu. "An introduction to a dynamic plant-wide optimization strategy for an integrated plant". In: *Comput Chem Eng* 29.1 (2004), pp. 199 –208.

[7] L. Würth, R. Hannemann, and W. Marquardt. "A two-layer architecture for economically optimal process control and operation". In: *J Process Control* 21.3 (2011), pp. 311 –321.

[8] M. Z. Jamaludin and C. L. E. Swartz. "Effects of closed-loop dynamics in dynamic real-time optimization". In: *AIChE Annual Meeting*. Atlanta, GA, USA, 2014.

[9] M. Z. Jamaludin and C. L. Swartz. "IFAC Symposium on Advanced Control of Chemical Processes (ADCHEM): A Bilevel Programming Formulation for Dynamic Real-time Optimization". In: *IFAC-PapersOnLine* 48.8 (2015), pp. 906 –911.

[10] S. J. Qin and T. A. Badgwell. "A survey of industrial model predictive control technology". In: *Control Eng Pract* 11.7 (2003), pp. 733 –764.

[11] G. Pannocchia. "Encyclopedia of Systems and Control". In: ed. by J. Baillieul and T. Samad. London: Springer London, 2013. Chap. Distributed Model Predictive Control, pp. 1–9.

[12] J. B. Rawlings and B. T. Stewart. "Coordinating multiple optimization-based controllers: New opportunities and challenges". In: *Journal of Process Control* 18.9 (2008), pp. 839 –845.

[13] R. Scattolini. "Architectures for distributed and hierarchical Model Predictive Control – A review". In: *Journal of Process Control* 19.5 (2009), pp. 723 –731.

[14] P. D. Christofides, R. Scattolini, D. M. de la Peña, and J. Liu. "Distributed model predictive control: A tutorial review and future research directions". In: ().

[15] R. Cheng, J. Forbes, and W. Yip. "Price-driven coordination method for solving plant-wide MPC problems". In: *Journal of Process Control* 17.5 (2007), pp. 429 –438.

[16] R. Cheng, J. F. Forbes, and W. Yip. "Dantzig-Wolfe decomposition and plant-wide MPC coordination". In: *Computers & Chemical Engineering* 32.7 (2008), pp. 1507 –1522.

[17] E. M. B. Aske, S. Strand, and S. Skogestad. "Coordinator MPC for maximizing plant throughput". In: *Computers & Chemical Engineering* 32.1-2 (2008), pp. 195 –204.

[18] Q. M. Shao and A. Cinar. "Coordination scheme and target tracking for distributed model predictive control". In: *Chemical Engineering Science* 136 (2015), pp. 20 –26.

[19] E. Camponogara, D. Jia, B. H. Krogh, and S. Talukdar. "Distributed model predictive control". In: *IEEE Control Systems* 22.1 (2002), pp. 44–52.

[20] Y. Sun and N. H. El-Farra. "Quasi-decentralized model-based networked control of process systems". In: *Computers & Chemical Engineering* 32.9 (2008), pp. 2016 –2029.

[21] J. Liu, D. Muñoz de la Peña, and P. D. Christofides. "Distributed model predictive control of nonlinear process systems". In: *AIChE Journal* 55.5 (2009), pp. 1171–1184.

[22] A. N. Venkat, J. B. Rawlings, and S. J. Wright. "Assessment and Future Directions of Nonlinear Model Predictive Control". In: ed. by R. Findeisen, F. Allgöwer, and L. T. Biegler. Berlin, Heidelberg: Springer Berlin Heidelberg, 2007. Chap. Distributed Model Predictive Control of Large-Scale Systems, pp. 591–605.

[23] B. T. Stewart, A. N. Venkat, J. B. Rawlings, S. J. Wright, and G. Pannocchia. "Cooperative distributed model predictive control". In: *Systems & Control Letters* 59.8 (2010), pp. 460 –469.

[24] B. T. Stewart, S. J. Wright, and J. B. Rawlings. "Cooperative distributed model predictive control for nonlinear systems". In: *Journal of Process Control* 21.5 (2011), pp. 698 –704.

[25] H. Scheu and W. Marquardt. "Sensitivity-based coordination in distributed model predictive control". In: *Journal of Process Control* 21.5 (2011), pp. 715 –728.

[26] M. Razzanelli and G. Pannocchia. "Parsimonious Cooperative Distributed MPC for Tracking Piece-Wise Constant Setpoints". In: *IFAC Symposium on Dynamics and Control of Process Systems, including Biosystems (DYCOBS-CAB)*. NTNU, Trondheim, Norway, 2016, pp. 520–525.

[27] J. M. Maciejowski. *Predictive Control with Constraints*. Essex, England: Prentice Hall, 2002.

[28] C. R. Cutler and B. L. Ramaker. "Dynamic Matrix Control - a computer control algorithm". In: *AIChE 86th National Meeting*. Houston, TX, USA, 1979.

[29] C. E. Garcia and A. M. Morshedi. "Quadratic programming solution of dynamic matrix control (QDMC)". In: *Chem Eng Commun* 46.1-3 (1986), pp. 73–87.

[30] A. Nikandrov and C. L. E. Swartz. "Sensitivity analysis of LP-MPC cascade control systems". In: *J Process Control* 19.1 (2009), pp. 16 –24.

[31] E. Zafiriou and A. L. Marchal. "Stability of SISO quadratic dynamic matrix control with hard output constraints". In: *AIChE J* 37.10 (1991), pp. 1550–1560.

[32] R. Baker and C. L. E. Swartz. "Interior point solution of multilevel quadratic programming problems in constrained model predictive control applications". In: *Ind Eng Chem Res* 47.1 (2008), pp. 81–91.

[33] B. Baumrucker, J. Renfro, and L. Biegler. "MPEC problem formulations and solution strategies with chemical engineering applications". In: *Comput Chem Eng* 32.12 (2008), pp. 2903 –2913.

[34] D. Ralph and S. J. Wright. "Some properties of regularization and penalization schemes for MPECs". In: *Optimization Methods and Software* 19.5 (2004), pp. 527–556.

[35] A. Wächter and L. T. Biegler. "On the implementation of an interior-point filter line-search algorithm for large-scale nonlinear programming". In: *Math Prog* 106.1 (2006), pp. 25–57.

[36] P. A. Bahri, J. A. Bandoni, and J. A. Romagnoli. "Integrated flexibility and controllability analysis in design of chemical processes". In: *AIChE Journal* 43.4 (1997), pp. 997–1015.

[37] C. Loeblein and J. Perkins. "Economic analysis of different structures of on-line process optimization systems". In: *Computers & Chemical Engineering* 22.9 (1998), pp. 1257 –1269.

[38] R. Baker. "Interior point solution of complementarity constrained problems arising in integrated design and control". Ph.D. Thesis. McMaster University, ON, Canada, 2006.

Chapter 6

Conclusion

This chapter summarizes the key contributions from this research, and highlights recommendations for future research avenues.

6.1 Summary and Key Contributions

The primary focus of this research is to design a DRTO strategy that optimizes process operations by taking into account the actions of the underlying plant control system. Our study is particularly driven by the industrial need to operate processes in a cost-optimal fashion, and therefore we align our framework to be consistent with the hierarhical industrial process automation architecture. The key contributions of this work are as follows:

1. **A multilevel DRTO formulation with embedded MPC subproblems**
   We propose a CL-DRTO strategy in the two-layer process automation architecture. It minimizes (or maximizes) an economic criterion based on the predicted closed-loop response dynamics of the process, formulated as a multilevel dynamic optimization problem with rigorous inclusion of the underlying MPC optimization subproblems. The multilevel problem is subsequently

reformulated as a single-level MPCC problem by transforming the convex MPC quadratic programming subproblems to algebraic equations using their necessary and sufficient, first-order KKT optimality conditions. The CL-DRTO strategy primarily computes optimal set-point trajectories for the lower-level MPC system, with an adaptive mechanism to update the tracking set-points at every optimization interval.

2. **Effects of closed-loop dynamics in DRTO calculations**
   Performance analysis shows that the proposed CL-DRTO strategy outperforms the traditional open-loop counterpart, particularly under detuned control settings due to control performance limitations posed by plant-model mismatch, RHPT zeros and dead time. It generates higher economic performance, inherits the embedded MPC tracking capability, improves process agility, and helps aid operational feasibility through appropriate adjustment of the controller set-point trajectories. Application to a polystyrene production case study also shows that the CL-DRTO strategy is able to drive the polymer grade transition in a cost-optimal fashion and maintain the polymer grades within the desired specifications in the presence of plant-model mismatch and disturbances.

3. **Simplified approaches to perform closed-loop prediction**
   We formulate and analyze multiple approximation approaches to perform the DRTO closed-loop prediction, which consist of: (i) a hybrid formulation, (ii) a bilevel formulation, and (iii) an input clipping formulation applied to an unconstrained MPC algorithm. The proposed approaches substantially reduce the complexity of the rigorous closed-loop DRTO formulation. Performance analysis on a MISO system demonstrates that the proposed approximation approaches provide accurate results at greatly reduced problem size and faster solution times in comparison to the rigorous formulation. Implementation on a polystyrene grade transition case study also shows that the approximation approaches successfully assist the grade transitions in a cost-optimal fashion, maintain the polymer productivity within the desired grade tolerances, and also minimize the impact of disturbances.

4. **Nonlinear DRTO formulation with linear MPC regulation**
   We compare the performance of the closed-loop DRTO strategy based on nonlinear and linear plant model predictions. Approximation of the rigorous DRTO closed-loop prediction is performed using a bilevel programming formulation with an embedded linear MPC optimization subproblem. We demonstrate that implementation of a nonlinear dynamic model in the bilevel CL-DRTO formulation to predict the closed-loop response dynamics helps to achieve superior economics and control performance to that obtained using a linear model for the plant response determination, while the problem size remains manageable.

5. **DRTO coordination in a distributed MPC system**
   We develop a CL-DRTO coordination strategy for application in a distributed MPC environment. The CL-DRTO coordination formulation is in the form of a bilevel programming problem with an embedded optimization subproblem of each MPC functioning in process. Interaction between process subsystems is naturally taken into account through the application of control inputs computed by the local MPC optimization subproblems to generate the optimal plantwide response dynamics. Performance of the proposed closed-loop DRTO coordination strategy is illustrated using a case study of two CSTRs in series with an intermediate feed regulated using two local MPC controllers. We analyzed coordination schemes based on economic and target tracking objective functions applied in the DRTO formulation. Excellent performance is obtained from both approaches.

6.2 Recommendations for Future Work

Several broad candidate areas for further exploration are identified. They are:

1. **Utilization of a nonlinear MPC for the underlying control system**
   The CL-DRTO strategy proposed in this thesis utilized an MPC formulation with a linear(ized) prediction model in a state-space formulation. The advantage is that the set of KKT conditions of the state-space formulation is general for various process applications. However, this approach may not be efficient for processes that exhibit strong nonlinear behaviour, hence applying nonlinear MPC is expected to improve the economics and control performance. A straight forward approach is to utilize a nonlinear DAE system that describes the process dynamics, but the challenge lies in the requirement to derive the Lagrange gradients of the KKT conditions symbolically, in which the complexity grows with the number of model variables and equations. However, such a challenge may be addressed with an automatic differentiation tool included in certain optimization platforms. An alternative approach is to approximate the nonlinear behaviour using local linear models which can be obtained by linearizing the nonlinear DAE system at every controller sampling instance, and the advantage of having a general form of KKT conditions is retained.

2. **Formulation of time-varying objective function and constraints**
   In all case studies presented in this thesis, we formulate the DRTO problem with time-invariant process economics such that pricing parameters in the objective function, product grade specification and production capacity are assumed constant. The implemented DRTO system then computes optimal decisions based on reactive action in which the optimization formulation is unaware of the future process transition. Improved performance is expected under preemptive

action with utilization of time-varying objective functions and demand constraints. For example, the inclusion of scheduled changes in the grade transition or production load in the optimization formulation allows appropriate changes be made before the actual transition time. Such a strategy is potentially helpful to further reduce the transition period, as well as the magnitude of constraint violations.

3. **Development of an override mechanism for the DRTO loop**
   In our study, the DRTO is executed at a fixed time interval that is multiple integer of the controller sample time, which constitutes multiple MPC calculations between a subsequent DRTO execution. Adjustment of the MPC set-point trajectories can be very effective if large magnitude disturbances enter the system just before the DRTO calculation instance. However, poor performance, such as insufficient backoff of set-point trajectories to minimize constraint violation, is possible if such disturbances enter the system right after a DRTO execution, with corrective action pending until the next DRTO calculation. We expect that the inclusion of an override mechanism in the DRTO loop is beneficial to provide early mitigation on the impact of large magnitude disturbances. The override strategy may be formulated based on the sensitivity of the closed-loop prediction towards disturbance dynamics where if the disturbances exceed a certain predetermined threshold, then override the system will activate the DRTO calculation without the need to wait until the next optimization interval.

4. **Formulation of DRTO coordination for plant under partial shutdown**
   A plant under partial shutdown involves a shutdown in certain process units while allowing the unaffected units to pursue certain courses of action until the process recovers its normal operation. A key advantage of a distributed MPC environment is that failure in one subsystem allows the other subsystems to remain under regulation with appropriate manipulation of plant degrees of freedom be made by the functioning controllers. We believe that implementation of a coordination scheme that supervises the underlying MPC subsystems is vital to handle interaction between the failure subsystem and the other functioning subsystems, and also to keep the plant operating in a cost-optimal fashion even during the partial shutdown period. A CL-DRTO coordination scheme with a partial shutdown policy may be cast as a mixed-integer dynamic optimization (MIDO) problem with model discontinuities handled using discrete formulations.